GRAVITY AND MAGNETIC STUDIES OF THE SUB-BASALT CASSITERITE DEPOSIT IN PLATEAU STATE, NIGERIA

BY

AVJAJIOKAN ENOCH IKPOKONTE - B.Sc. (BENIN)

A THESIS SUBMITTED TO THE POSTGRADUATE SCHOOL, AHMADU BELLO UNIVERSITY, IN PARTIAL FULFILMENT OF THE REQUIREMENTS FOR THE DEGREE OF MASTER OF SCIENCE, APPLIED GEOPHYSICS.

DEPARTMENT OF PHYSICS,
AHMADU BELLO UNIVERSITY,
ZARIA-NIGERIA.

OCTOBER$_t$ 1984

D E C L A R A T I O N

The work "Gravity and Magnetic Studies of the Sub-basalt Cassiterite Deposit In Plateau State, Nigeria" is the original work carried out by the author. The work of others are duely acknowledged. No part thereof has been submitted to any other institution, organisation or bodies for any award other than to the AHMADU BELLO UNIVERSITY, ZARIA, NIGERIA.

DR. M. B. AWAD
(Supervisor)

A. E. IKPOKONTE
(Author)

PROFESSOR D.E. AJAKAIYE (Supervisor)
(Prof. and Head of Dept.)

AHMADU BELLO UNIVERSITY, ZARIA

OCTOBER, 1984

ACKNOWLEDGEMENTS

I wish to express my gratitude to the Head, Department of Physics, Ahmadu Bello University, Prof. D.E. Ajakaiye, for her contributions towards the choice, organisation and supervision of the project. Her devoted sense of advice and encouragement leaves me tireless.

I will always thank Dr. M. B. Awad for his close concern, directives and supervision throughout the duration of the project. To Dr. S.B. Ojo and Dr. M.A. Daniyan, I say thanks for personal contributions, made towards the successful completion of this project.

My special thanks go to the Manager, (Exploration Division), Nigerian Mining Corporation, Dr. S.O. Ford and the Prospecting Superintendent, A.T.M.N., Mr. C.I.B. Cox, for their interests, directives and contributions towards the successful completion of the project. The N.M.C. Provided vehicle and field assistants and the A.T.M.N. are highly commended for their individual contributions; I am indebted to them. I am also indebted to the Workers of the Computer Centre, Ahmadu Bello University, for their contributions towards the use of facilities during the computations.

ABSTRACT

A detailed gravity and magnetic survey carried out on the N'Gall basalt area of Jos Plateau region, was aimed at studying which analytical technigue is practically suitable to the exploration of sub-basalt deposits, with a view to estimating the basalt thickness and removing its masking effect from the acguired data in problem areas such as the sub-basalt cassiterite fields.

It was thought that this approach will further reveal a knowledge of the relative variation of the bedrock surfaces, tne v/eathered/v/eak zones of the bedrock, and the ancient river channel along which tin-bearing sands are believed to be deposited and later covered by sediments overlain by thick hard basalt flow.

Results show that the area of investigation includes a possible downstream extension of the ancient N'gell river flowing to the NE-SW direction into a basement low surface, resulting into a thick pile of sediments, later covered by basalt flow and compacted. Dopth estimates from the potential field sources are comparable with those done on an available control borehole section and are in aggreement with the borehole results. The basaltic layer thicknesses obtained from gravity data ranges from 10 to 29 m„, and from magnetics a range of 11 to 40 m.

Statistical correlation of both results is fair (0.44 to 0.99). The basalt overburden depth from gravity ranges from 9 - 36 m. with an average of 16 m. while estimate from magnetics ranges from 14 - 21 m. with average of 17 m. B' ::'-!t overburden, depths was then fairly obtained from total field magnetic data and compared with those from gravity. The gravimetric depths to basement ranges from 60 - 80 m. with an average of 65 m. and a range of 47 - 69 m„ was obtained from magnetic data. An estimate done on gravity gradients in the area yielded a depth range (to source) of 32.4 - 44„5 m» with an average of 38.0 m. which is indicative of the approximate depth to the base of basaltic layer and is in aggreement with the: borehole results.

From these results, it was then possible to remove the basaltic masking effect from gravity data observed on the basalt, by a stripping technigue and this enabled a fair estimation of approximate depths to sub-basalt bedrock -and'interpretation of the sub-basalt basin outline.

From the stripped gravity data then, bedrock depths ranges from (49 - 65) m„ in the north - western part of the study area; (52 - 100) m. with bedrock dipping towards south-west in the middle part, and a range of (45 - 70) m. in the south-eastern part of the study area. The sub-basalt sedimentary thickness ranges from 10 - 30 m. in the north-western part, 30 - 80 m. in the middle part, with average of 70 m. and 3 - 30 m. with

average of 20 m. in the South-eastern part of the study-area. This residual gravity data stripped to the base (38.0 m. depth) of the basalt layer further compares well with the 3rd spacing (45.7 m.) downward continued Bouguer gravity data.

These results, coupled with the results of the interpretation of the original Bouguer, residual and stripped gravity maps; second ..vertical derivative and analytical downward continuation maps of both gravity and vertical component magnetic data of the area further reveals the possibility of the ancient river channel originally following a probable contact or weak/fracture zone oriented in a NE-SW into a basement low surface downstream. This area may then be favourable for the preservation of the early mineralised wash sands.

CONTENTS

		Page
Acknowledgement		i
Abstract		ii
Table of Contents		v
List of Figures		viii
List of Tables		xi
Chapter		
1.1	Introduction	1
1.1.1	Location and General Geology of the Study Area	1
1.1.2	Geological Setting And Sub-surface Geology of the Study Area	3
1.2	Previous Geophysical Work	7
1.3	Some Geophysical Problem of Sub-basalt Exploration	9
1.4	Scope of the Present Study	11
Chapter Two -	Field Survey	
2.1	Preliminary Field Reconnaisance Survey	14
2.2	Field Procedure	14
2.2.1	Gravity Survey	15
2.2.2	Magnetic Survey	18
Chapter Three -	Reduction And Analysis of The Available Data	
3.1	Borehole Gravity And Magnetic Data ...	19
3.2	Density And Susceptibility Measurements..	20

3.3 Data Reduction 23

3.3.1 Gravity Data 23

3.3.2 Magnetic Data 26

Chapter Four - Interpretation Techniques

4.1 Introduction 27

4.2 Resolution of Anomalies 28

4.2.1 Removal of Regionals By Graphical And Visual Smoothing 28

4.2.2 Analytical Methods

a) Second vertical Derivative Computation 29

b) Analytical Downward Continuation 32

4.3 Gravity Stripping Technique 34

4.4 Depth Estimates 37

4.4.1 Basement Depths 37

4.4.2(a) Estimation of Fault Parameters 38

(b) Semi-infinite horizontal slab approximation 41

Chapter Five - Qualitative and Quantitative Interpretation of the data.

I Qualitative Interpretation

5.1 Features of the Bouguer and its related components 44

5.1.1 The regional anomaly 44

5.1.2 The residual anomaly 45

5.2 Features of the Total and Vertical field magnetic data 48

5.3 The second vertical derivative and analytical downward continuation data ... 56

5.3.1(a) Second derivative gravity data 56

(b) Magnetic derivative data 58

5.3.2 Features of the analytical downward continuation maps 58

(a) Gravity continuation data 60

(b) Magnetic continuation data 66

5.4 Features of the Stripped gravity data .. 66

II Quantitative Interpretation

5.5 Gravity depths 70

5.6 Magnetic depths 72

5.7 Isopach map of the basaltic layer 74

5.8 Depth estimates from downward continuation maps 74

5.9 Isopachte of the sub-basalt sedimentary unit and the bedrock depth maps. 76

Chapter Six - Summary and Conclusion

6.1 Summary and discussions 80

6.2 Related error sources and precautions .. 88

6.3 Conclusion 89

6.4 Recommendations 94

Appendix 96

References 106

LIST OF FIGURES

FIGURE	DESCRIPTION	PAGE
1.1.1	Surface Geology and Location map of the study area	2
1.1.2	Schematic diagrams showing stages in geological setting of the area of study	5
1.1.1(b)	The north-westerly trend of Quarternary Jos Alkali Basalt Volcanoes	4.
1.1.2(b)	Subsurface Geology of part of the study area	6
2.2.1	Drift curves for Worden Gravimeter No. 135	16
2.2	Relative elevation map of the Study Area	17
4.2.1	A stripped gravity result on drill-hole gravity profile over the N'Gell basalt	35
4.4.1	Gravity effect of a faulted horizontal slab showing parameters	39
4.4.2	Gravity effect of a semi-infinite thick horizontal slab showing parameters	43
5.1	A map showing the Bouguer Anomaly of the study area	46
5.1.1(a)	Regional anomaly map of the study area (obtained by 2-dimensioal graphical smoothing)	50

5.1.1(b)	Regional anomaly map of the study area (obtained by visual smoothing)	51
5.1.2	A map showing the Residual gravity anomaly of the study area	49
5.2(a)	A map showing the Total Intensity magnetic field of the study area	53
5.2(b)	Large broad Total field magnetic anomaly over a graben-hollow	54
5.3.1.(a)	A map showing the 2nd vertical Derivative component of the gravity field (45.7 m spacing)	57
5.3.1.(b)	A map showing the 2nd Vertical Derivative magnetic field of the study area (45.7 m spacing)	59
5.3.2(b)	A map showing the Analytical Downward-continued gravity field of the study area (30.5 m spacing)...	62
5.3.2.(c)	A map showing the Analytical Downward-continued gravity field of the study area (45.7 m spacing....	63
5.3.2(d)	A map showing the Analytical Downward-continued gravity field of the study area (61. m spacing).....	64

5.3.2.(c)	A map showing the Analytical downward-continued magnetic field of the study area (45.7 m spacing).....	65
5.4	A map showing the stripped gravity anomaly of the study area	67
5.6	Total field magnetic profile on the reference borehole section	73
5.7	A map showing the thickness of the basaltic layer in the study area	75
5.8	Histograms of the overburden depths on some profiles in the study area ...	71
5.9(a)	A map showing the (sub-basalt) bedrock surface depths of the study area	77
5.9(b)	A map showing the thickness of the sub-basalt sedimentary unit in the study area	78
6.1(a)	A geological section showing the probable bedrock profile	81
6.1(b)	A geological section showing the probable bedrock channel of the ancient N'gell river	82
6.3(a)	A geological interpretation (with borehole) results along line 288 in the study area.....	90
6.3(b)	A geological interpretation along line 304 in the study area:.....	91
6.3(c)	A geological interpretation model along line 324 in the study area.....	92

LIST OF TABLES

TABLE	DESCRIPTION	PAGE
3.2(a)	Density of Rocks from the N'Gell basin	21
3.2(b)	Susceptibility of Rocks from the N'Gell Basin	22
5.5(a)	Basalt and overburden thicknesses on the reference Borehole Section	100
5.5(b)	Compiled depths to basaltic layer from gravity and magnetics	101
5.0	Qualitative interpretation of the gravity and magnetic anomalies polarities in the area	96
5.5(c)	Depths to source from stripped gravity closures	102
5.5(d)	Depths estimated from gravity and magnetic closures	103
5.6(e)	Parameters of geological flexure on the sharp gravity zone (B)	104
5.6	Statistical correlation of the basalt thicknesses from gravity and magnetics ..	105
6.1	Bedrock parameters of the deepest zones .	104

CHAPTER ONE

1.1 INTRODUCTION

1.1.1 Location and general geology of the study area:

The area of study lies between latitudes 9° 47' 3" and 9° 48" and longitudes 8° 45' 2" and 8° 46' 41" and covers an area of about 1 km^2, (fig, 1.1.1 (a)). It is often referred to as the N'Gell Basalt area of the Jos Plateau region.

The geology of the Plateau region has been well documented (Falconer and Beaburn, 1923; Falconer et al, 1926; Mackay et al, 1949; Jacobson et al, 1958; Macleod et al, 1971; Buchanan et al, 1971; Jacobson and MacLeod, 1977).

The area lies within the Basement Complex Rocks which compose of migmatities gneisses, granites and granite-gneisses of the Pre-Cambrian to Lower Paleozoic age. These rocks are intruded by a more resistant Younger Granite ring complexes which consists mainly of syenites, rhyolites, quartz and quartz-fayalite-prophyry, granites and hornblende-biotite and biotite-fayalite granites, biotite-granites, riebeckite-biotite and riebeckite-aegirine and arfedsonite granites.

These intrusions form contract dip angles of not less than 60° with the host rocks. Their eroded remnant form major hills (or watershed) in the area.

Almost all the Nigeria's cassiterite is derived from alluvial concentrations, shed from roof and contract zones of the biottite granites. A large area

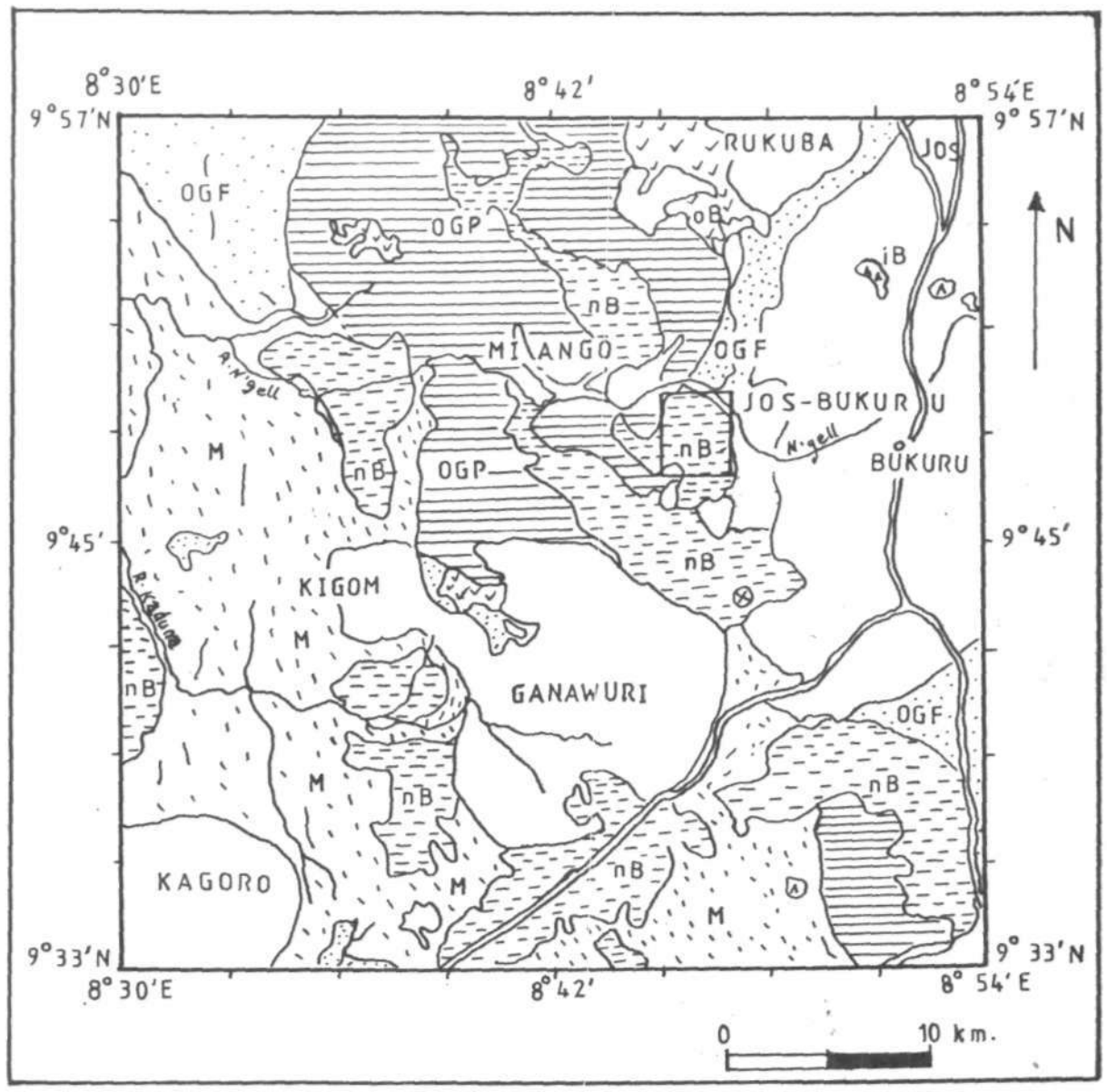


FIG: 1·1·1 (a)· SURFACE GEOLOGY
(after MacLeod et al·, 1971)

nB — Area of study

nB — newer basalt
iB — lateritised older basalt
oB — older basalt

Younger granite

OGF — fine and medium grained biotite, and biotite-muscovite granite

OGP — porphyritic biotite and biotite-hornblende granite

trend of foliation

⊗ probable volcanic vent

M — migmatites

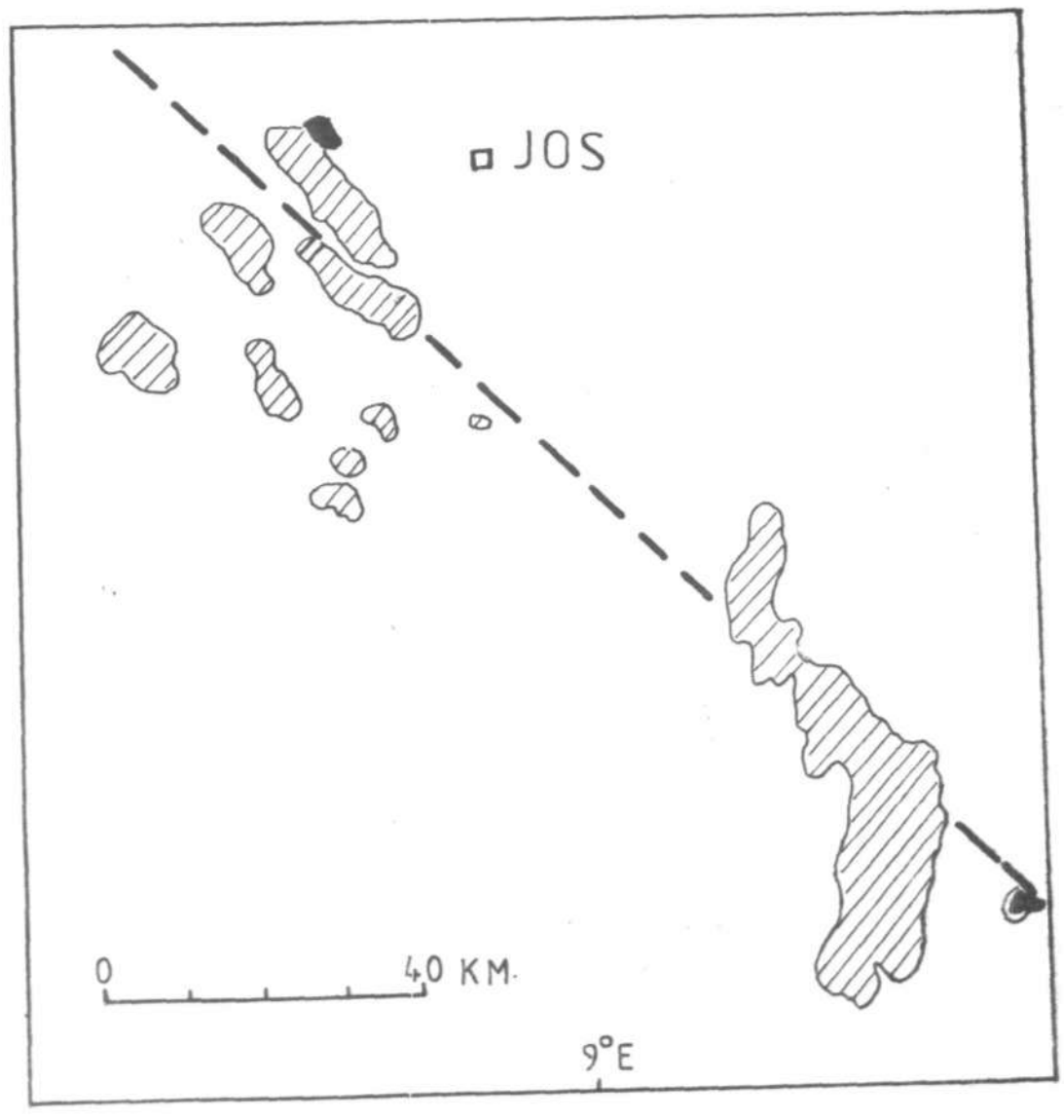
of the rich alluvial deposit are located along stream channels, covered by late series of basalt flows.

The basaltic series are mainly the (older) basaltic clays of Tertiary age which are often mixed with sediments of granitic origin and often referred to as "fluvio-volcanics", and a late Quaternary (Newer) hard basalts and lateritized basalt clays. The late series of basaltic eruption is known to have characterised the geology of much of the eastern border of Nigeria with upliftment along the Cameroun volcanic line about 1,100 km long (fig. 1.1.1(b)).

1.1.2 Geological Setting and Subsurface geology of the study area:

The geological setting of the study area is summarised in Cox, 1979; and the schematic description shown in fig. 1.1.2(a), in which the former valley floor was covered by shallow richly mineralised gravel beds eroded from adjacent hills. The granitic bedrock surface was cut by the ancient stream forming U-shaped valleys. Lake conditions probably existed following a block of the drainage downstream resulting in a diversion and meandering of the stream. Finally, the valley was partially flooded by basalt lava and the modern stream now flows along the edge of the basalt.

A careful study of the available borehole data along several profiles covering parts of the area, fig. 1.1.2(b), gave an indication of the subsurface geological structure. This consists of older granites bedrock, sub-basalt



Lava flows

Volcanic Cones

Fig. 1:1:1(b) The north-westerly trend of the Quanternary Jos Alkali basalt volcanoes. The trend of Lineaments in the alkali basalt on the N'Gell is parallel to this trend. (based on 1:100,000 sheets of the Geological Survey of Nigeria, after Ajakaiye, 1976).

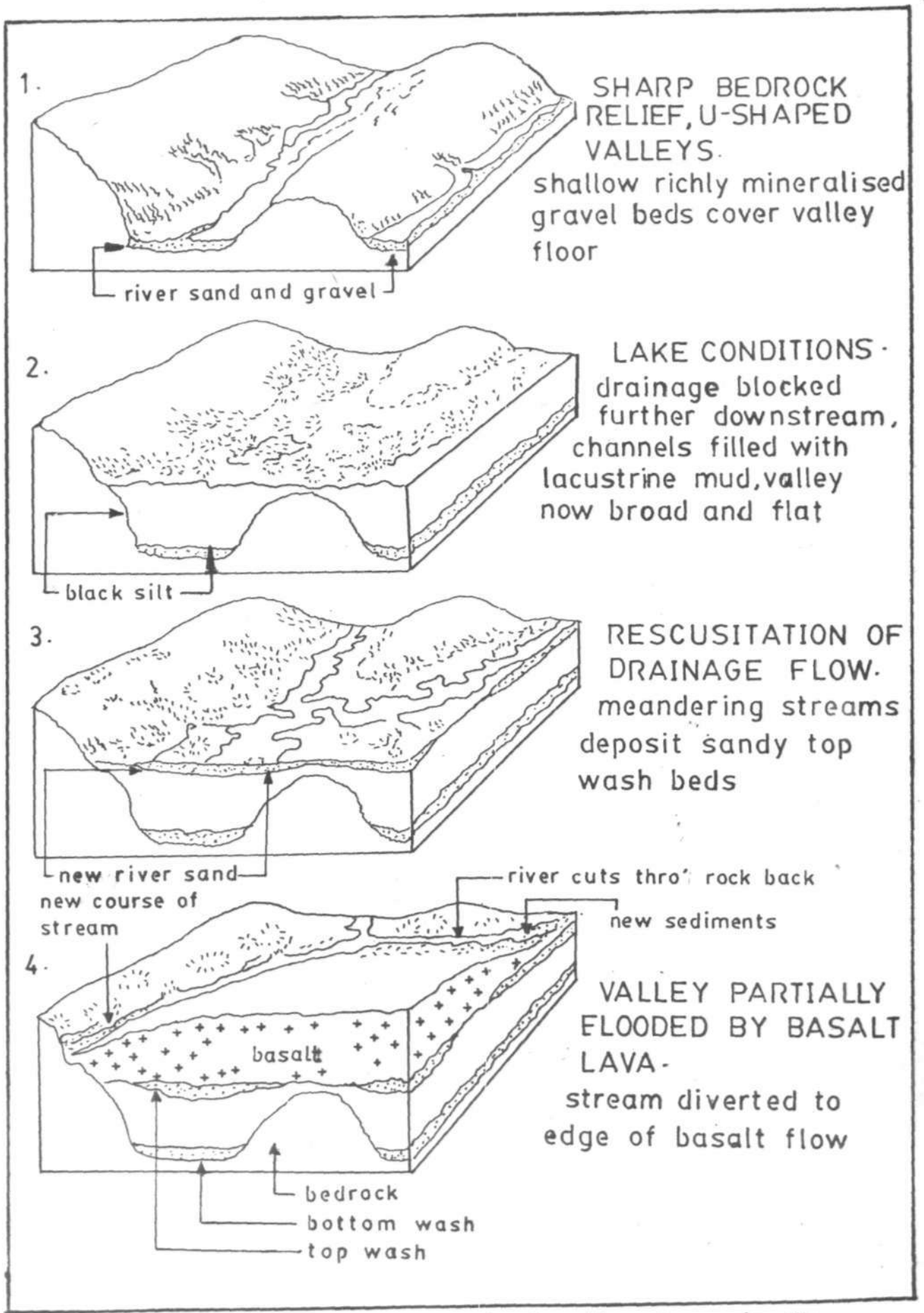


Fig: 1-1-2 (a) A schematic diagram showing the stages in the geological setting of Sabon-Gida N'Gell valley and the N'Gell sub-basalt basin (adapted from Cox, 1979).

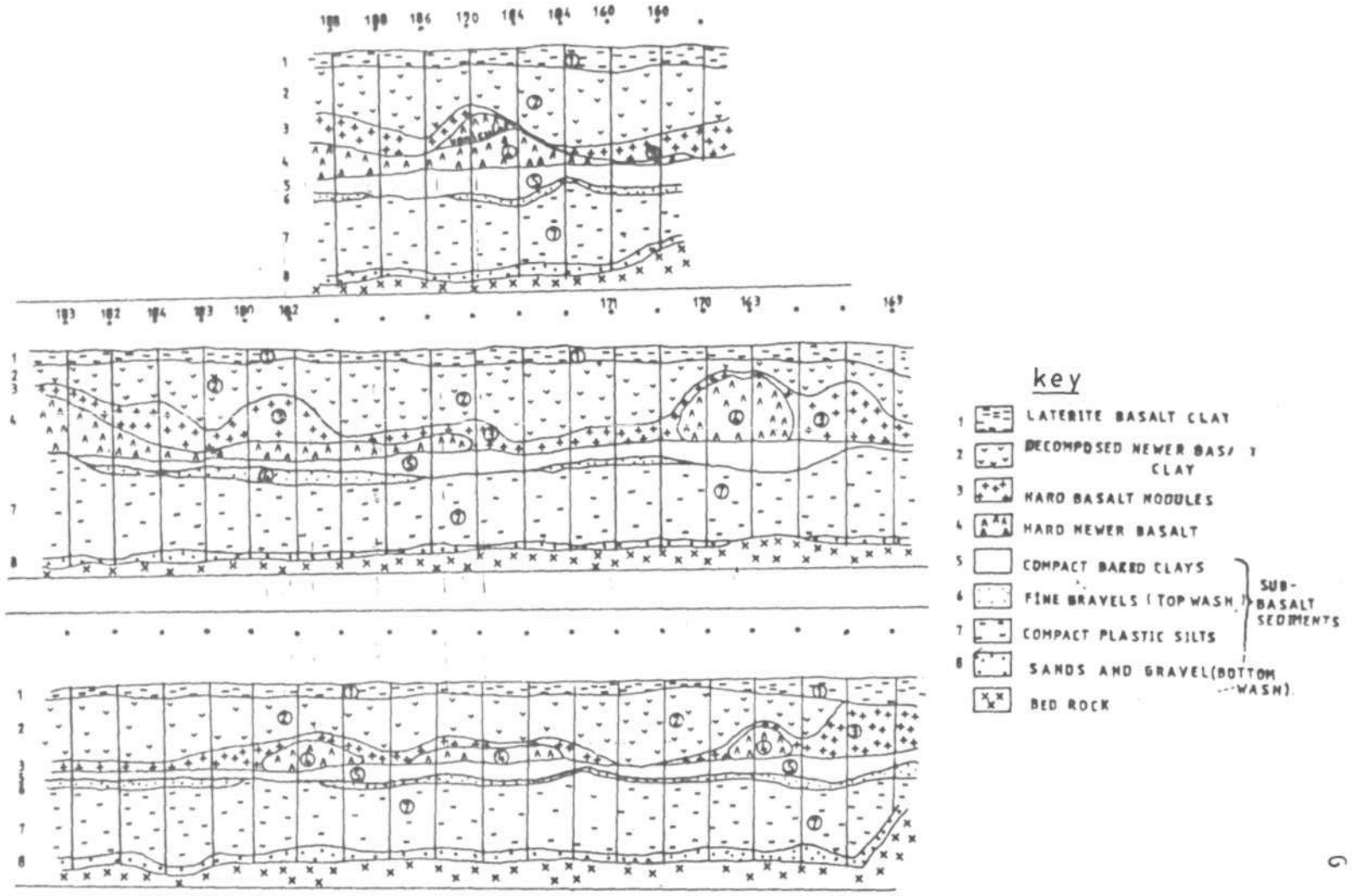


Fig.1-1-2(b) Sub-surface geology of part of the study area. Vertical lines show drill-holes with depths (ft) to bedrock. (Courtesy of A.T.M.N. Nig. Ltd., adapted from Ajakaiye, et al., 1975).

sedimentary deposits, the hard (newer) and decomposed basalts.

The geological sequence from the borehole data is as follows:

i. Pre-Cambrian to Lower-Paleozoic rocks of the Basement (older granites) which form the bedrock and which are weathered in places.

ii. Paleooene to Mid-Pliocene sediments consisting of sands and sandy alluvium derived from the granitic terrain.

iii. Mid-Pliocene to Upper-Pleistocene sediments which are mainly the shallow valley sandy alluvium and carbonaceous clays (Bond, 1956).

iv. Decomposed Older and hard Newer basalts. The older basalts are probably of Mid-Tertiary while the Newer basalts are most likely of Late-Pleistocene to Quaternary age (Turner, 1971; Burke and Durotoye, 1970).

The following were deduced from the borehole data:

i. density and magnetic properties of the different formations;

ii. the relative variation in thickness of the different stratification and the overburden depth to the top of basalt layer and basement.

1.2 Previous geophysical work:

The earliest geophysical work carried out on the Plateau area were for exploration purposes and is said to cover an area of not more than 500 km^2 (Ajakaiye, 1976). Electrical resistivity and magnetic methods were used to locate the channels of old rivers buried

by volcanic/alluvial materials thus enabling a reduction in the amount and cost of exploration drilling in the search for tin (Du Preez, 1948: Shaw, 1951).

An aeromagnetic map (Sheet 168, Naraguta, S.E.) covering a limited part of the Younger Granite province has also been published (Canadian Aero-Service Limited, 1963). As a follow-up of this a comprehensive geophysical study of the sub-basalt tin deposit, (350 km^2 area) was carried out in 1964 to 1965 under the auspices of the United Nations Mineral Project and the British Overseas Geological Surveys (Ajakaiye, 1976). Gravity, Seismic, resistivity and magnetic techniques were used in the study (Mason-Smith, 1965). The results show that Gravity and Seismic methods were equally useful in the areas of decomposed basalt but are complementary in hard basalt areas. Detail gravity work on a 122 m^2 grid was recommended in the area (Mason-Smith, 1965).

Gravity, seismic reflection and refraction (using both shallow shot holes and hammer) test surveys were carried out with the main purpose of finding the relative usefulness of these methods in mapping the bedrock topography under the hard basalt (Ajakaiye, et al, 1975).

Extensive regional gravity surveys has been carried out on the Jos Plateau (Mason-Smith, 1965; Ajakaiye, 1976). The area is known to be characterised by negative Bouguer/ gravity and a broad regional anomalies with wavelength of about 100 km and a north-westerly strike ranging from about -30 mGal to about-65 mGal which tend to be more negative

towards the centre of the Province (Ajakaiye, 1976). A Bouguer gravity map of some parts of Nigeria (Ajakaiye, 1970; Burke and Ajakaiye, 1974) shows that a gravity low of about - 80 to - 85 mGal passes through the area, of the present study.

1.3 Some geological problems of sub-basalt exploration:

Problems associated with the use of some geophysical methods in sub-basalt exploration have been identified from the results of past test geophysical methods in the area.

Application of the electrical resistivity method indicate that moderate electric current is incapable of penetrating the hard basalt. Depth-sounding did give fairly reliable depth to top of basalt in hard basalt areas (Mason-Smith, 1965). Very high electrical current will be required to penetrate any thick basaltic sheet in the area assuming the following five geophysical layers, that is, upper layer of basalt clay, decomposed basalt, hard basalt, sub-basalt sediments, and granitic bedrock, with average (wet) resistivity values of 0.90, 10.0, 3000,0, 0.90 and 3000.0 kilohm m. respectively. (Mason-Smith, 1965; Telford, et al, 1980). Thus resistivity measurements may not give reliable information of the sub-surface structure below the hard basalt layer.

If a high velocity layer overly a lower velocity zone, efforts to obtain informations from the underlying low velocity zone using seismic method is less feasible. The seismic velocity of hard basalts (5.43 - 6.40 km/s) and unweathered granite (5.03 - 6.10 km/s) with average velocities of 6.40 and 5.64 km/s respectively (Dobrin, 1976), are approximately the same at various location in the area (Mason-Smith 1965). In some areas such as the Kassa basalt in Kuru, where the base of the basalt is in direct contact with the bedrock or separated from it by a thin alluvium layer, seismic refractions or reflections from the hard basalt base are obtainable. Where sub-basalt alluvium is thick, even with shot points at the edges of the basalt, multiple reflections may result. Seismic refraction may succeed in picking up the depth to hard basalt.

A study of the geological map and the aeromagnetic survey data over the area reveals a good correlation between the magnetic anomalies and the Newer basalt flows (Ajakaiye, 1976). This correlation may reflect a varying thickness of the basalt flows (assuming uniform susceptibility) or the degree of weathering of the basalts (Ajakaiye, 1976) Basalt thickness from borehole data ranges from 15-25 m. in most areas and well below 15 m. at the flanks and areas of deep weathering. Since aeromagnetic surveys were done at a normal flight line spacing of 2 km, any analysis that may involve digitised spacing of less than 1 km, with a

view to investigating the thickness variation of basaltic sheet, may not yield reliable results. This is due partly to the fact that aliasing may be produced and that shallow depth (about 45 m.) is of interest. In a similar case history, tin-bearing deep leads occur near Inverel (in Australia), in valleys later filled by basalt. The occurence of this basalt can be detected by aeromagnetic anomalies (Forsyth, 1960). The observed correlation of this data with the geology encouraged the use of total field ground magnetic survey, in this study.

1.4 Scope of the present study:

Problems associated with the location of the original stream pattern and the presence of the overlying hard undecomposed basalt are powerful deterent to both mining and geophysical exploration and exploitation of the sub-basalt alluvial tin deposits.

The main purpose of the present work is to study which analytical technique is best suited to the exploration of sub-basalt deposits using both gravity and magnetic ground surveys.

For this purpose the area was covered with detailed gravity and magnetic ground surveys on a 60.96 m. regular square grid pattern. This was done in order to estimate the basalt thickness with a view to removing its masking effect from the acquired data in the study area. The available drill-hole data will be used to aid in the

analysis and interpretation (Hammer, 1963).

The analytical techniques applied are as follows:

i) the acquired Bouguer gravity and Total Field magnetic contour maps are used to calculate

a) the 2nd vertical derivative components based on application of Rosenbach's technique (1954);

b) the Analytical Downward continuation based on Constantinescu, (1961),

with a view of studying the effects of shallower and smaller disturbing masses and to locate sources of anomalous field and probably depth extent of basaltic layer.

ii) A compuation of effective basaltic thickness and depths from

a) gravity data using the assumption of infinite horizontal basaltic slab of uniform density.

b) total field intensity magnetic values using slope-half-slope method along the principal profiles (Peter's, 1949).

c) gravity and magnetic closures based on Both and Smith's, 1958, and thin slab approximations.

iii) the residual gravity is subjected to a stripping correction with the aid of the limited borehole informations and the results of the above compatations (based on Hammer 1963) in order to map out the sub-basalt bedrock surface topography and the effects of deeper origin. Careful studies of all the obtained results together with the available geological informations is hoped to reveal:

a) the usefulness or otherwise of such practical technique of stripping off calculated shallower gravity effects to improve the definition of deeper gravity prospects (Hammer, 1963), in problems areas such as the sub-basalt cassiterite fields.

b) estimation of the relative thickness of the hard basaltic cover from the acquired ground magnetic and gravity data as reflected on the aeromagnetic survey data in tin-field areas (Forysth, 1960; Ajakaiye, 1976).

c) a knowledge of the relative variation of the bedrock surfaces, the sedimentary thickness, and the weathered/ weak zones of the bedrock, under the hard basalt cover.

CHAPTER TWO

FIELD SURVEY

2.1 Preliminary field reconnaisance survey:

Prior to the actual geophysical work, about three reconnaisance trips were made. The first one undertaken with the Amalgamated Tin Mines of Nigeria (A.T.M.N.) team led by the Prospecting Superintendent. The main objective of the trips was to get acquainted with the location sites for the present study as well as collect fresh rock samples from the active mining casts.

By use of the surface geological map, the structural positions of the rock bodies adjacent to the area of study were examined on the topographical map during one of the trips.

2.2 Field procedure:

A total of 15 parallel (principal) profile lines each extending to about 0.85 km in the N.W. direction were laid out. Also about 14 parallel cross-profile lines each extending about 0.84 km. S.W. were laid.

All the principal profiles were oriented in the direction 320^{o} for lines 288 to 332 at intervals of about 61 m. The spacing between line 332 and 336 is exceptionally increased to about 106.7 m. to approcch a regional trend. The crossprofiles were numbered from 64 to 120, with the normal 61 m. spacing. This gives an areal coverage of about 1 km^2.

All the profiles were laid using a WILD T1 micrometer Theodolite and stations marked at intervals of 61.0 ± 0.1 m. on a 1:2,500 map.

Heights were determined using level and reduced relative to a datum of about 1194 ± 0.1 m. on a base station at a borehole 288/88 (fig. 2.2). Two sites were surveyed and named test-site and main probe site, each overlapping with borehole profiles.

2.2.1. Gravity survey:

The instrument used for the actual gravity work was the Worden Gravimeter Model N_o. 135 with a scale constant of 0.09267 mGal per division, from Department of Physics, Ahmadu Bello University.

Prior to the field work, the instrument was observed in the Geophysics Laboratory for two consecutive days. The daily tidal variation was smooth (see fig. 2.2.1) with a maximum amplitude fluctuation of about 0.3 meter reading (0.028 mGal). The linear trends in the curves are attributable to instrumental drift. The variations due to this is considered just adequate as compared with the value of 0.03 mGal per day recommended by the manufacturers for the instrument. The variation amplitude is not greater than 0.1 meter reading (0.001 mGal).

However, because of the nature of the surveyed area and the level of expected anomaly, the instrument needed resetting for the field work. The instrument was also observed for about 3 hours after each day work during which a maximum amplitude range of about 0.009 - 0.019 mGal was being recorded. This was considered reasonable.

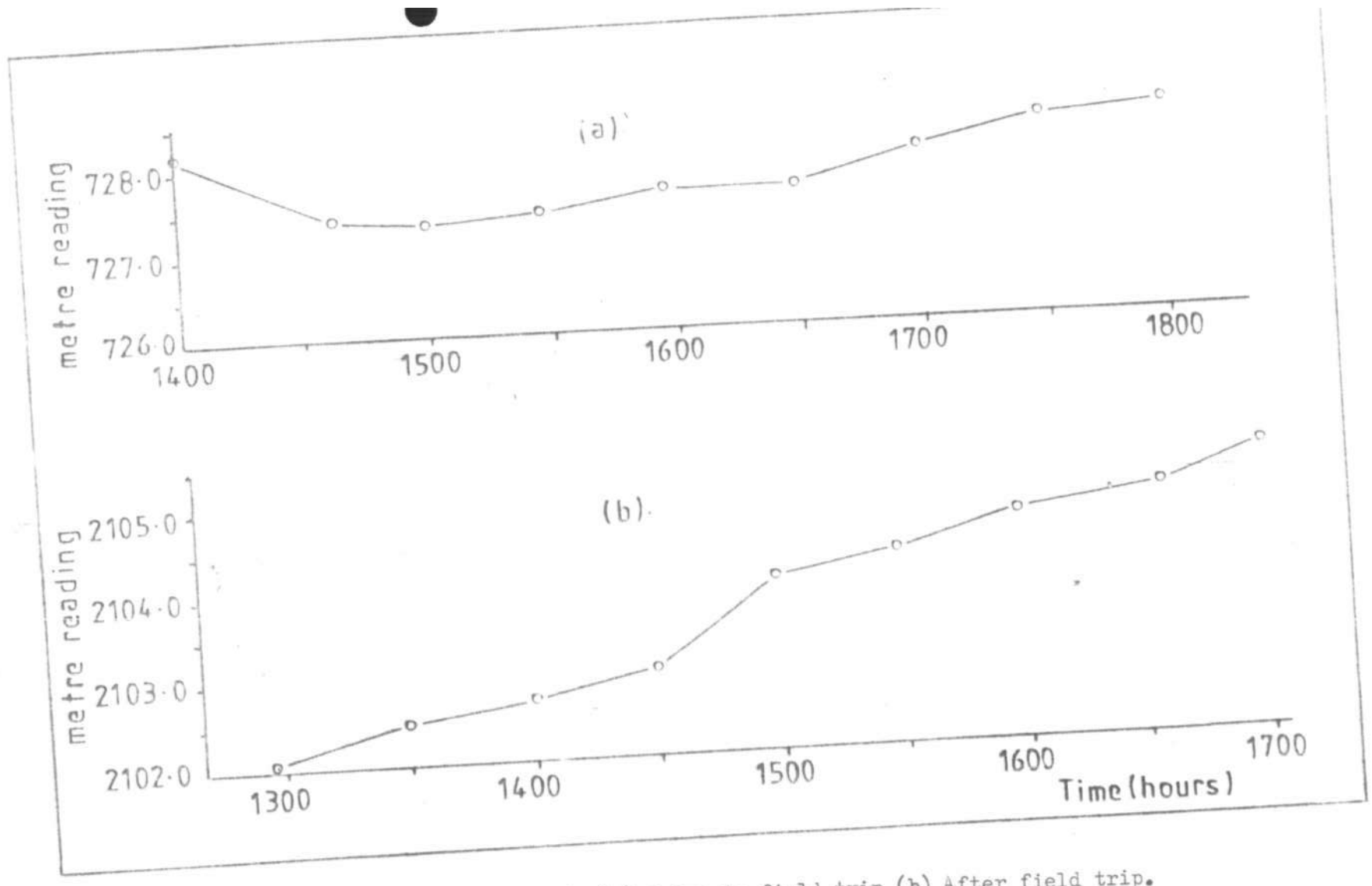


FIG. 2.2.1. Drift curves for Worden Gravimeter No 135. (a) Prior to field trip (b) After field trip.

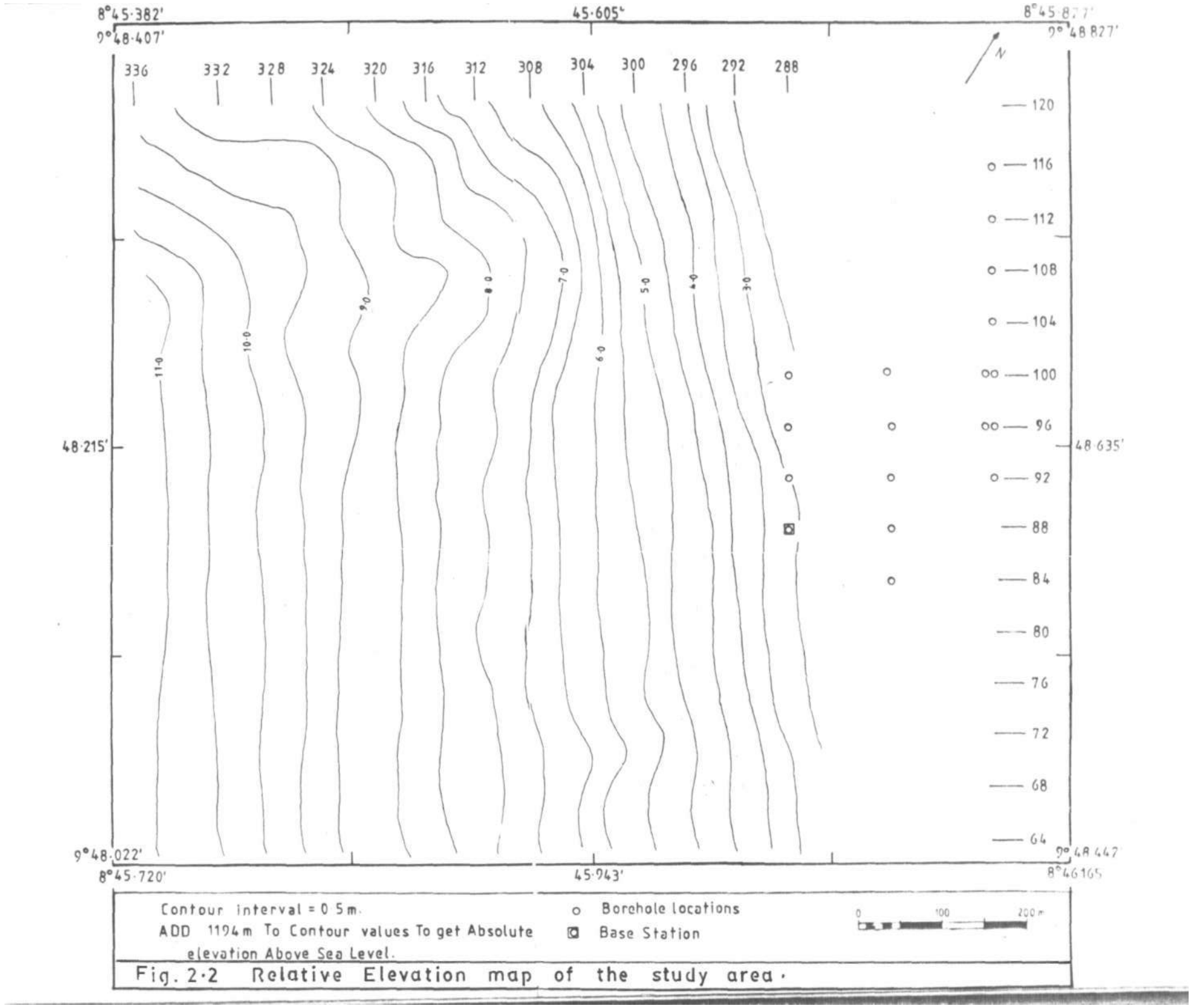


Fig. 2·2 Relative Elevation map of the study area.

All gravity values were reduced relative to that of absolute gravity Base station at the Jos Survey Headquarters (Lat. 9° 54' 42"; Long. 8° 54' 24" established by Ajakaiye and Verheijen, in 1978, (9777962.041 ± 0.014 mGal) which was tied to the Base Station 288/88 and 220/70 at both the main probe site and test site respectively, using close-loop method of Nettleton (1976).

Other base stations (about 21) were established and interconnected. The detailed stations were occupied using the usual Nettleton's ABABCBCD----- method between interconnected base stations of the order A,B,C,D ---- on the grid profiles (Telford, et al, 1980). Few repeated readings taken along the cross-profiles did not show any difference greater than about.0.0003 mGal. from those on the principal profiles.

2.2.2 Magnetic survey:

Magnetic field observations were made using proton precession total field magnetometer, Geometric G 826. This instrument measures the total field magnetic component in gammas to an accuracy of 1 gamma.

Since consistent readings were obtained only at a distance greater than 120 m. from any iron structures, vehicles used during the surveys were thus kept at distances not less than this, from any observed station.

Magnetic measurements were made at the locations of the gravity stations on the grid pattern. Reoccupation of the base stations (about 21) were done in not more than 5 minutes and detailing done using the Nettleton's methods as in above.

CHAPTER THREE

REDUC TION AND ANALYSIS OF THE AVAILABLE DATA

3.1 Borehole gravity and magnetic data:

The typical local section of the basaltcovered area of study simplified for gravity and magnetic purpose is as follows:

Rock Layer	Density in 10^3(kg m^{-3})	Susceptibility in 10^{-3} c.g.s.
Overburden laterised basalt clay	2.3	0.1
Decomposed basalt (with hard noddles)	2.3-2.56	0.3
Hard to vesicular basalts	3.0-2.56	0.6-0.5
Sub-basalt alluvium (lenses of sands, carbonaceous clays, wash)	2.3	0.0-0.1
Hard to weathered bedrock granite	2.67-2.5	0.1-0.0
Hard bedrock granite	2.67	0.2

The bedrock granite have fairly uniform density and susceptibility except where there are or high level intrusions or where it is weathered. Gravity and magnetic anomalies may arise due to changes

in thickness or degree of decomposition and susceptibility of any of these layers.

The average overburden depth is 17.24 ± 2.8 m. and the thickness of basalt ranges from 14.6 - 25.9 m. with an average of 19.58 ± 4.5 m. while the thickness of the sub-basalt sediments ranges from about 4.3 m. at the flanks to about 25.3 m. towards the centre of the valley.

3.2 Density and susceptibility measurements:

A total of about 18 representative samples were collected during field surveys. Both drill-core and open-cast mine samples were subjected to both density (table 3.2(a)) and susceptibility (table 3.2(b)) measurements. Wet and dry desity were determined using both the Mettler PS 15 Balance, the chemical balance and pycnometer (for friable samples); while the susceptibility determination was carried out using a battery operated SCINTREX SM-5 Susceptimeter.

The highest density (2.93 ± 0.01 kg. m^{-3}) and susceptibility (0.6 ± 0.05 x 10^{-3} c.g.s.) recorded for the unweathered "newer" hard basalts; while the sub-basalt black clay gave the least density (1.36 ± 0.06 kg. m^{-3}) and susceptibility (0.0-0.03 x 10^{-3} c.g.s.).

The measured mean values of density, however, are comparable with the range of both standard values and those from other localities in the area. (Telford, et al, 1980).

Table 3.2(a) Density of Rocks from N'Gell basin

rock type	Samples	Range of Density in 10^3 (kg m-3)	Average Wet Density in 10^3 (kg m-3)	Values from other localities (in 10^3) (kg m-3)
Bed Rock Granite	3	2.57-2.70	2.64±0.06	2.66 + 0.05* (Granite Gneiss)
Basaltic Noddle	3	2.94-2.95	2.94±0.01	2.83-2.93** (Olivine Basalts)
Basaltic (Vessicular)	3	2.54-2.56	2.55±0.01	-
Hard (Newer)	3	2.92-2.94	2.93±0.01	2.73-2.79** (Calcitic Basalt
Basalt				2.83-2.93** (Olivine Basalt)
Bottom Wash (Gravel Sands	4 (Part-samples)	2.63-2.65	2.64+0.01	1.70-2.30+ (Pure Sands)
Wet Black Clay	4 (Part-samples)	1.2301.4	1.36±0.06	1.63-2.60+ (Clay)
Decomposed Older Basalt Clay	3 (part-samples	1.91-2.5	2.21±0.30	1.70-2.50+ (Sands and clays)
Top Wash (Dry)	4	1.81-2.52	1.98±0.30	1.70-2.40+ (gravels)
Greyish	4 (Part-samples)	1.65-1.85	1.83±0.08	1.63-2.6+ (clays)
Weathered or Decomposed Bedrock	4	1.65-2.00	1.826±0.2	1.63-2.6+ (Clays)

* After Ajakaiye, 1976.

* * After Ibe, 1982

\+ After Telford, et al, 1980, pp.25

Table 3.2(b) Susceptibility of Rocks from N'Gell Basin.

Rock Type	Samples	Range of Susceptibility in 10^{-3} c.g.s.	Average Susceptibility in 10^{-3} c.g.s.
Bedrock Granite	3	0.1-0.2	0.13±0.06
Basaltic Noddle (Olivine Neddle)	5	0.1-0.2	0.18±0.04
Newer Hard Basalt	5	0.5-0.6	0.58±0.05
Bottom Wash (Gravel and Sands)	4	0.3-0.4	0.35±0.06
Wet-Black Clays	3	0.0-0.1	0.03±0.04
Decomposed Older Basaltic Clay	3	0.3	0.30
Creyish Clay	2	0.1-0.2	0.15±0.07
Decomposed (Weathered)	2	0.0	0.00
Top Wash	3	0.00-0.1	0.07±0.06

3.3. Data reduction

3.3.1 Gravity data:

The necessary corrections - drift, latitude and elevation corrections were applied to the gravity field data.

(i) Drift correction:

Each base station having been occupied twice in a sequence of measurement, the drift correction was done assuming a linear variation of metre readings with time. Looping between stations were done within 15 minutes or less, and it was possible that tidal effects were fully incorporated into the instrumental drift curves.

The computations were done with a simple computer programme, using the relation:

$$\Delta g = \pm K \, (\Delta R_{(A)} + \Delta R_{(B)})/2.$$

where:

g = change in gravity value between two base stations A and B;

$\Delta R_{(A)}$ & $\Delta R_{(B)}$ = changes in scale readings of the metre, between the base stations from drift curves;

K = instrument constant;

and the following relation gives the drift rate,

$$\sigma = \frac{(R_{(A)} - R_{(B)}) - (\Delta g/K)}{t_{(B)} - t_{(A)}}$$

where:

σ = drift rate between base A and B;

R_A and R_B = base stations metre reading at detailing;

t_A and t_B = time of observation.

The absolute gravity values at detail stations are then given by the relation:

$$g_s = g_{(A)} + K(R_s - R_A) - \sigma (T_s - T_A)$$

where:

g_s = absolute gravity value at a detailed station, s;

R_s, T_s = scale readings and time of observation at the detail station respectively.

ii. Latitude correction:

The theoretical gravity acceleration, g_ϕ, at sea level is given by the International Gravity formulae for 1973, thus:

$$g_\phi = 978031.85\ (1 + 0.0053024\ \sin^2\phi - 0.0000059\ \sin^2 2\phi)$$

where:

ϕ = Latitude

The computation was made to obtain the difference between the reference spheroid values described by the above formulae, and the actual Geoidal gravity values described by the field measurements.

(iii) Elevation correction:

The free-air correction, $g_{(F.A)}$, was carried out using the relation:

$$g_{(F.A)} = 0.3086\ h\ (mGal)$$

which takes into account the altitude variation between the stations, assuming they are freely suspends in the air; where h is the elevation from sea level in meters. On the other hand, the Bouguer correction, $g_{(B)}$, was made using the relation $g_{(B)} = 0.04188\ \sigma\ h$, (mGal) which takes into account the mass effect of the horizontal slab included between the stations level and a standard datum level (sea level); σ is taken as the 2.67 in 10^3 kg m^{-3} (the average crustal density).

The Bouguer Gravity anomaly was the reduced using a computer programme thus:

$$g_{(B)} = g_{(obs.)} \pm dg_{(\phi)} \pm dg_{(F.A)} \mp dg_{(B)} + dg_{(T)}$$

where:

$g_{(obs.)}$ = observed station reading.

dg_{ϕ} = latitude correction

$dg_{(F.A.)}$ = free air correction

$dg_{(B)}$ = Bouguer correction.

$dg_{(T)}$ = Terrain correction (negligible).

3.3.2. Magnetic data:

The correction for diurnal and possible erratic variations of the geomagnetic field and the changes in the instrument caused by temperature and drift was carried out by plotting drift curves assuming linear variation with time. A simple program was written to reduce the values in the computer.

CHAPTER FOUR

INTERPRETATION TECHNIQUES

4.1 Introduction

The main target of this study is to locate the bedrock surface configuration and its associated cassiterite deposition. The interesting anomalies resulting from smaller or shallower features on the potential field maps are often masked by effects of large scale deep-seated structures. Thus the removal of regionals resulting from deep-seated sources is often done by various anomaly seperation techniques.

Procedures of regional/residual anomaly separation are mainly of two types, either graphically or by numerical application of analytical methods.

In the present study, knowledge of the local geology is utilised in the choice of the techniques.

The inspection of the gravity map revealed the following types of anomalies:

i. sharp anomalies which may be of shallow origin;

ii. anomalies of intermediate dimensions which are probably indicative of interesting geological sources;

iii. large broad anomalies which are of a regional nature.

The anomaly classification in the above manner require the application of various established methods such as smoothing, second derivatives and analytical continuation techniques. On each of the resulting maps, a closure pattern of gravity and / or magnetic field(s) may be regarded as an indication of a distinct geeological structure.

4.2 Resolution of anomalies:

4.2.1 Removal of regionals and residuals by graphical and visual smoothing:

Removal of the regional anomaly will leave us with the superficial effects (residual anomalies). In the area of study, these residual anomalies may be due to the varying thicknesses of the top basalt layer and other sub-basalt layers.

Assuming a thin or uniform horizontal hard basalt layer, the sub-basalt bed-rock surface configuration of the area could be more apparent on the observed gravity residual map.

Graphical and visual smoothing techniques were employed due to the nature of the available map (fig. 5.1). Two trends may be recognised on this map:

(1) a general strike direction NE - SW parallel to the profiles (64 - 96).

ii. another strike, NNW - SSE, direction perpendicular to the profiles (100 - 120).

Consequently, the simple visual smoothing process was not quite effective when applied to the data. Profiles plotted on the lines perpendicular to the strike directions were used to reduce the regionals in each case as a two-dimensional graphical smoothing (Telford, et al, 1980), (figs. 5.1.1(a)).

Fig. 5.1.1.(b) and the resulting residual map (not shown) was obtained by a straight forward graphical smoothing - by plotting and recognising a general regional trend on each principal profile.

4.2.2. Analytical methods:

These methods involved using a grid of Bouguer gravity and Total field magnetic values observed on the surface. A 50 x 56 point values of the acquired gravity and magnetic data at corners of a squared mesh of 15.24 m. spacing were digitised from the Bouguer gravity and vertical field magnetic maps of fig. 5.1. and 5.2 respectively.

(a) Second vertical derivative computation and mapping

The Second Vertical Derivative is a measure of curvature of the gravity field. When Laplace equation is applied to any potential field,

$$\frac{\delta^2 U}{\delta x^2} + \frac{\delta^2 U}{\delta y^2} + \frac{\delta^2 U}{\delta z^2} = 0$$

the second vertical derivative is the partial derivative w.r.t. vertical, that is

$$\left(- \frac{\delta^2 U}{\delta x^2} \right),$$ (Rosenbach, 1953).

Details of the theoretical principles and application of such technique are documented in Evjen (1936), Peters ((1949), Henderson and Sietz (1949a), Elkins (1951), Nettleton (1954), Steiner (1963), and others.

Second vertical derivative formulas are generally in the form:

$$Vzz = \frac{C}{s^2} (W_o V_o + W_1 V_1 + W_2 V_2 + \ldots . + W_n V_n)$$

where:

Vzz	=	second vertical derivative or residual at the point of calculation.
C	=	constant for particular system.
s	=	Grid spacing.
Wo,W1,W2, ...	=	weighing factors (positive or negative)
Vo	=	gravity or magnetic at the point of calculation and
V1, V2, ...	=	average field values around successive circles.

The method involves the calculation of the averages of gravity/magnetic values on concentric circles of successive radii S, S $\sqrt{2}$, S $\sqrt{5}$, ..., etc. These averages are multiplied by certain numerical weighing coefficients. Such coefficients may be considered to provide linear filtering process applied to the original map.

The Rosenbach's working formulae used in the present work have the following form:

$$Vzz = \frac{1}{24s^2}\left[96(V_0) - 18\sum_{i=1}^{4} Vi\,(s) - 8\sum_{i=1}^{4} Vi(s\sqrt{2}) + \sum_{i=1}^{8} Vi(s\sqrt{5})\right]$$

The choice of weighing factors depends on the preference of the interpreter and the nature of the data (Dobrin, 1977). The summation of all the weighing coefficients of the general equation (Vzz) is always equal to zero, and the resulting map shows positive and negative anomalies equally likely. In general, reversed polarities in a second derivative map are not all attributed to a specific structural origin. Fictitious anomalies are not uncommon in such maps (Roy, 1961). Moreover, the dimension of grid spacing plays an important role. Calculations with smaller grid spacing may accommodate smaller details, while those carried out with larger spacing may reflect

the effect of larger features.

(b) The analytical downward continuation:

The continuation of a certain potential field, is the process of measuring the field at a higher or lower levels (upward or downward continuation respectively). Computation at such a level of continuation is possible in principle if there is no disturbing body within the range of continuation.

Downward continuation is applied for anomaly separation, such as **resolution**of overlapping effects of sources close together. If two separate but nearly sources are under homogenous overlying material, the downward continuation could be made to a level closely above the sources where the effect would be clearly separated whereas they would be confused by overlap at the level of measurement. Continued field to depths greater than the source will begin to oscilate (Nettleton, 1971), and we use this as depth criterion.

The importance of continuation methods as well as its interpretation usefulness have been documented (Hammer, 1947; Evjin, 1936; Haug's, 1942; Bullard and Cooper, 1948; Henderson and Sietz, 1949; Peters, 1949; Trejo, 1953; Henderson, 1960; and Constantinescu, 1961). Peters, 1949, proposed that downward continuation can be used to determine the shapes of interfaces between uniformly but differently magnetized media.

In this work, we have applied Constantinescu's formulae (1961), which used the Laplace equation in cylinderical co-ordinates system by the approximation of Fourier-Bessel function.

Constantinescu (1961), pointed out that the potential and its derivative in a space free from sources are continuous and the gravity/magnetic values at depth Z = -d can be represented by a Maclaurin's series. On the other hand, the vertical derivatives of various orders can be obtained by successive derivation of Laplace's equation in the approximation of Fourier-Bessel function. Constantinescu's (1961), working formulae using two concentric circles having radii, d and $(d\sqrt{2})$ has the form:

$$V_{(-d)} = 8.395745 \left[V_{(o)} + 6.9041 \; Vi(d) - 4.517417 \; Vi(d\sqrt{2}) \right]$$

where:

$$Co = + 8.395745$$

$$C1 = + 6.9041 \quad \text{and}$$

$$C2 = - 4.517417.$$

It must be pointed out that the vertical components of the total magnetic field, ΔZ, are used in continuation methods. The inclination of magnetisation in the magnetised body (in this case, the basaltic layer), has been tested by a simple rule of

thumb (Sharma, 1976), on the data and ΔZ component obtained from the Total field, thus:

$$\Delta Z = \Delta T \sin I$$

where: I = inclination of the magnetic field.

Computations involving the above analytical methods were done using Computer Programmes (Award, personal communication) modified and adapted for the present work.

4.3 Gravity stripping technique:

In principle, the gravity layer stripping technique is used to extend gravity interpretation to deeper horizons. By calculating and subtracting the gravity effects of overlying strata whose structure and density relations become known in detail from shallower development, deep prospect horizons are uncovered (Hammer, 1963).

Combined stratigraphic and density informations from shallow development holes defines the mass anomalies in the upper strata.

Hammer (1963), pointed out that gravity features seen on the surface datum level after subtracting known shallower subsurface gravitional influences to clarify the gravity picture of deeper structure, defines "deeper gravity anomaly". In other words, the gravity stripping technique expresses the portion of gravity anomalies originating below the stripping datum as

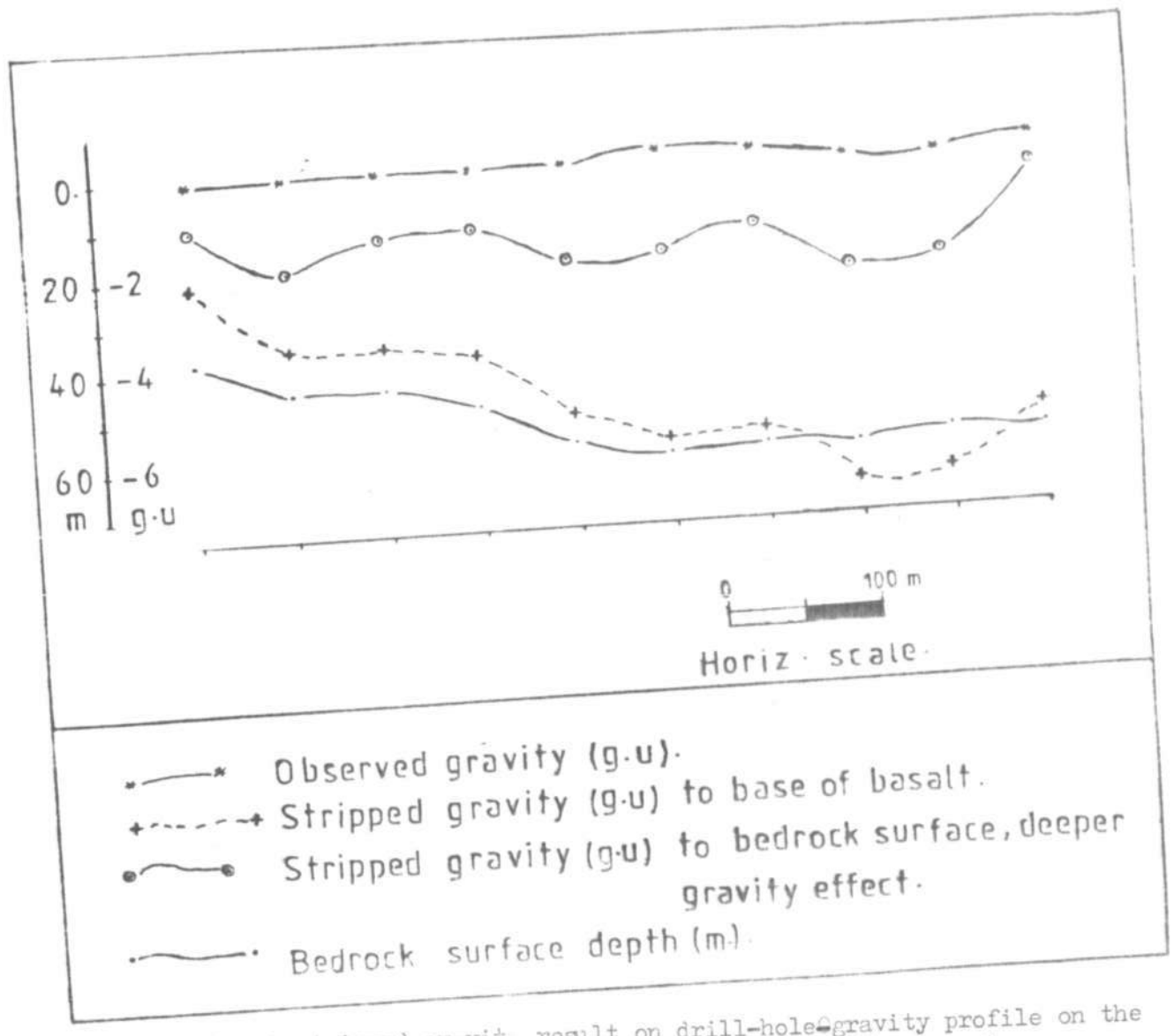


Fig. 4.2.1. A stripped gravity result on drill-hole gravity profile on the N'Gell basalt. (adapted after Ajakaiye, et al, 1975).

mapped on the surface.

We have employed this technique in this study because of the need to determine the approximate depth to bedrock and the removal of the unwanted effect of the basaltic layer from gravity data acquired on the surface. Moreover, the idea of depth approximation to bedrock is reflected in the stripped data since the stripping to the bedrock surface makes the data oscilate (fig. 4.2.1).

Two basic assumptions are made in the use of this technique (Hammer, 1963):

i. available test drillings carried out to various moderate depths to define subsurface structures and formation-thicknesses.

ii. available (well defined) density relations of the various strata.

In this study, these conditions are however, partially met. Few borehole profiles are available in the study sites although the sub-basalt borizons and structures are well defined. The density informations from the different drill-holes are insufficient for accurate computations covering the unknown part of the study area.

The gravity "stripping correction datum" in this study is taken as the base of the basaltic layer which may not necessarily be horizontal.

Calculations of the gravity effects of the various density strata are carried out separately by standard techniques (Hammer, 1963). Usually, except in the case of very steep dips, the infinite flat plate approximation is considered adequate. In this study, computation was performed at each gravity station in a two-dimensional array of the surface survey by use of a gravity program (Nagy, 1964; Ojo, personal communication) modified and adapted to the present work. The calculations give gravity differences in terms of density contrasts referred to the surface stratum which therefore, has zero effect (Hammer, 1963).

4.4 Depth estimates:

4.4.1 Basement depths:

Basement depth calculations are discussed in Nettleton (1975), Bullard and Cooper (1948), and in Bott and Smith (1958, 60, 61).

We have applied Bott and Smith's technique and made use of the information available from boreholes drilled in the area.

Bott and Smith introduced several formulae for rapid estimation of maximum possible depth to the top of gravitating body. The maximum depth (h) corresponding to the maximum observed anomaly $(\delta g)max'$ and its corresponding gradient

$\left|\frac{\delta g}{\delta R}\right|_{max.}$ is given by

$$h \leq \frac{3\sqrt{3}}{8} \frac{(\delta g)_{max.}}{\left|\frac{\delta g}{\delta R}\right|_{max.}}$$

or

$$h \leq 0.65 \ \Delta R$$

where:

ΔR = minimum radius of the anomaly closure

This formulae was applied to each of the anomaly closure on the observed residual gravity.

4.4.2 Estimation of fault parameters:

A Bouguer gravity map may include both linear and closed anomalies, which are likely due to structures separated by faults, or lithologic changes in formations.

Three parameters of a fault, namely, the amount of down-throw (T), and the depths to upper and lower surfaces (Z_1 and Z_2) were given by Nettleton (1942), Sharma and Vyas (1970), and Sazhina (1971), see fig. 4.4.1.

The formulae for the vertical attraction of gravity (g) and its horizontal gradient ($\frac{\delta g}{\delta x}$), caused by anomalous escarpment are given by:

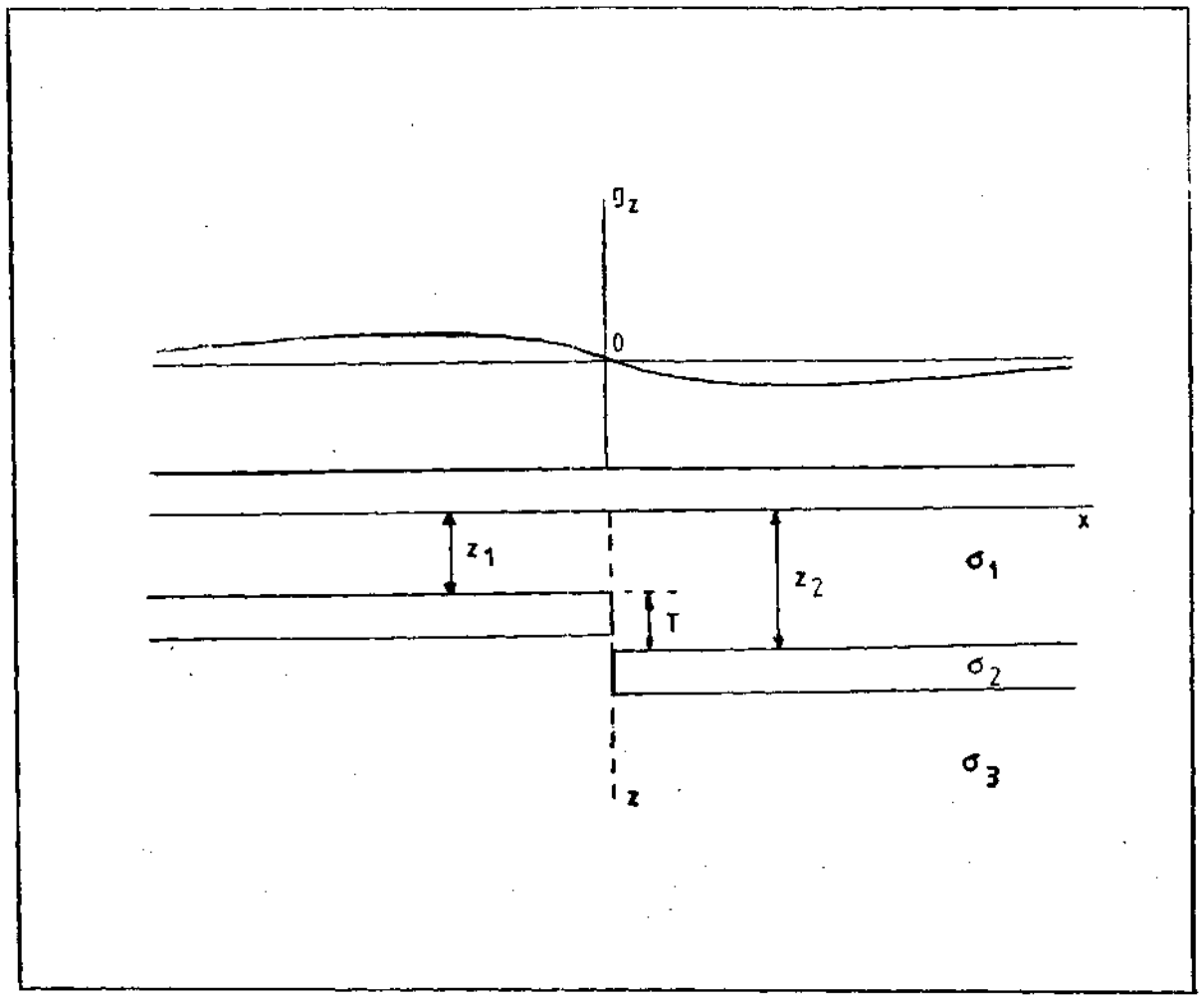


Fig.4·4·1 Gravity effect of a faulted horizontal slab showing parameters.

$$g = \sigma G\left[\pi (Z_2 - Z_1) + 2 Z_2 \operatorname{arctan} \frac{X}{Z_2} - 2 Z_2 \operatorname{arctan} \frac{X}{Z_1} + X \ln \left(\frac{X^2 - Z_2}{X^2 - Z_1^2}\right)^2\right]$$

and,

$$\frac{\delta g}{\delta X} = \sigma G \ln \left(\frac{X^2 - Z_2^2}{X^2 - Z_1^2}\right)$$

when $X = 0$, $g = \sigma G \pi (Z_2 - Z_1)$

$X = \infty$ $g = 2 \sigma G \pi (Z_2 - Z_1)$

$X = -\infty$ $g = 0$.

Using these relations, the values of Z_1 and Z_2 can be determined. Also, since the $(\frac{\delta g}{\delta x})$ - curve shows a maximum at point $X = 0$,

then

$$T = \frac{g_{max.}}{2 \pi G \sigma} = \frac{g_{max.}}{42 \sigma}$$

and $\frac{\delta g}{\delta x} = 2 \sigma G \ln \frac{Z_2}{Z_1}$

Where:

$g_{max.}$ = amplitude of the anomaly associated with the fault.

σ = density contrast of the slab material with the overburden

G = universal gravitational constant.

Semi-infinite horizontal slab approximation:

It is often practical to substitute a vertical prismal body whose width, b, is very great to a semi-infite horizontal slab. The gravity effect, g, for a semi-infinite horizontal slab is given (Telford, et al, 1980) by

$$g = 4.07 \times 10^{-3} \sigma \left\{ \frac{x}{2} \log \left(\frac{D^2 - x^2}{d^2 + x^2} \right) + D \left(\pi/2 + \tan^{-1} (x / D) \right) \right\} - d \left\{ \pi/2 + \tan^{-1} (x/d) \right\}$$

Where:

x = horizontal distance along profile from origin.

d = depth to the top of the body, and

D = depth to the bottom.

σ = density contrast with the surrounding

$$g_{max} = g_{+\infty} - g_{-\infty}$$

$$= 4.07 \times 10^{-3} \sigma \pi (D-d)$$

also, differentiating, w.r.t. x at origin, we have,

$$\left(\frac{dg}{dx}\right)_{x=0} = 4.07 \times 10^{-3} \sigma \log \left(\frac{D}{d}\right)$$

$$(D-d) = g_{max} / 12.77 \times 10^{-3}$$

$$\log\ (D/d) = \frac{1}{4.07 \times 10^{-3}\ \sigma} \left(\frac{dx}{dg}\right)_{X=0}$$

From these relations, we can find D and d assuming a density contrast, σ . See fig. 4.4.2.

From the Bouguer correction given in chapter three of this study, and the above effect of a semi-infinite horizontal slab, we can have some idea of the magnitude of a sudden change in overburden thickness. Thus, from the above relations,

when (d=0), the slab outcrops, we have

$$g_{max} = 12.77 \times 10^{-3}\ \sigma\ D \quad (\text{m Gal/ft}).$$

or $g_{max} = 0.04188$ (mGal/m)

wher :

σ = density contrast with the overburden

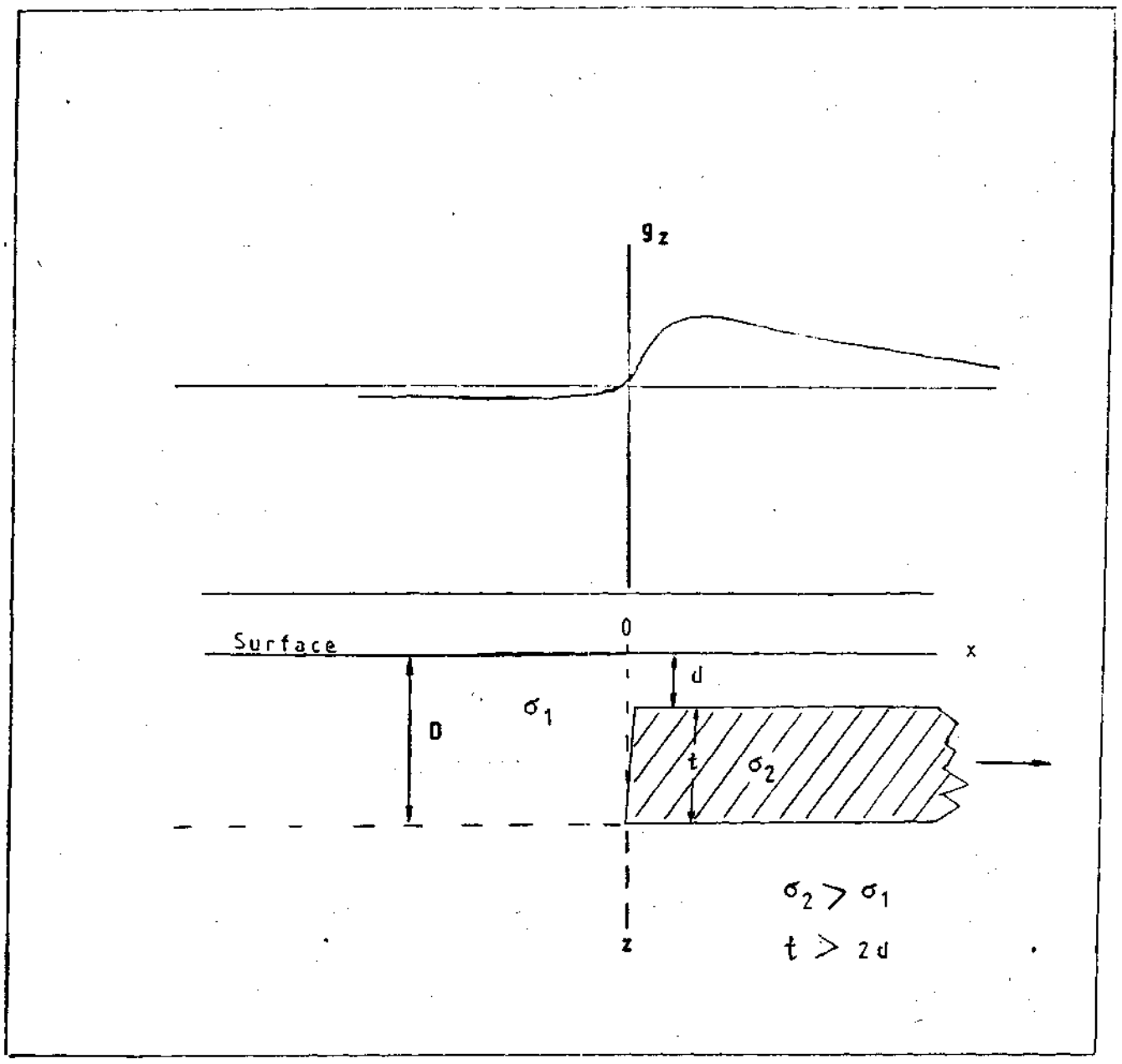


Fig.4.4.2 Gravity effect of a semi-infinite thick horizontal slab showing parameters.

CHAPTER FIVE

QUALITATIVE AND QUANTITATIVE INTERPRETATIONS OF THE DATA

1 Qualitative Interpretation.

5.1 Features of the Bouguer gravity and its related components:

The Bouguer anamaly (map) of the area (fig.5.1) has negative values ranging from - 78.0 to - 85.2 mGal. Three gravity belts are identified and marked on the map by probable structural boundaries as follows:

(a) - the north-western belt (A) characterised by relatively lower negative gravity and a NNW - SSE strike.

(b) - the middle belt (B) with highly negative Bouguer ranging from - 80.5 to -85.2 mGal. in a linear trend (NE - SW). (The gravity high (-80.5 mGal) is along line 88).

(c) - the South-eastern belt (c) whose boundary with belt (B) is almost along line 80, with a strike of NNW-SSE direction. These zones and their closures are delineated considering attitude, behaviour and configuration of the contour lines.

5.1.1 The regional anomaly:

Both the regional gravity data of fig 5.1.1 (a) obtained from two-dimensional graphical filtering and that of fig. 5.1.1 (b) from visual smoothing, have a

general trend of about N20°E.

Both maps have values ranging from -79.0 mGal in the Western corner to about -82.9 mGal at the eastern corner of the area. Both trials are acceptable since their trends are observed to follow the structural trend of the Central Ring structure (Jos-Bukuru complex). Their values indicate a "drag" of larger negative Bouguer gravity component towards the Central Plateau.

5.1.2 The residual anomaly:

The residual gravity map of fig. 5.1.2 obtained from graphical filtering is characterised by major and minor anomalies.

(a) The major anomalies:

The major anomaly occupies belt (B), striking NE - SW. The anomaly amplitude on this main feature ranges from - 4.4 ± 0.1 to 0.4 ± 0.1 mGal. The possitive high is between two linear gravity lows and form a narrow "nose" of gravity expression.

(b) The minor anomalies:

Minor anomalies closures of amplitude range of 0.2 ± 0.1 to 0.3 ± 0.1 mGal, marked G1, G2,..... G4 occupy belt (A) and those marked G5, G6,....., G9 occupy belt (c) with amplitude range of 0.0 to - 2.4 ± 0.1 mGal.

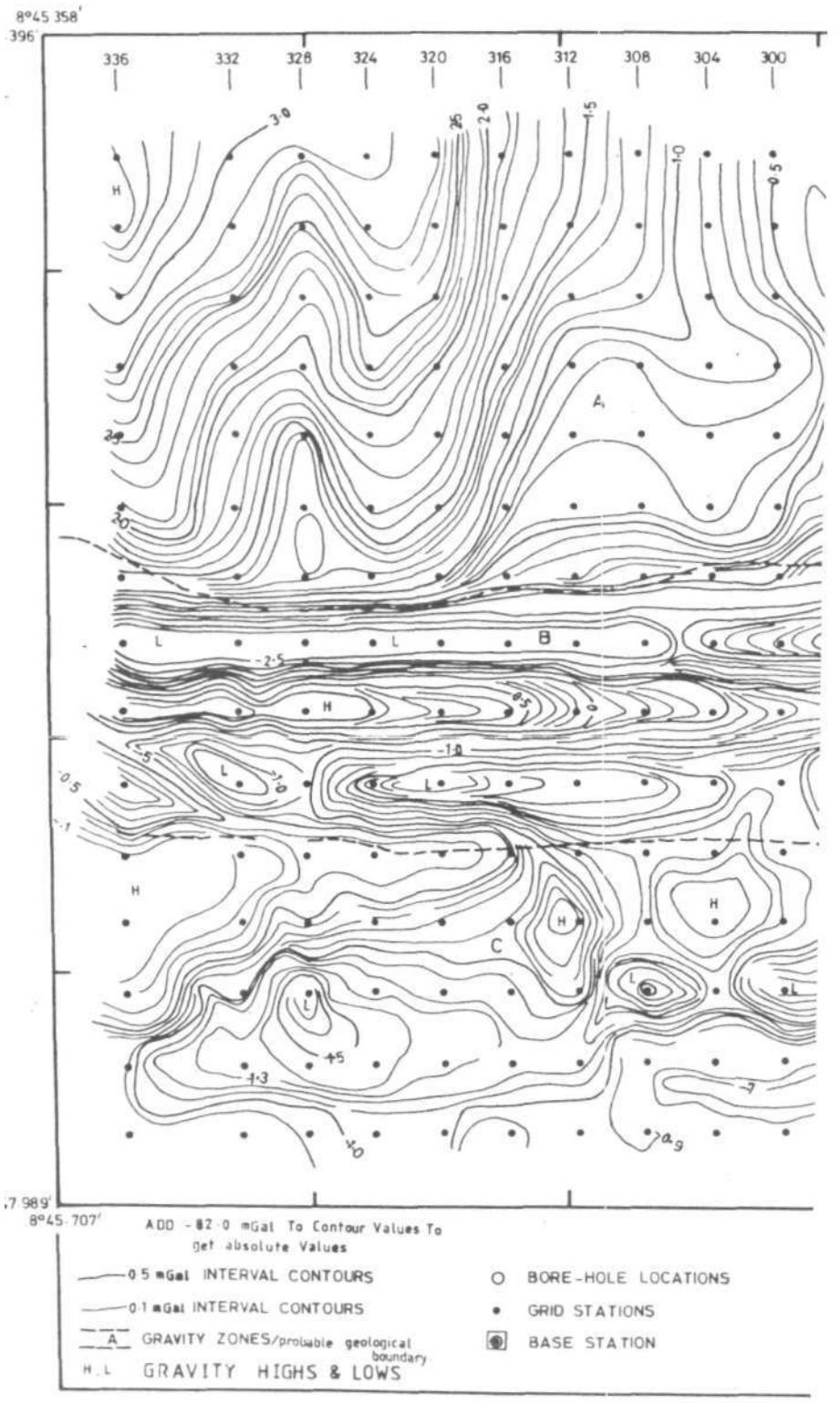


Fig. 5·1 A map showing the Bouguer of the study area.

The major anomaly of belt (B) is considered to indicate either a linear tectonic feature with structural boundaries, and/or accumulation of sediments (fluvio-marine/fluvio-volcanic/estuarine and/or lacustrine) in some huge amount filling the ancient river and its channels, and by compaction following the thick basaltic cover, became of slightly higher density than the underlying materials. Of course, the mixing made during structural and sedimentological settings could be a third probability. The author assumes the third one of the basis of the following:-

1. - gravity high delineation does not appear on the magnetic maps (Total or vertical field intensity) This could mean that this type of gravity high did not arise from fissure-like structure causing a dyke-like basic intrusion for example.

2. - the high gravity middle belt is actually bounded by two lows from its north-western and south-eastern sides respectively. These may be as a result of some fracture zones affecting the old sediments (sub-basalt sediments). This point is some-how in agreement with the vertical magnetic (fig. 5.2) and the downward continued magnetic maps (5.3.2.(e)), which shows some high gradients on both sides.

3. - the degree of density of gravity contours covering the south-western side of the middle belt area is slightly higher than its south-eastern side.

This is in agreement with the interpretation taken along two profiles shown in figs 6.1 (a) and 6.1 (b), which shows that the thickness of the filled sediments is increasing towards the south-western side (down-stream). The contour density most probably obey this feature. Again, the interpretation taken along a reference borehole profile line 288 shown in fig. 6.3(a) confirms the compaction of the sub-basalt sediments.

4. Moreover, this assumption is in fairly well agreement with map of fig. 5.9 (b) which shows that the thickness of the sub-basalt sedimentary unit reaches a maximum of more than 70.0 m. in this belt in comparison with the whole map area.

5.2 Features of the total field and vertical field magnetic data:

The total field magnetic data is shown in fig. 5.2 (a) and the vertical field component in fig. 5.2. The later map was prepared by assuming a magnetic inclination (I) of about 5.5^{o} for the area.

A close study of the total field map reveals an anomaly intensity order of 150 - 900 for the area An intensity order of 700 - 870 occupy much of the middle belt of the area, along 316 -336. (This is also apparent on fig. 5.2 (b)). This anomaly is considered to be indicative of a basaltic langer overlying a thick fluvio-volcanic/or metamorphosed sediments on the

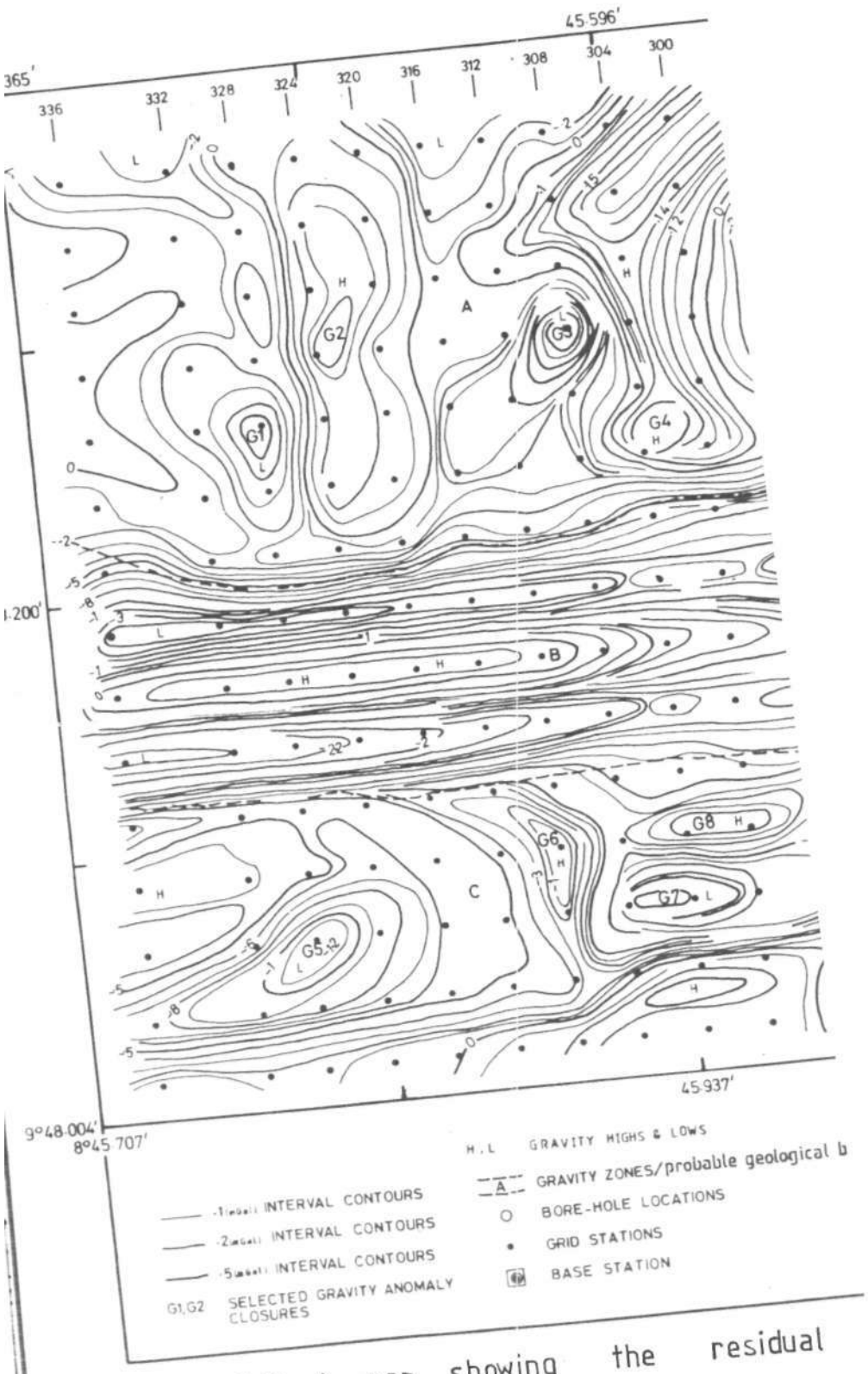


Fig. 5.1.2 A map showing the residual the study Area.

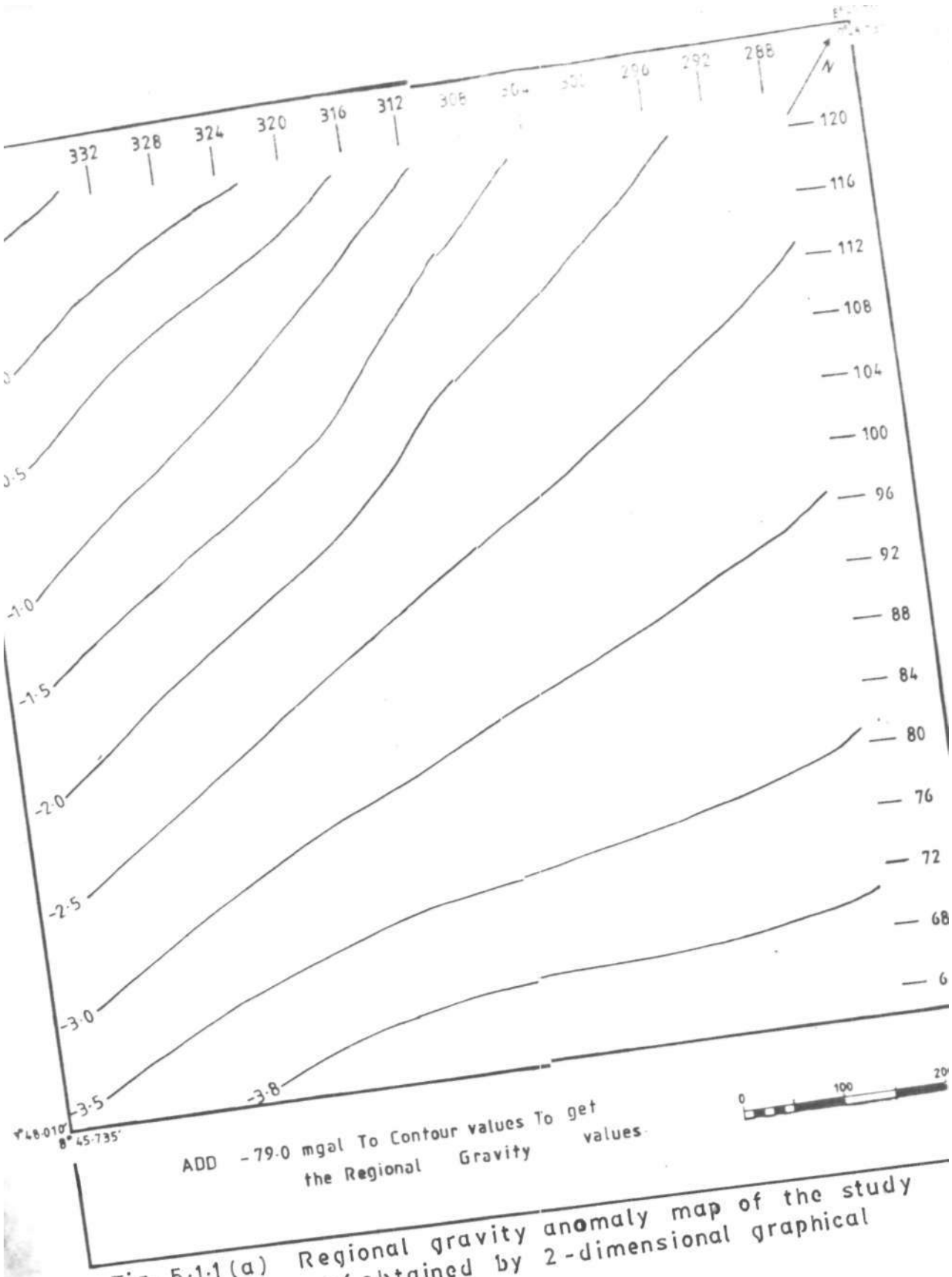


Fig. 5·1·1 (a) Regional gravity anomaly map of the study area (obtained by 2-dimensional graphical smoothing).

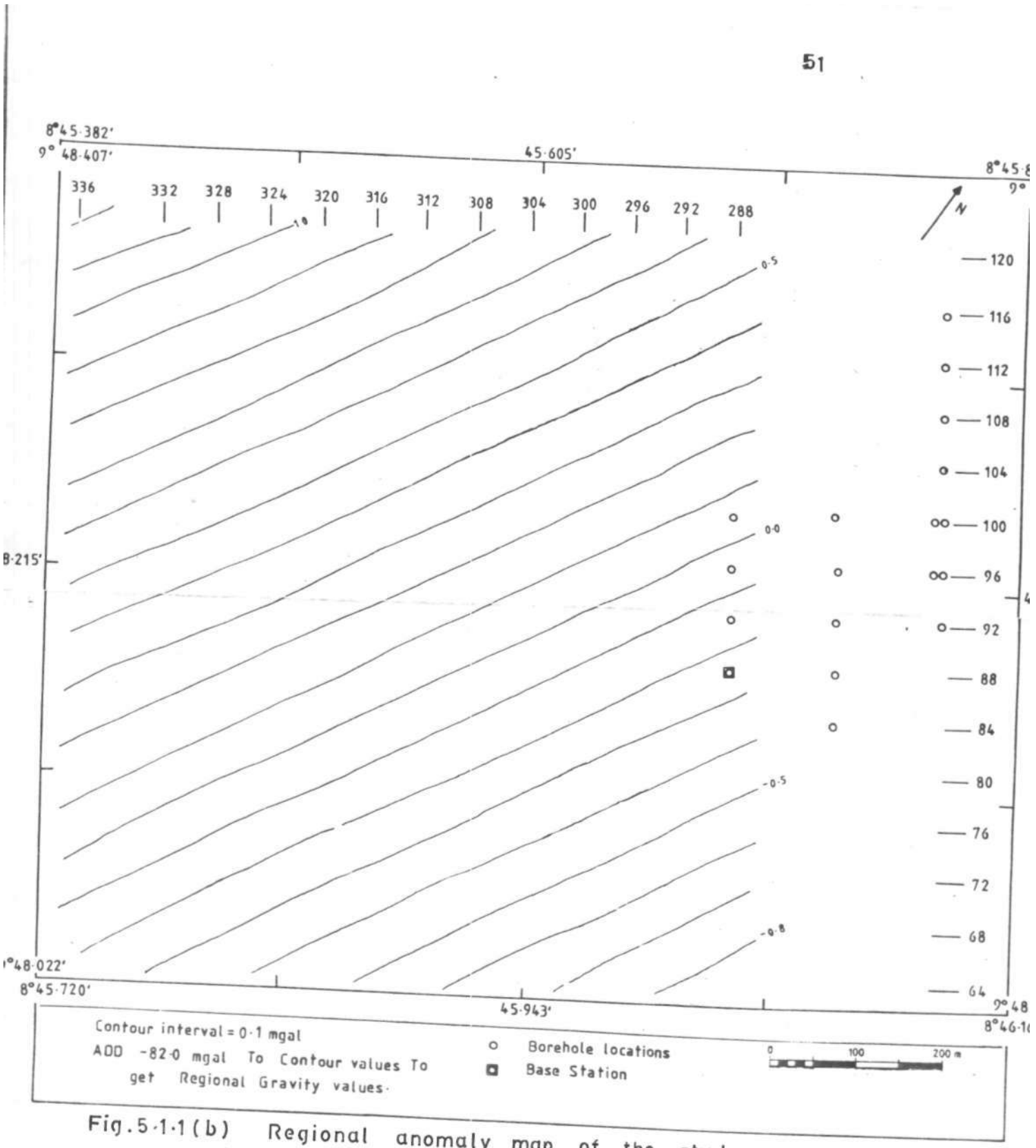
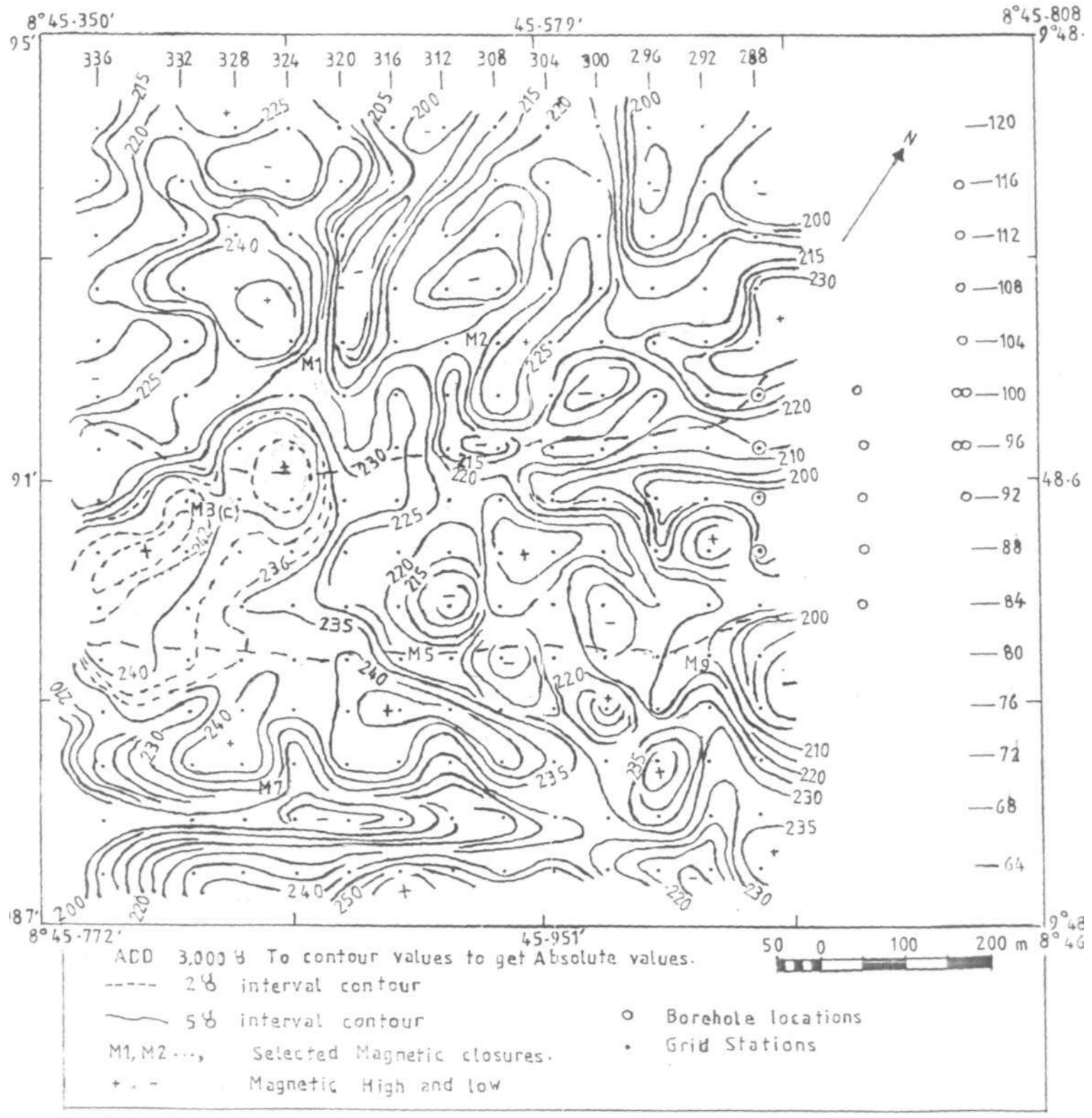


Fig.5·1·1(b) Regional anomaly map of the study area. (obtained by visual smoothing).



Fig· 5·2 A map showing the Vertical field magnetic component of the study area·

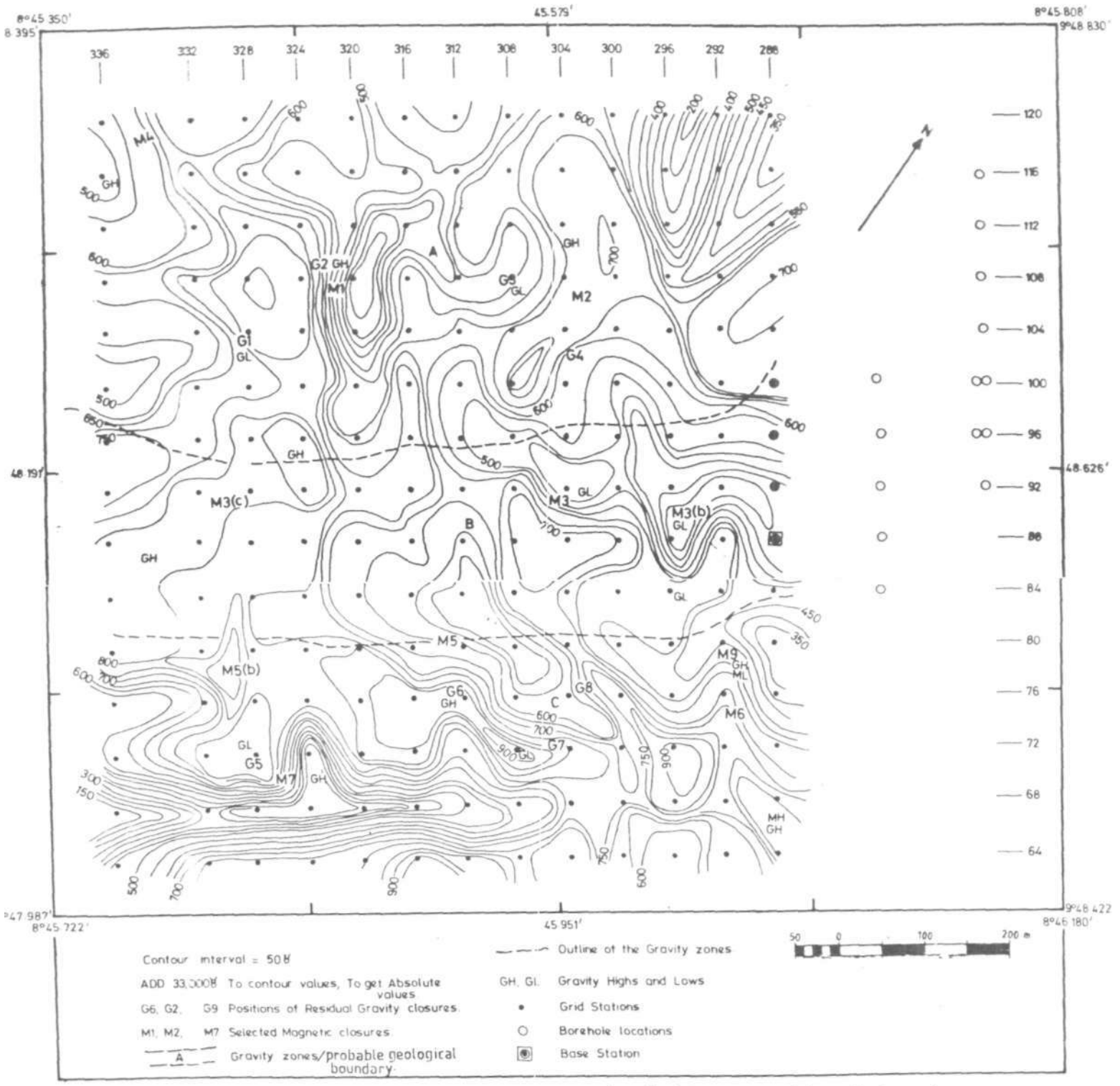
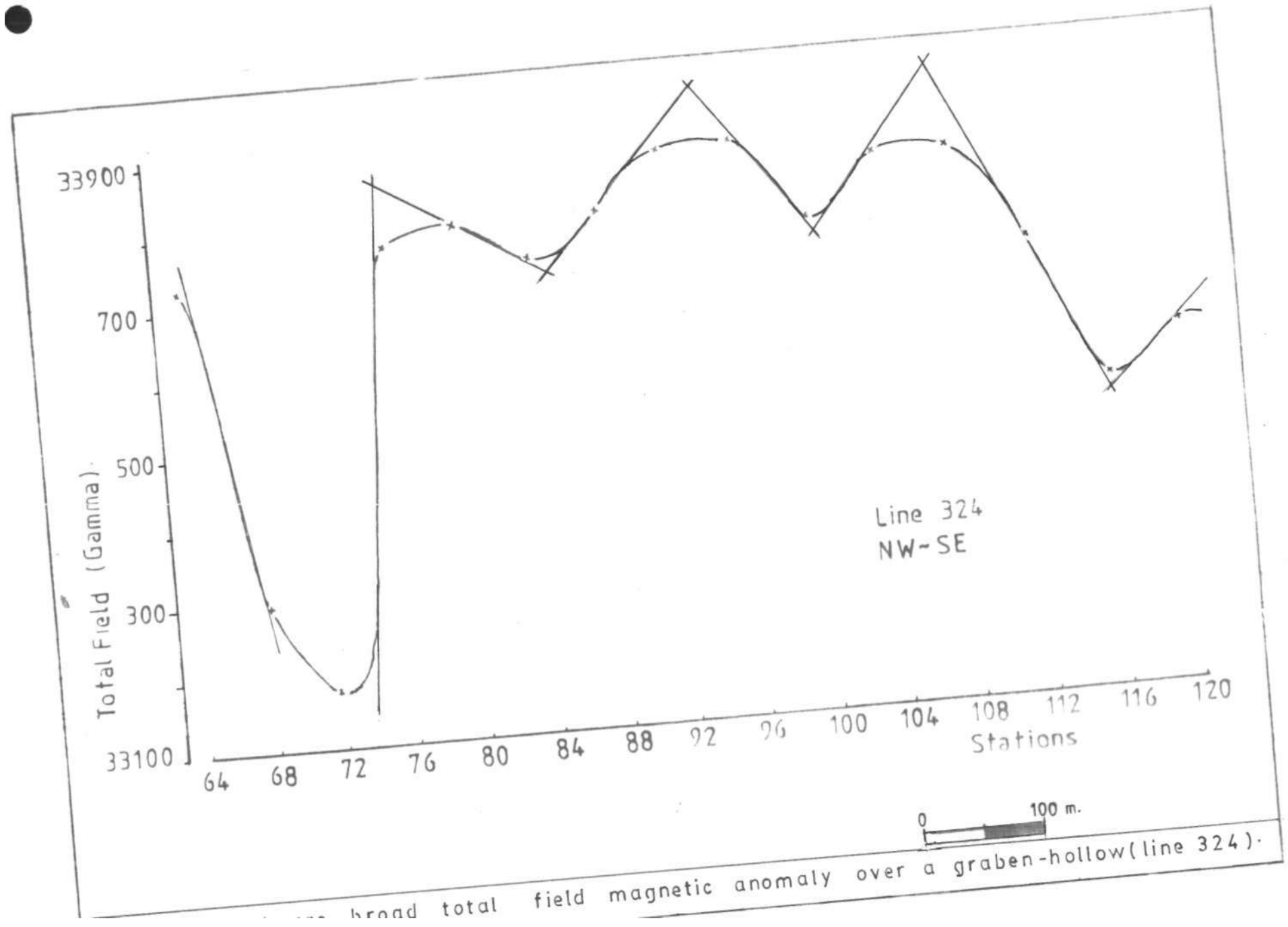


Fig. 5.2 (a) A map showing the Total field magnetic intensity of the study area.



broad total field magnetic anomaly over a graben-hollow (line 324).

paleozoic basement-low (Sazhina and Grushinsky, 1971)

There is no correlation generally between the total field magnetic closures (marked M1, M2, ...M7) and those of the residual gravity (marked G1, G2,...G9) except for the closures marked M1/G2 and M7/G5. This may be because the direction of magnetisation on these two later closures are near horizontal and/or near to the direction of the total field, contrary to other closures.

The vertical field magnetic component, however, compares better with the residual gravity map than the total field.

The lack of one-to-one correspondence observed between the gravity and magnetic closures may be due to a random direction of remanence magnetisation within the basalt.

The vertical magnetic field component also show some high gradient on both sides of a high along line 88 in the middle belt. This is in agreement with the gravity data earlier discussed.

By considering the nature and/or polarity correlation of each corresponding gravity and vertical field magnetic closures (Sazhina and Grushinsky, 1971) some geological interpretations have been compiled in table 5.0 (appendix 1) for the area of study. Informations derived from continuation maps are also utilized in this respect.

5.3 The second vertical derivative and analytical downward continuation data:

Since the approximate depth to the basaltic layer (earlier discussed in chapter 3.), is about 17. m. (overburden depth), and the depth to its base about 36. m; and the approximate depth to our target bedrock is about 61 m., the original Bouguer gravity and the vertical magnetic field maps were therefore digitised at a spacing interval of 15.2 m. (contour interval of Bouguer map is 0.1 mGal and for magnetic map, 10 ϑ) for these analytical methods of computation.

Maps were then constructed for any of the spacings (4 consecutive spacings) approximating to bedrock depth. These spacings are believed to enabled interpretation of structures and sources near to their equivalent depth (in case of analytical downward continuation) or enhancement of local features (in case of derivative data) and hence anomaly features at depths in the unknown area of study.

5.3.1(a) Second derivative gravity data:

The second vertical derivation map constructed from gravity data (fig. 5.3.1.(1) shows that features of the middle part of the area are still consistent with the NE-SW linear trend as has been indicated on the original Bouguer and its residual gravity maps.

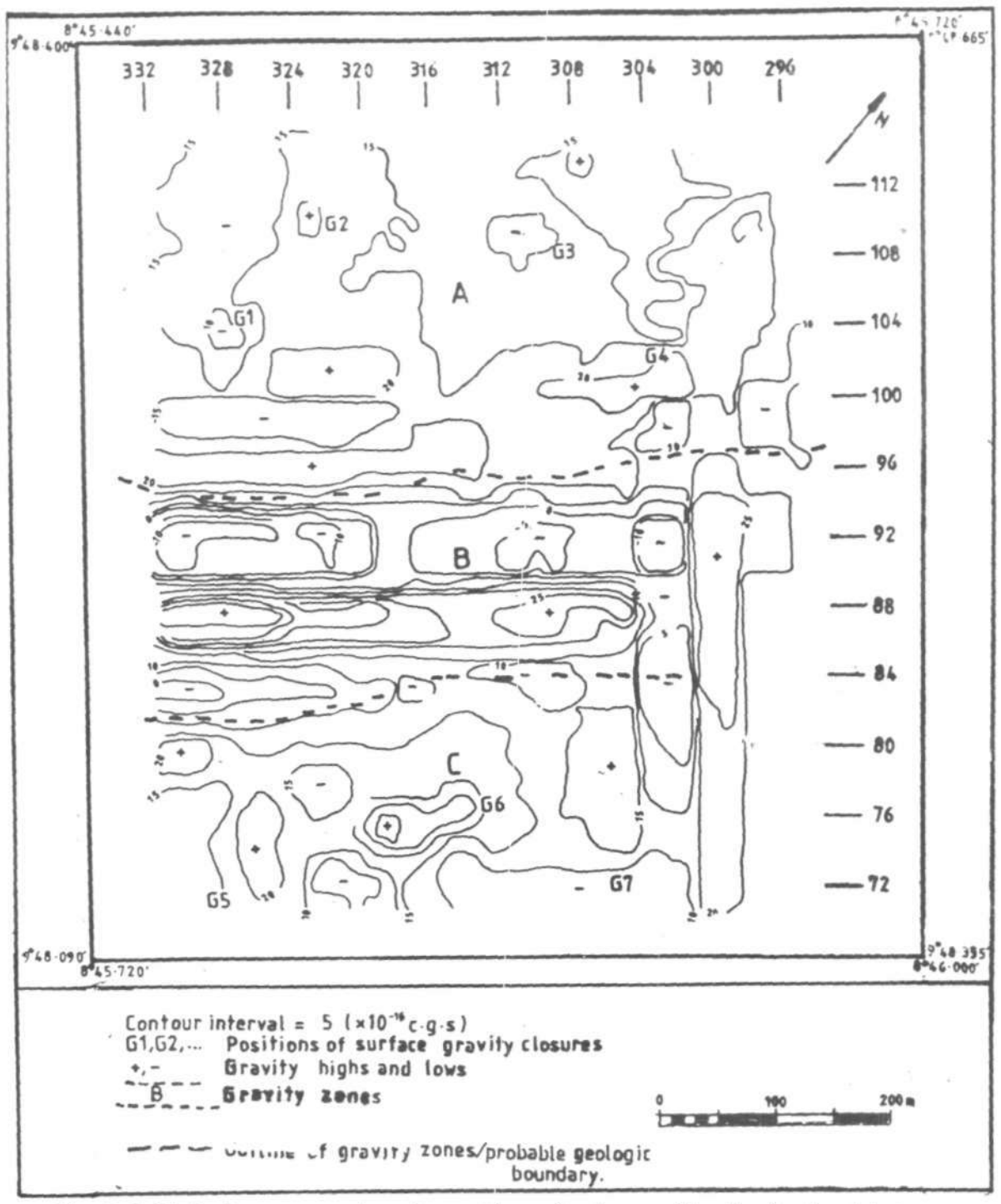


Fig.5·3·1(a) A map showing the 2nd vertical derivative gravity component of the study area (45·7 m spacing) (based on Rosenbach,1953).

These features on this map are considered to originate from lateral variation of lithology within the shallow sub-surface setting, and is indicative of a possible fracture originating from the basement.

Some of the minor gravity closures are not pronounced on the derivative map. A NW-SE linear trend emphasised within the basaltic layer (discussed later for fig. 5.3.2 (a), 15.2 m downward continued data), becomes more prominent.

5.3.1(b) Magnetic derivative data:

The second vertical derivative magnetic map was constructed, as shown in fig. 5.3.1 (b). The prominent expressions of the features on this map are probably indicative of the petrological and/or structural differences within the most upper level of the basement. The variation of the basic property of the basement rock is also of interest. The map has emphasised anomalies marked G2/M1, M3, M3 (b), G6/M5 and G3. These anomalies are indicative of probable variation in magnetic properties of rocks within the subsurface zone more than the structural configuration.

Other anomalies apparent on this map, namely, G5/M7, M5(b) and G1 may have origin from near basement surface.

5.3.2 Features of the analytical downward continuation maps.

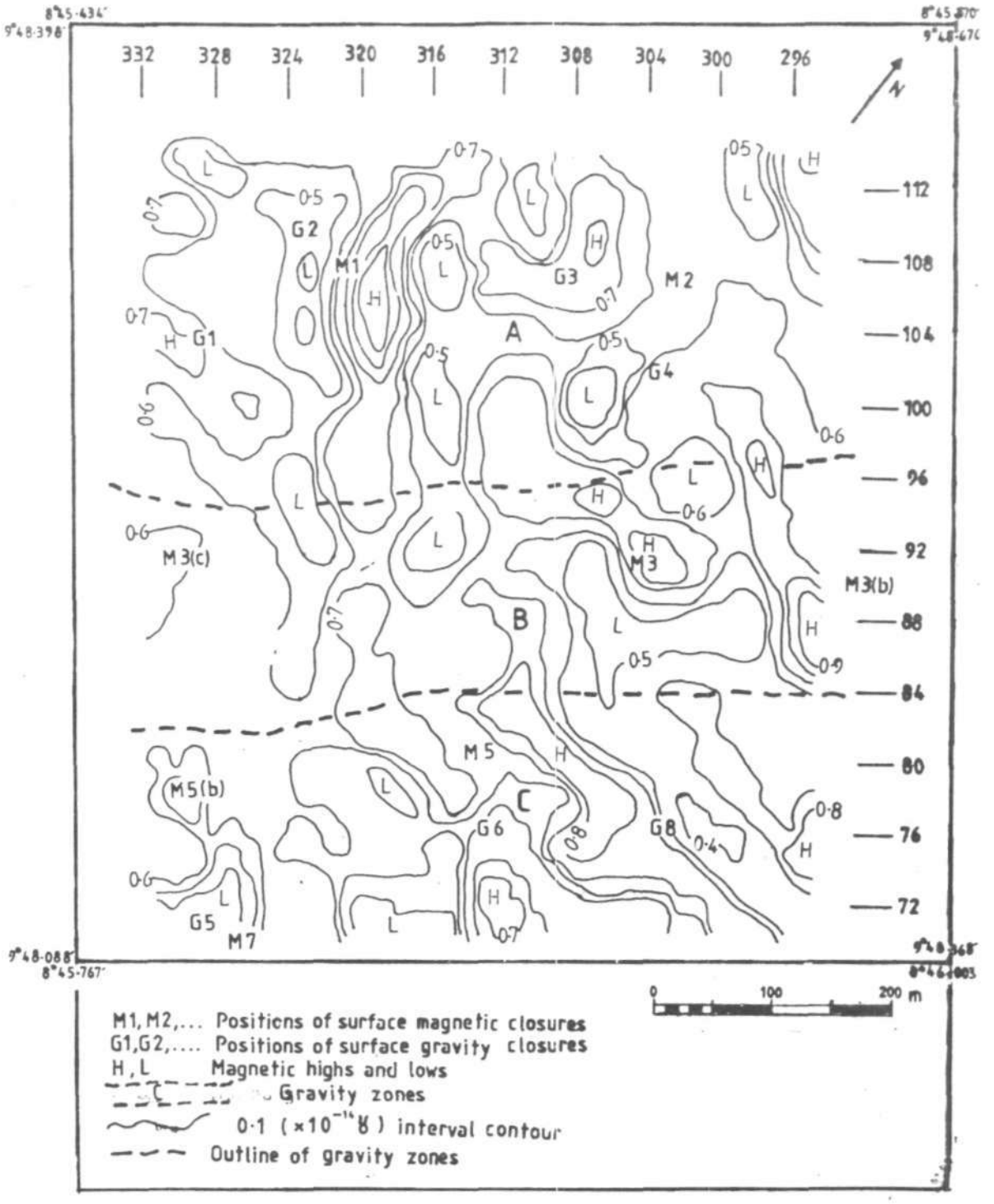


Fig. 5.3.1(b) A map showing the 2nd Vertical Derivative magnetic field of the study Area (45.7m spacing)

(based on Rosenbach, 1953)

5.3.2(a) Gravity continuation data:

Constantinescu's formulae (1961), was used to construct 4 downward continuation maps for spacings 15.2, 30.5, 45.7, and 61 m.

The following observations could be deduced from the maps:

(i) - the belts A, B, and C demarked on the Bouguer residual and second derivative gravity maps could also be delineated on these maps.

(ii) - a NW-SE lineaments persist throughout the 4 continued data (maps) in belt (c).

(iii) - an inspection of figures 5.3.2 (c)-(d) shows the residual closures G1, G2, ..., on these maps. These two continued depths are equivalent to depths below the basaltic layer, and most probably considered to be indicative of the approximate basement surface depths and simply implies an increased oscillation of the potential field.

Belt (A) is also observed to show a relatively less number of small anomalies than belt (c) at 61 m. level. This is believed to be indicative of a higher basement altitude in belt (c), deeper altitude in belt (A), and probably deepest in (B).

Structurally, the downward continued gravity field is considered to show that the study area is affected by possible geotectonic fractures of about (N 42°W) and (N50°E) trends, the former of which is probably related to the instrusion of the basalts within the same period (Recent)as the erruption.

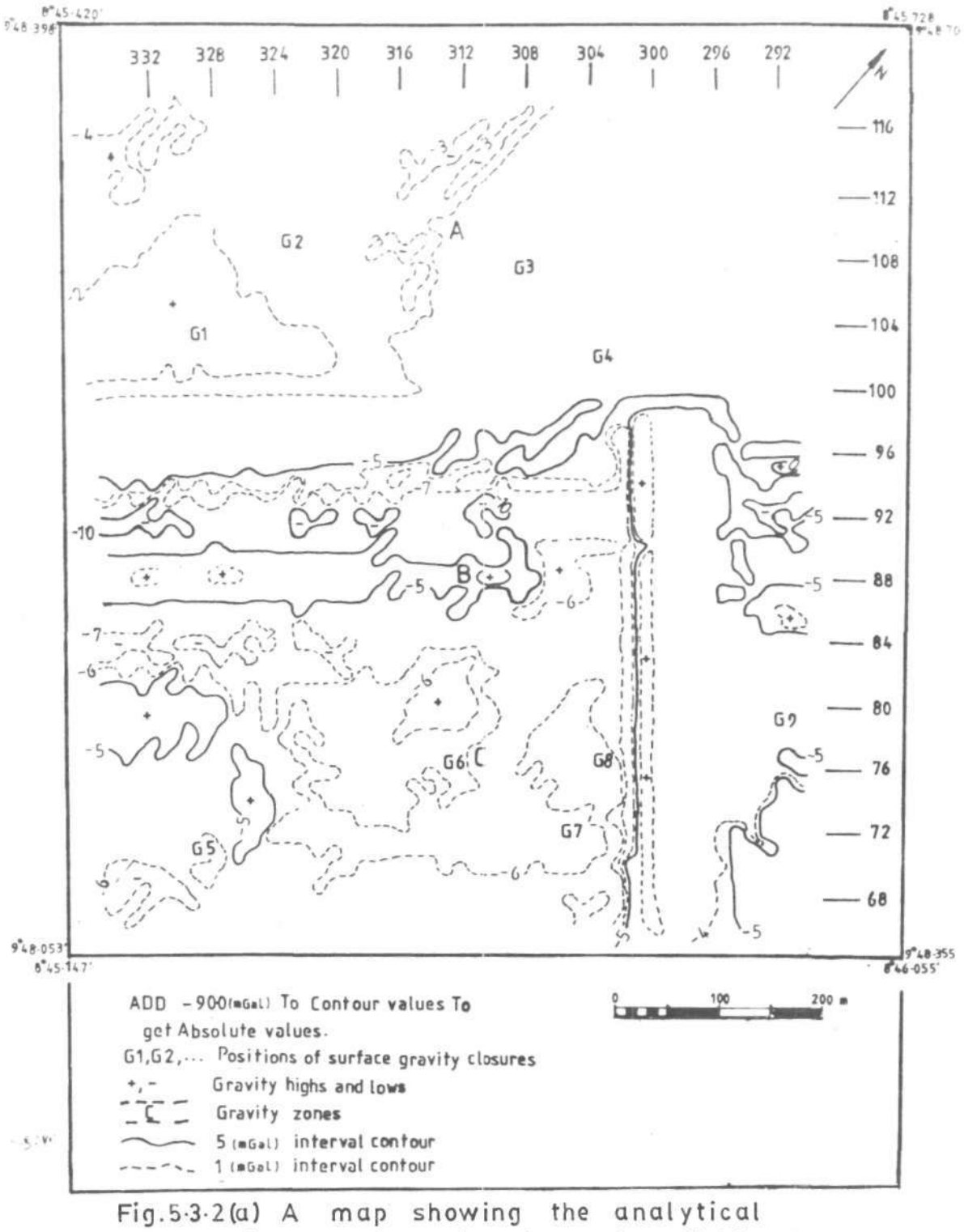


Fig.5·3·2(a) A map showing the analytical downward-continued gravity field of the study area.
(15·2 m. spacing)
(based on Constantinescus', 1961)

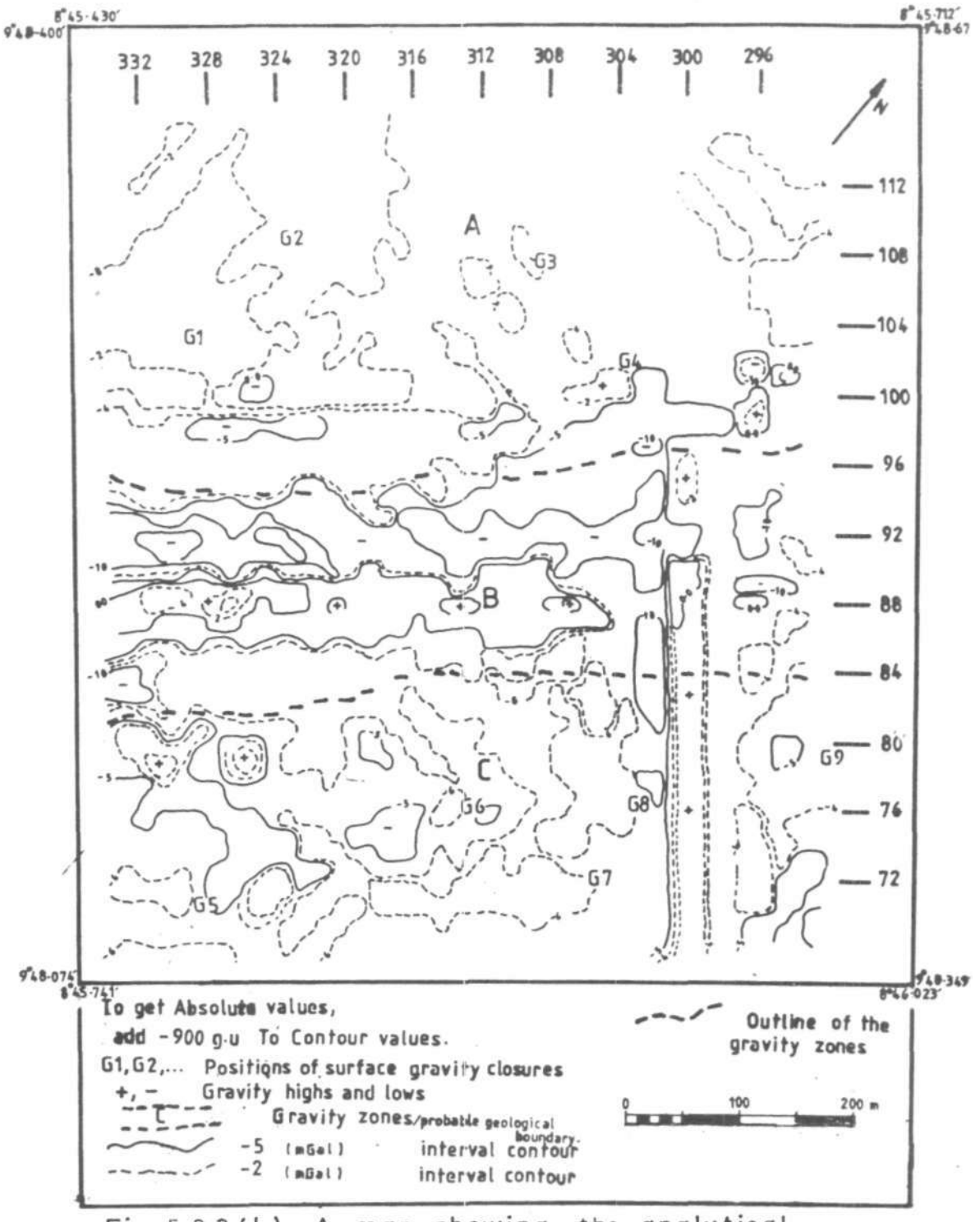


Fig.5·3·2(b) A map showing the analytical downward-continued gravity field of the study area.
(30·5 m. spacing)
(based on Constantinescus', 1961)

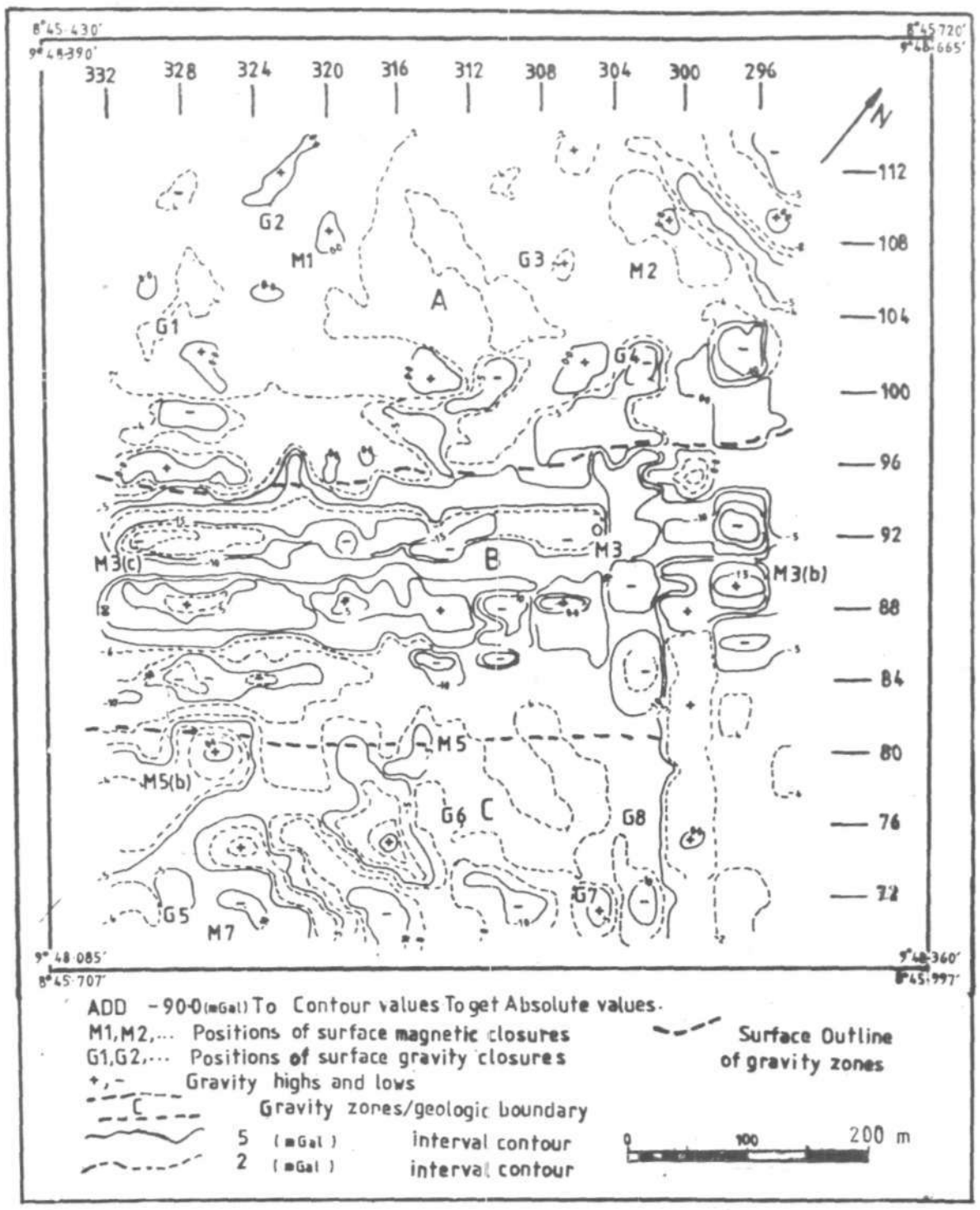


Fig.5.3.2(c) A map showing the analytical downward-continued gravity field of the study Area (45·7m spacing) (based on Constantinescu, 1961)

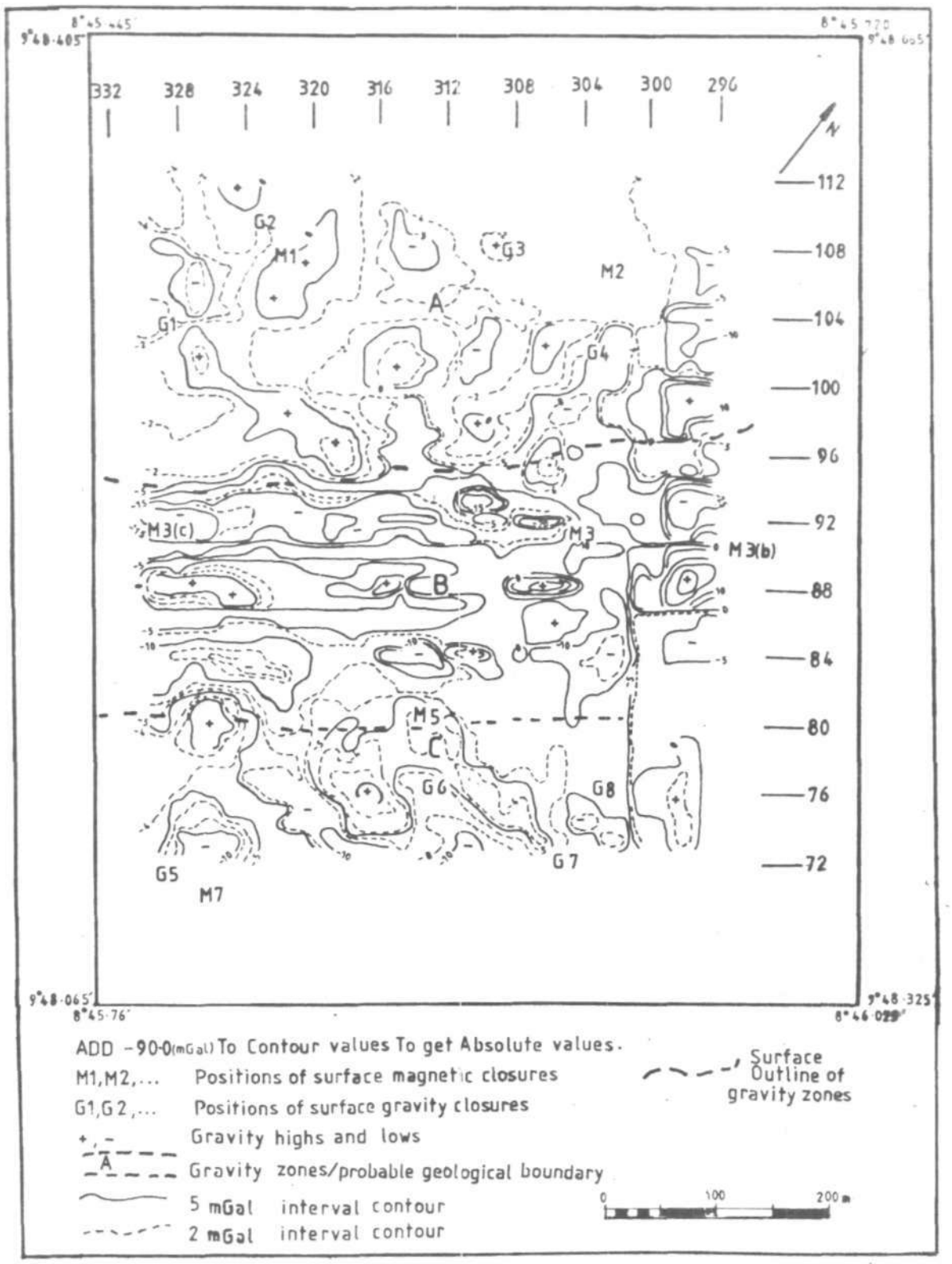


Fig.5·3·2(d) A map showing the analytical downward-continued gravity field of the study area. (61 m. spacing) (based on Constantinescus, 1961)

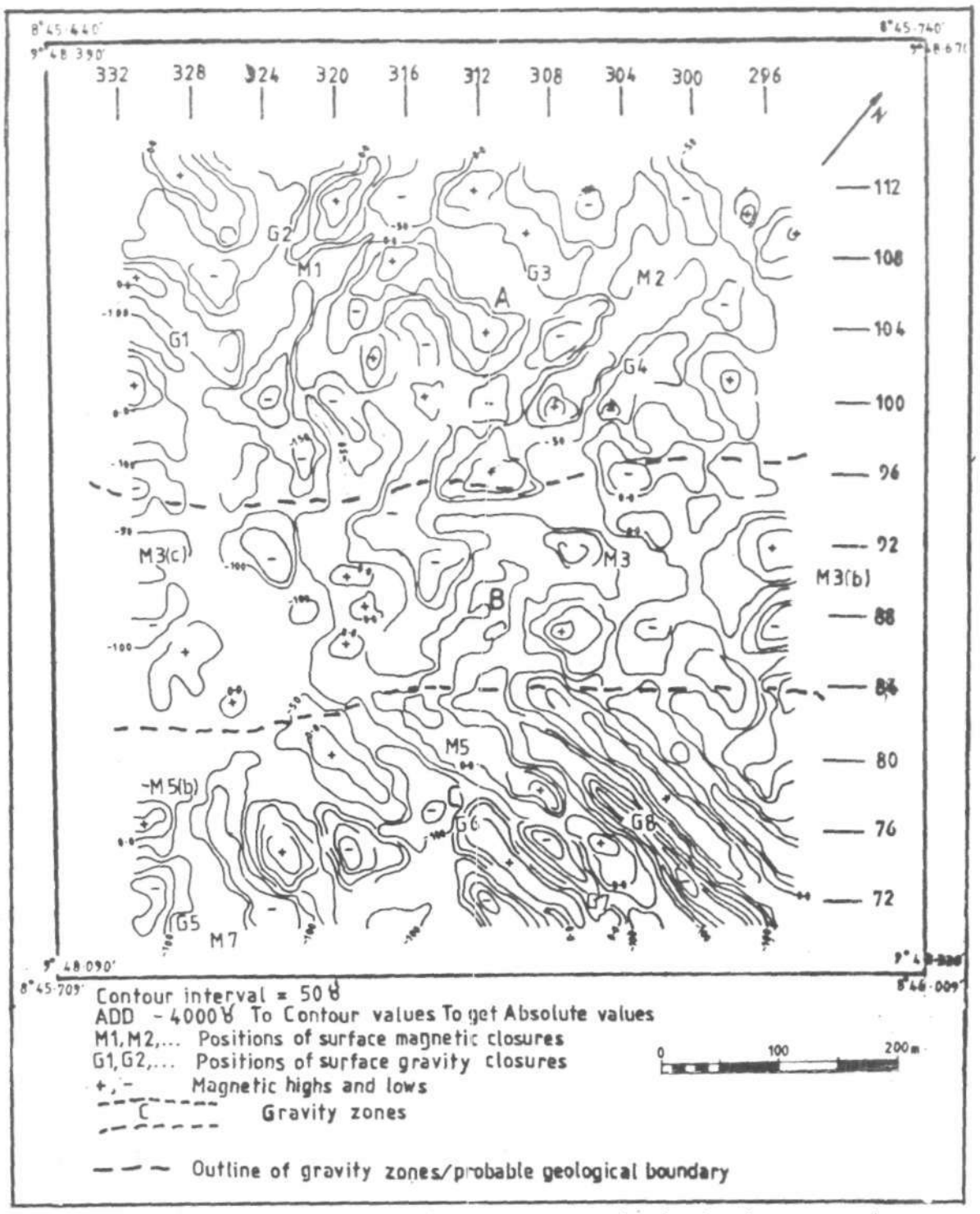


Fig. 5·3·2(e) A map showing the analytical downward-continued magnetic field of the study area. (45·7 m spacing) (based on Constantinescus', 1961)

5.3.2(b) Magnetic downward continued data:

Based on Constantinescu, (1961), analytical down-ward continuation map (fig. 5.3.2 (e) was constructed for the 3rd spacing (45.7 m) of magnetic data.

The following observations could be made from the map:

(i) the three gravity belts earlier discussed are observable.

(ii) a magnetic high is observed as prominent as in the corresponding gravity maps along line 88., and are thought to be indicative of some fractures affecting the sedmiments and the basement.

(iii) the behaviour of the contours in belt (c) (E-W strike contours) indicates that this part of the map is most shallow. This fact is also apparent on the bedrock depth maps (fig 5.9) discussed later.

5.4 Features of the stripped gravity data:

Gravity stripping technique applied in this study was used in an attempt to remove the gravity effect of the basalts from the observed gravity residual data. As earlier mentioned, computations were carried out at each gravity station in a two - dimensional array of the surface survey assuming an infinite flat plate approximation (Hammer, 1963)

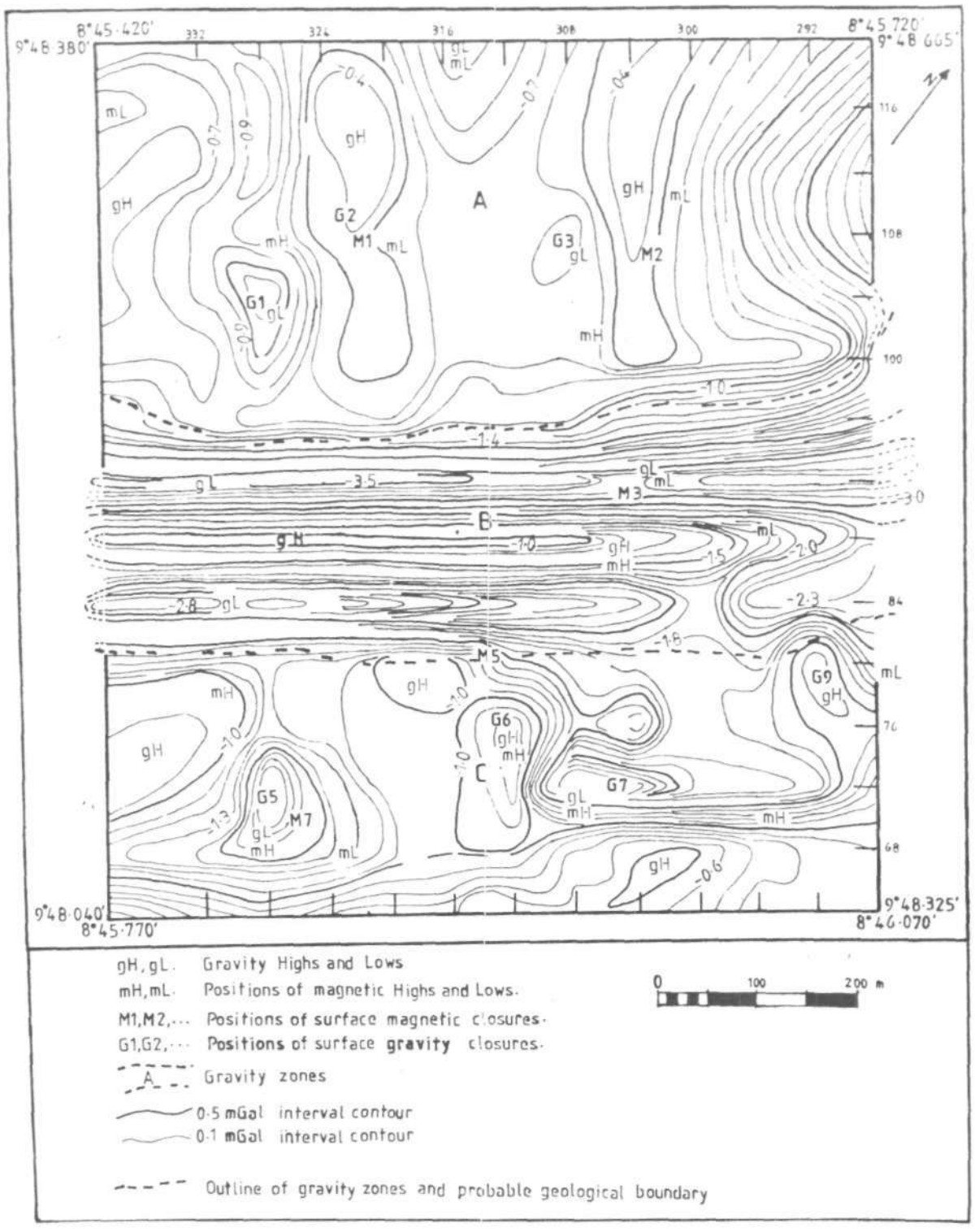


Fig. 5.4 A map showing the stripped gravity anomaly of the study Area (based on Hammer, 1963)

The resulting stripped gravity map is shown in fig. 5.4; and the following points are worth noting concerning the nature of the data:

(i) - the gravity gradient may not change at any point after stripping was applied unless the stripped layers varied in thickness (assuming uniform density). Where the basaltic layer was fairly uniform, the gravity values at points will increase in magnitude and polarity and the characteristic sub-basalt features not changed.

(ii) - below the "strip correction datum" (where we may loose the borehole depth control), the resulting gravity expression is likely to be fairly comparable with a downwardly continued data to the spacing equivalent to depth of the correction datum. If this is correct, we then compare the stripped data with the 45.7 m. spacing continuation of the gravity data.

The above mentioned discussion would allow us to make estimates of the gravitating bedrock depths, and sub-basalt sedimentary thickness as mentioned later.

Comparing fig. 5.4. with the 45.7 m. spacing of gravity downward-continued map (fig. 5.3.2(c)) shows the following:

(i) -in belt (A) of fig 5.4 . , along lines 300, 304 and 308, is a gravity high of 0.3 mGal with a low amplitude of 0.8 mGal at a point marked G3/M2. In the corresponding fig 5.3.2(c) is a dominant positive gravity.

(ii) - there is also a gravity high in belt (A) covered by anomalies G2/M1 along lines 320 and 324 on both figs 5.4 and 5.3.2 (c).

(iii) -the (middle) belt (B), is also dearly comparable on both maps.

(iv) - also the anomalies marked G5/M7, G7 and G8 appear on both maps with change of polarity.

From the above results, there is somehow a general correlation of results of two independent techniques applied which are - the original Bouguer values treated by applying Constantinescu's method, (1961), and the stripped gravity residual data, applying Hammer's method, (1963).

II Quantitative Interpretation

5.5 Gravitating depths:

Depths to bedrock and basaltic layer were estimated using Both and smith's rule on gravity closures, and with the assumption of infinite horizontal slab extension of both basalt and overburden layers on gravity profiles.

(i) Results in table 5.5 (a) (appendix 2.) were first obtained on reference borehole profiles. Density contrast of basalt and overburden clay was taken as 0.99×10^3 kg m^{-3}. Estimate done from gravity and magnetics are shown in (appendix 3). In general, overburden depth from gravity varies within a range of 8.6 - 36.4 m. with an average of 15.8 ± 1 m. Results show that the effective basalt thickness is less for gravity than magnetics probably as a result of insitu weathering of the basalt. Histograms of overburden depths are shown in fig 5.5.

(ii) The gravity depths to basement is in the range of 60.0 - 79.6 m. with an average of 65.0 ± 1 m. (table 5.5 (d), appendix 5).

(iii) Estimates of fault parameters were done assuming a geologic flexure or scarp along profiles 84 - 96. Depths to source ranges from 32.4 m. to 44.5 m. with an average of 38.0 ± 0.4 m. (table 5.5 (e).

(iv) Depth estimates done on stripped gravity data assuming a semi-infinite horizontal slab extension of a sedimentary flat basin, (Tellord; et al, 1980),

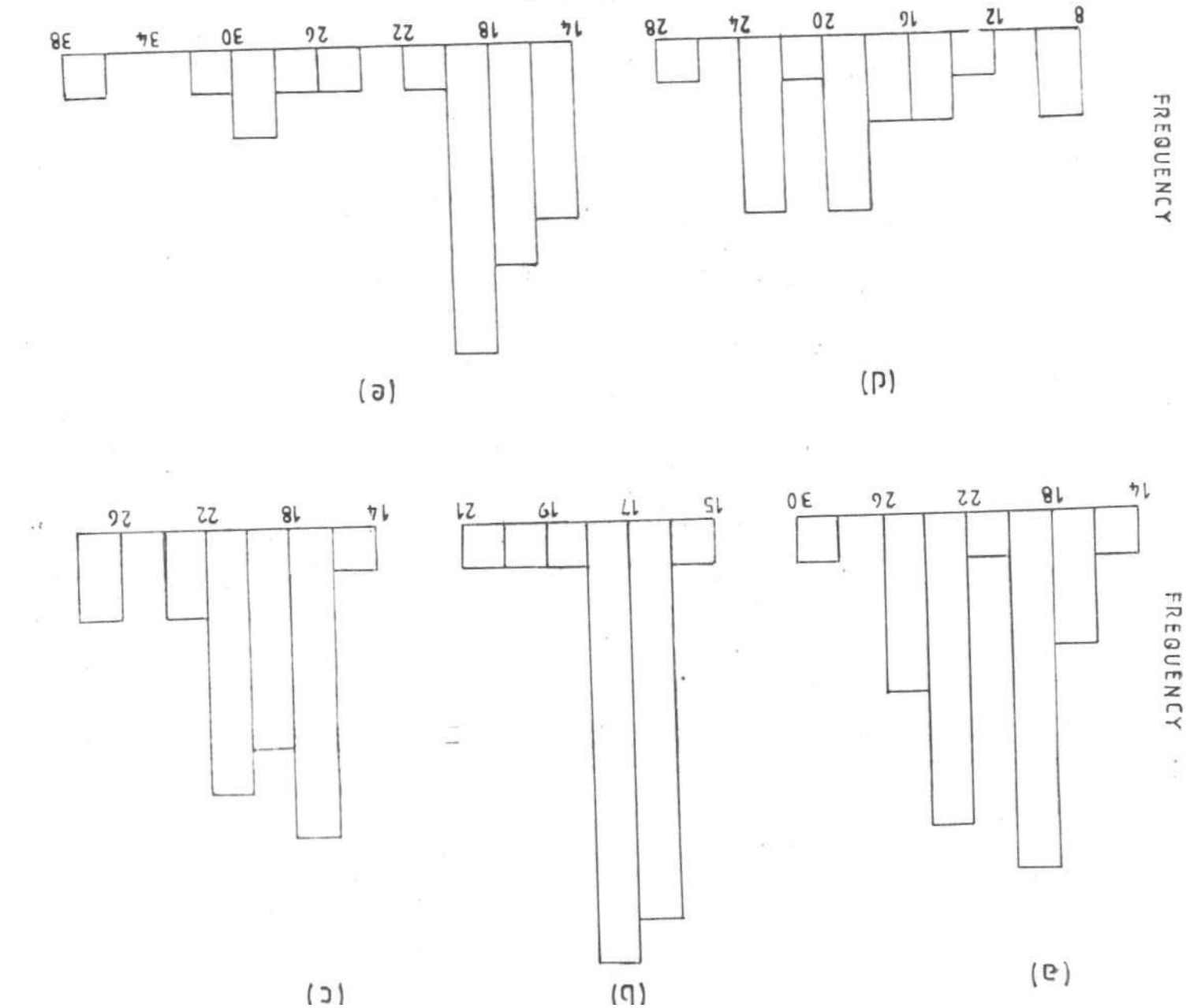


Fig. 5.5 Histogram of the overburden depths on some profiles in the study area (a) Line 204 (b) Line 208 (c) 316 (d) Line 300 (e) Line320.

enabled the construction of the sub-basalt bedrock surface structural map (fig 5.9). In belt (A) of the map, bedrock range of 49. - 65 m. depth is recorded; in (B), a range of 62 - 100 m. is recorded with a max. bedrock dip of about 3.2° towards S.W; and in belt (C), a range of 49-70 m. Belts (A) and (c) have much varied basement surface.

(v) Computed basaltic thicknesses are given in table 5.6 (appendix 7.).

5.6 Magnetic depths:

Magnetic depth estimates were found very useful in this study (table 5.5 (a) - (d), appendix 2.3 & 5) and compares fairly well with the gravity results on borehole profile.

Estimates were made on defined closures and on profiles - corrections were applied for azimuthal deviation of the profile axis from the North. Approximate depths to basement and overburden were estimated using Peter's slope-half-slope method (Peter's, 1949) (fig 5.6).

(i) Overburden depths from magnetic ranges from 13.7 - 21.4 m. on the reference bore-hore with an average of 17.0 ± 1 m. Estimate from closures gives a range of 13.8 - 20.0 with and average of 17.0 ± 1 m.

(ii) Computed basaltic thickness are given in appendix - 7, table 5.6, for some principal profile lines.

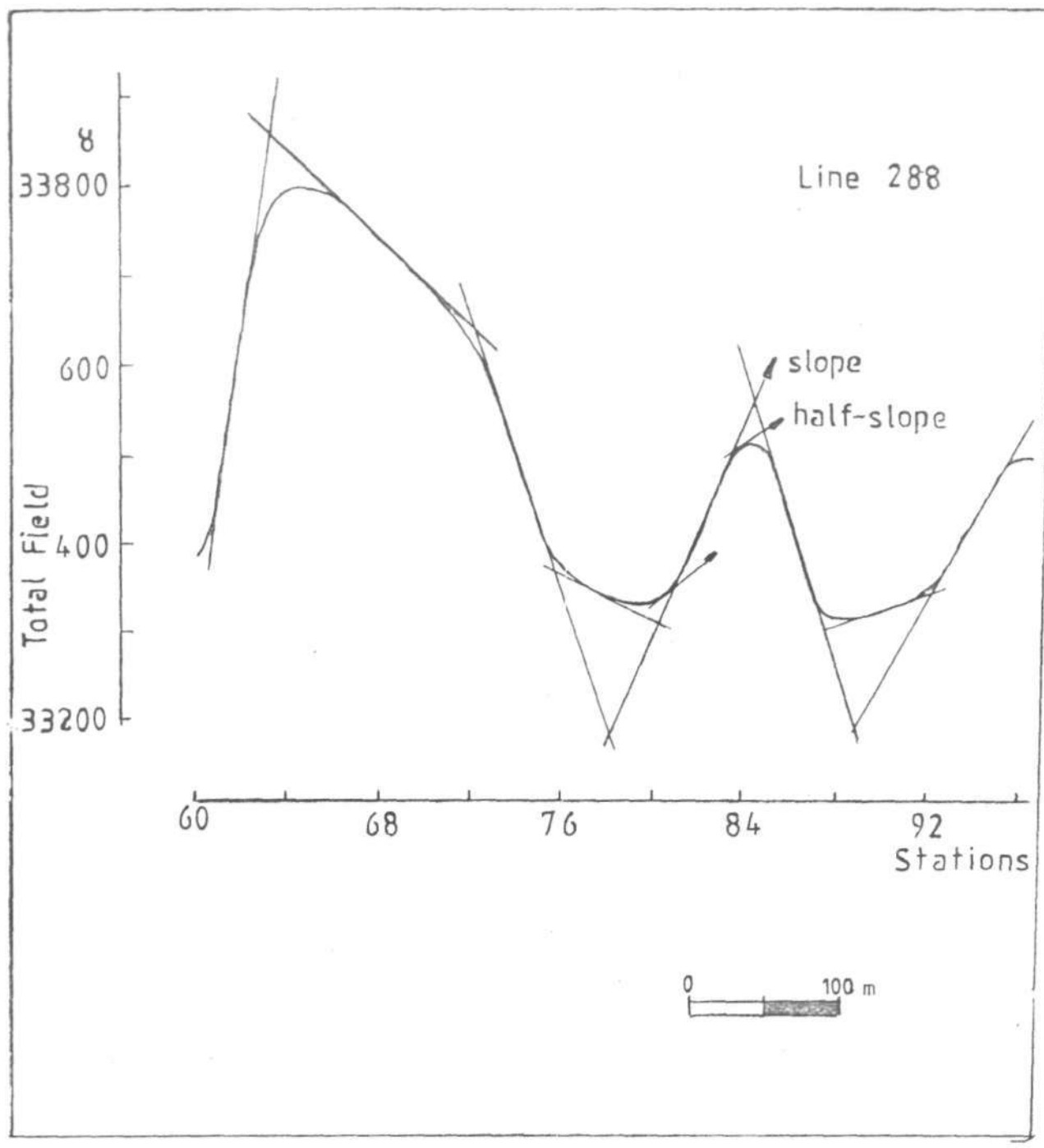


Fig. 5.6. Total field magnetic profile on the reference borehole section. Slope-half-slope depths yield approx. depths to the basaltic layer. (based on Peters, 1949).

Statistical correlation of the values from magnetic with those of gravity is fair.

5.7 Isopach map of the basaltic layer:

Fig. 5.7 shows the estimated thickness (map) of the basaltic layer over the area. This map was constructed as a result of the estimated overburden depths and approximate depths to base of basalt, from both gravity and magnetics with borehole profile correlation.

The pattern of the variation in basaltic thickness will reflect the pattern of the pre-basalt paleogeomorphological surface as well as areas of easy drilling for further investigation of the sub-basalt prospect. Moreover, a direct or inverse relation study of the basalt thickness variation with the sub-basalt sedimentary surface will lead us to some idea about the geological history of the study area.

5.8 Depth estimates from downward continuation maps

As earlier mentioned, the features expressed on the 3rd and 4th. spacings continuation maps as compared with those of the Ist and 2nd spacings gives an indication of a maximum depth of about 46 m. to the base of basalt layer beyond which the gravity values were not uniform.

The study of the 3rd and 4th continuation spacings (45.7 and 61 m respectively) maps for both gravity and magnetics readily indicates that the lateral configuration of depths of all probable gravitating and magnetic

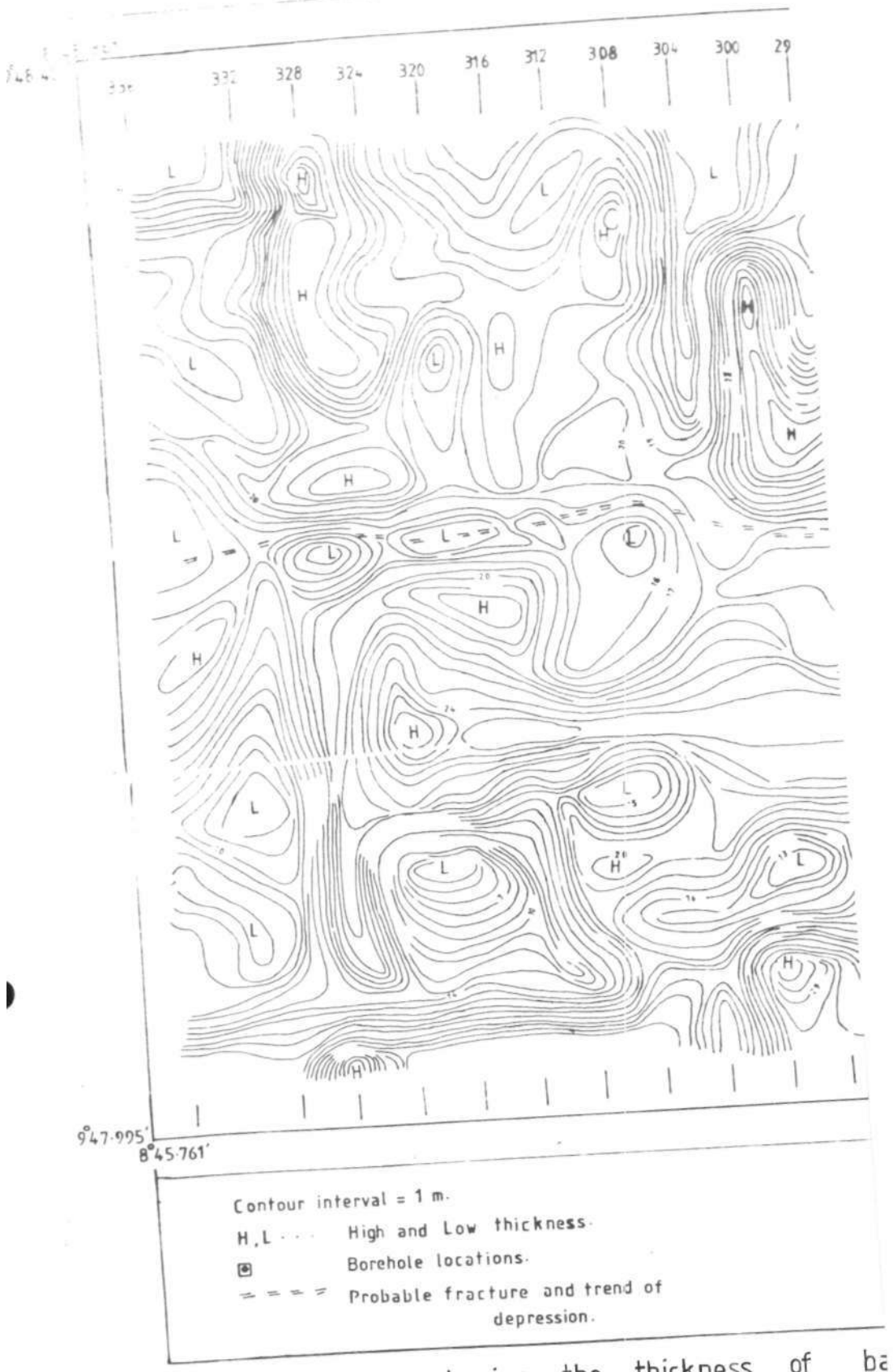


Fig. 5.7 A map showing the thickness of ba
the study Area.

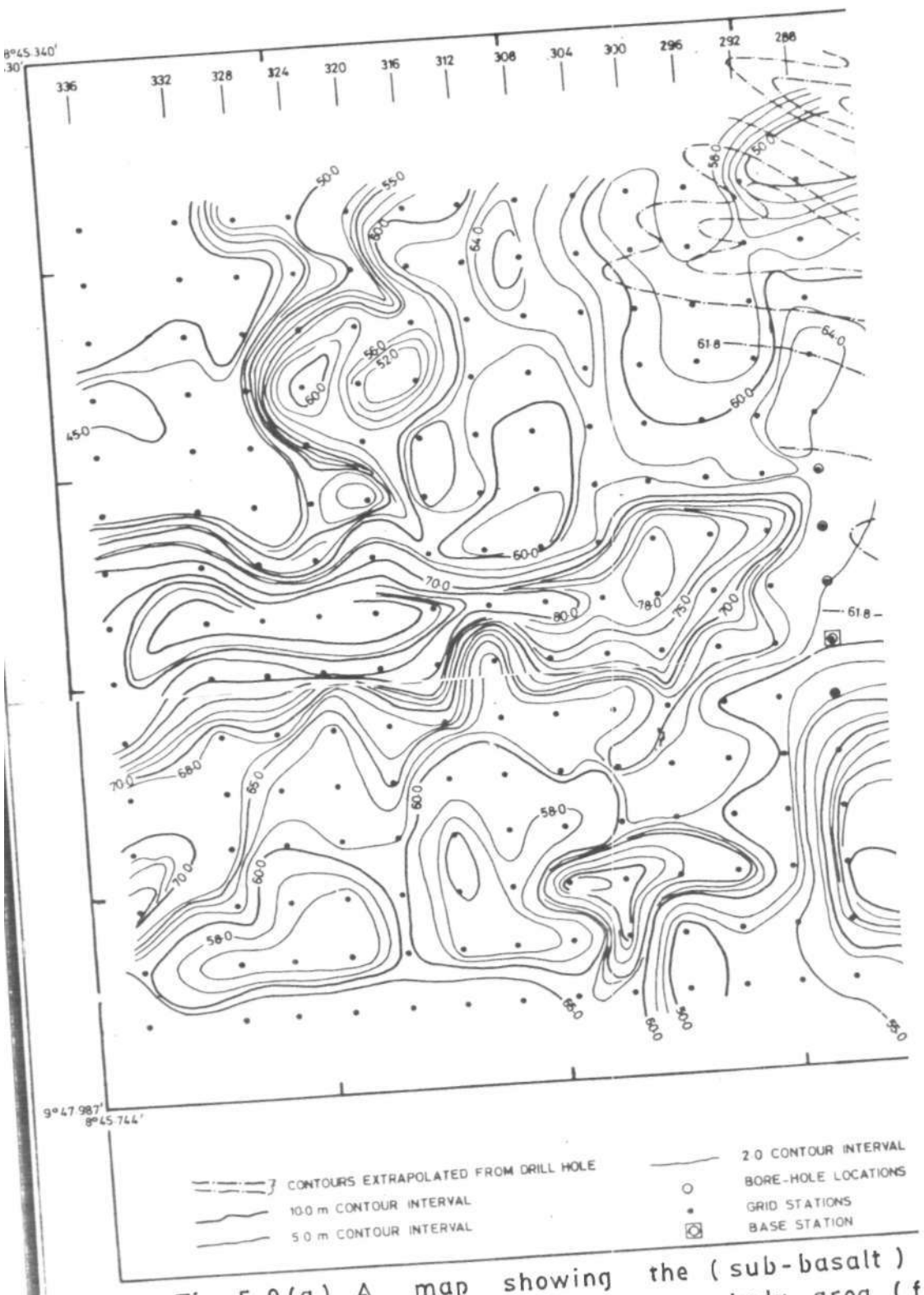


Fig. 5·9(a) A map showing the (sub-basalt) surface depths of the study area (f gravity data, based on Hammer, 1963).

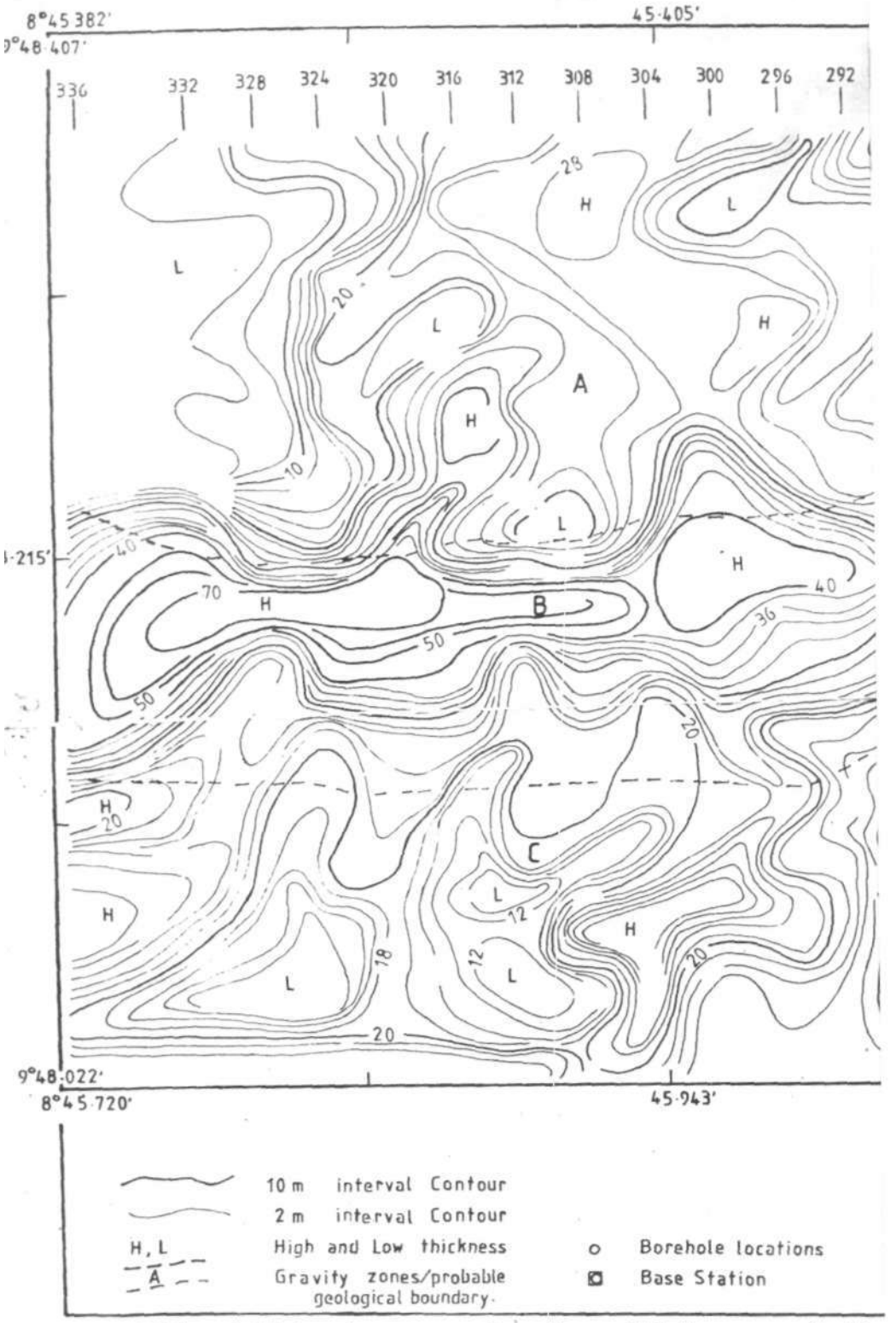


Fig. 5·9 (b) A map showing thickness of the sedimentary unit of the study area

CHAPTER SIX

SUMMARY AND CONCLUSION

6.1 Summary and discussion:

I The area of study is characterised by a strong NNE - SSW trending negative Bouguer anomalies in the range of - 78.0 to - 85.2 mGal. The regional gradient rises negatively by about 4.9 mGal/km., towards the central Ring structure of the Jos - Bukuru complex, from the area of study.

The observed trend conforms with that of the central Ring complex in terms of its structural outline. The large negative Bouguer is most probably due to the large Ring Complex structure of deeper origin.

II Analysis of the original Bouguer, its regional and the residual components shows that 3 gravity belts (A, B, and C) are identifiable on the maps, with probable structural boundaries.

The major anomaly of the middle part of the map (belt B) is considered indicative of sediments accumulation on a basement low surface downstream of an ancient river channel (fig. 6.1 (a) - (b)). These sediments could have been compacted and affected by some fractures (NE - SW) on the basement.

About 4 minor anomaly closures are located in belt (A) and 5 in belt (C), and are considered later in the derivative and continuation maps.

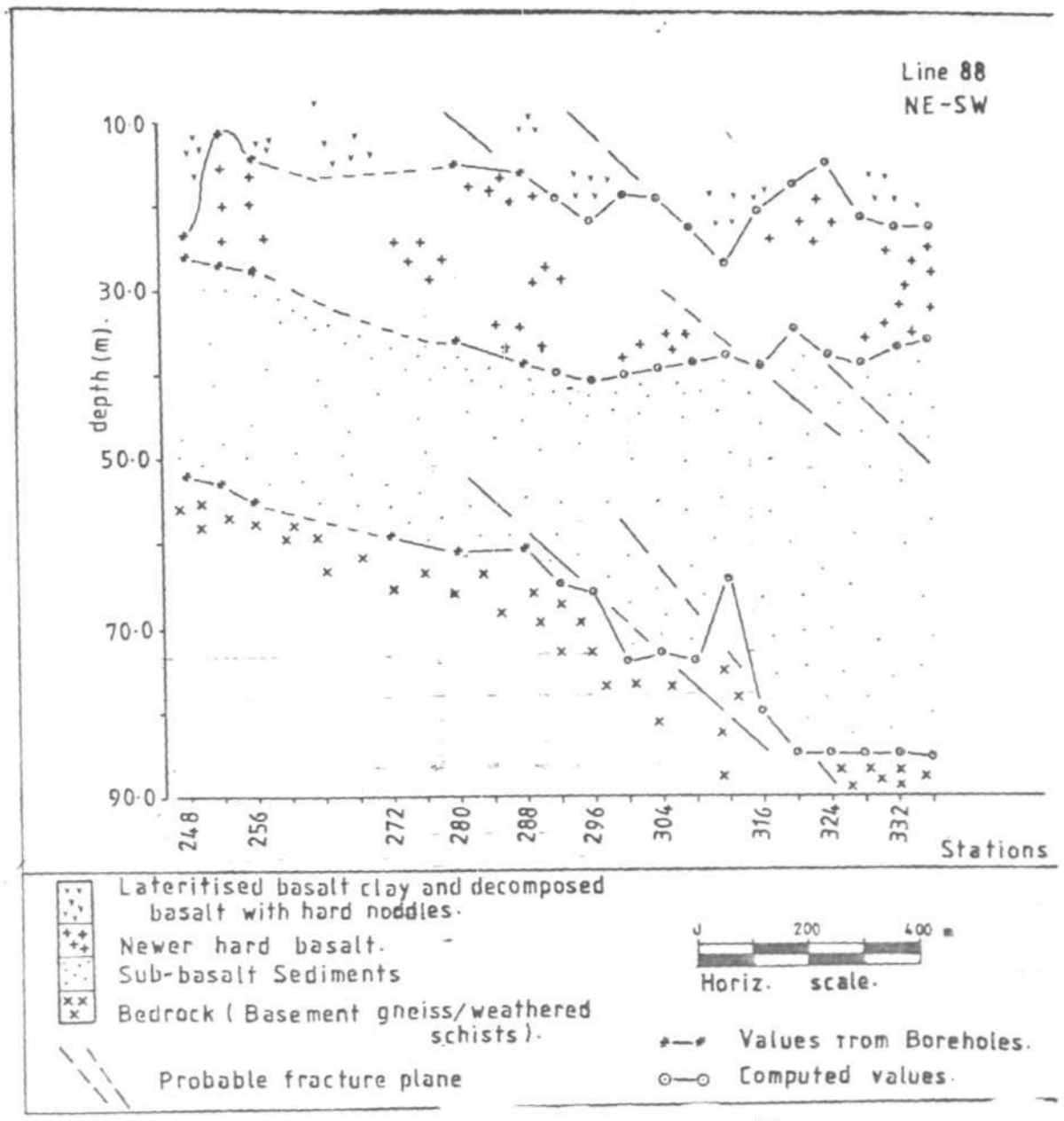


Fig. 6·1 (a) A geological section showing the probable bedrock profile in the study Area.

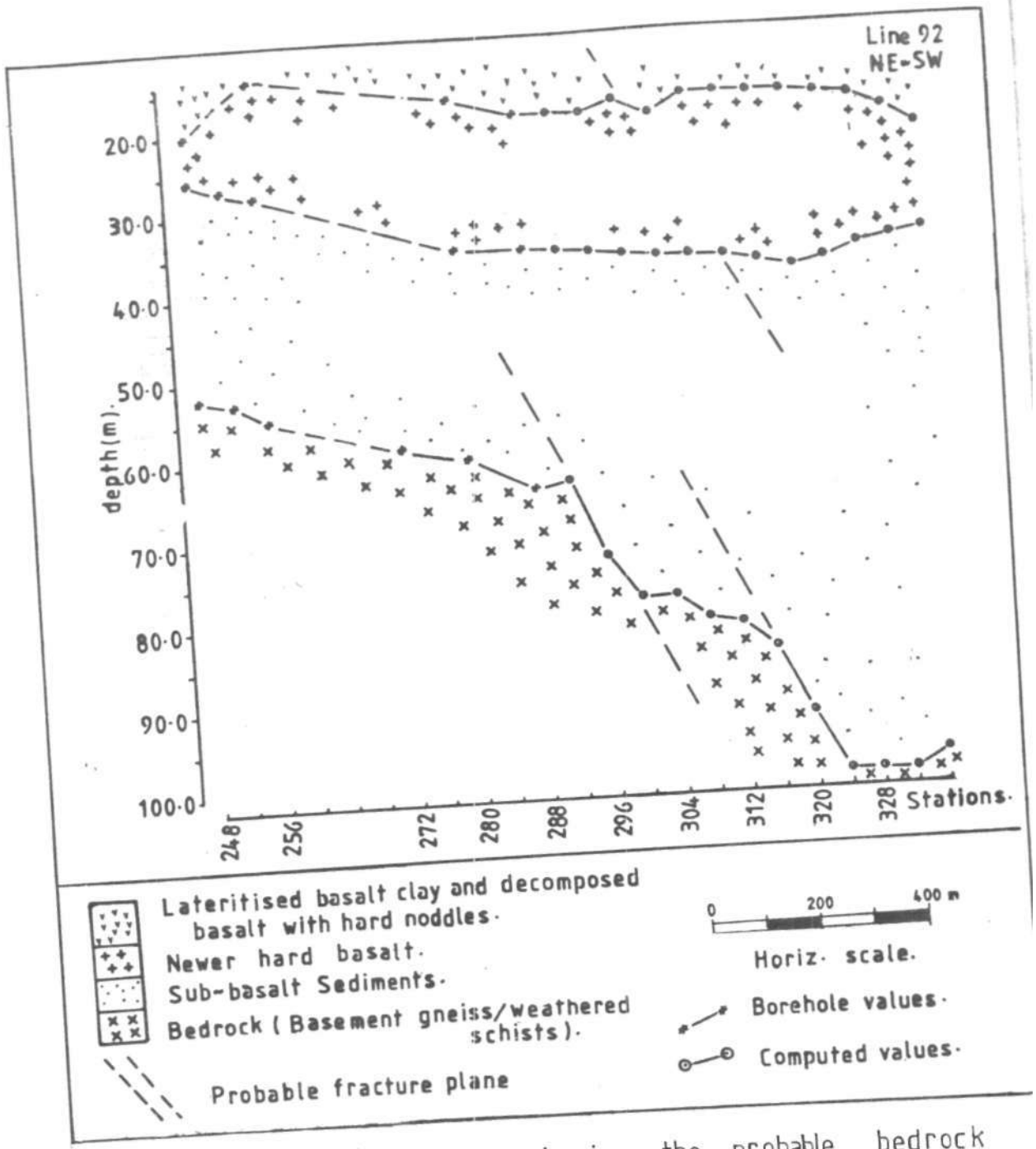


Fig. 6·1(b) A geological section showing the probable bedrock profile followed by the ancient Ngell river.

III From the second vertical derivative maps, the following conclusions may be drawn:

i. - on the gravity derivative map, conspicuous anomaly of the middle part of the map earlier mentioned is well defined, and has a width of about 180 m. This anomaly further indicates some fractures oriented in a NE - SW direction in the most shallow level of subsurface of the area of study. The low gravity closures of belts (A) and (C) are still apparent on this map.

ii. - the derivative magnetic map indicates a rise in the basic properties of the sub-basalt rocks and/or some anomalies that are probably from small lithologic variations. Two small magnetic bodies are found in belt (A) (G1/M1, and G3); two in belt (B) (M3 and M3 (b); and one in belt (C) (G6/M5). Limiting depths to these bodies are shown in table 5.5 (d) and shows that these bodies has little or no basement surface expression.

IV The interpretation of the downward continuation gravity maps for the 1st, 2nd, 3rd and 4th spacing (15.2, 30.5, 45.7 and 61 m respectively), has led to the following:

i. - most of the structural features represented on the original Bouguer, residual and 2nd vertical derivative maps are apparent on the continuation maps,

on the 3rd and 4th spacing. This is most probably indicative of the depths extent of 36 - 45 m. for the base of the basaltic layer as also confirmed from the nearby horeholes.

2. - the feature of the middle part of the map which is clearly observed on the Bouguer and residual gravity maps and apparent from the 1st - 4th spacings of continuation maps are well indicative of some fractures affecting both the basalts, sub-basalt sediments and the basement. These results also show that the middle part of the study area has the higher bedrock depth and the thickest sub-basalt sediments which is in agreement with figs. 6.1 (a) - (b) and 5.9 (b).

3. - the study of the 3rd and 4th spacing continuation maps shows that the depth extent of the basement surface below the basaltic layer is reliably confined to a range of 45 - 61 m. which is also confirmed well from the nearby borehole data from the area.

4. - a deformational trend of lineament in the basalt as evident on the continuation maps, oriented in a NW - SE direction is considered to be approximately parallel to the alignment of the 15 Quaternary alkaline

basalt volcanoes (the Newer basalts) on the plateau. This could indicate a development within the same structural age but however requires investigation on a larger scale (fig. 1.1.1. (b)).

V Estimate of the basaltic layer thicknesses from gravity data shows a variation in the range of 10 - 29m. Areas of very deep weathering exhibit low basalt thickness of less than 10 m. Basalt thickness is higher in belt (A) and (C), and compares with areas of slightly higher surface elevation.

Statistical correlation is fair with the thickness from magnetic as shown in table 5.6 (appendix 7). See also fig. 5.7.

VI Estimate of overburden depth to the basaltic layer from gravity varies from 8.6 - 36.4 m. with an average of 16.0 ± 1 m. while estimate from magnetics is in the range of 13.7 - 21.4 m. on the reference borehole profile. (with an average of 17.0 ± 1 m.). Estimate from magnetic surface closures gives a range of 13.8 - 20.0 m. with an average of 17.0 ± 1 m. Histograms. of overburden depths are shown in fig. 5.5.

These results show that the effective basalt thickness is less for gravity than magnetics probably as a result of insitu weathering of the basalt.

VII The surface gravimetric depths to basement is in the range of 60.0 - 79.6 m. with an average of 65.0 ± 1 m. as shown in table 5.5 (d), appendix 5

With assumption of geologic flexure or scarp on the high gravity gradient in belt (B) - along profiles 84 - 96, depths to source ranges from 32.4 - 44.5 m. with an average of 38.0 ± 1 m. as shown in table 5.5 (e), (appendix). This is indicative of approximate depth to the base of the basaltic layer, and is in agreement with a depth range of 36 - 45 m. apparent from the continuation maps and the borehole data.

VIII The stripped gravity data shows:-

1. - 2 positive gravity highs in belt (A) corresponding to the anomalies observed on Bouguer residual and continuation data (3rd and 4th spacings) and the second derivative gravity and magnetics. These anomalies are probably indicative of small basic plugs in the basement.

2. - most of the gravity anomalies are clearly defined on the stripped gravity map. There is a general correspondence with the 3rd. spacing (45.7 m.) gravity continuation.

3. - the stripped gravity data has enabled the calculation of approximate dpeths to bedrock which

compares fairly with the borehole profile results and results from surface gravity using Bott & Smith (1958) rule.

The sub-basalt bedrock surface maps constructed from these results (fig. 5.9) shows a bedrock depth range of 49 - 65 m. in belt (A); a range of 62 - 100 m. with a bedrock dip towards S.W. in belt (B); and a range of 45 - 70 m. in belt (C) which have much varied basement surface. Isopach map of the sub-basalt sedimentary unit is consequently compiled (using the idea of the depth extent of the basaltic layer base) to supplement the bedrock surface structural map in sub-basalt interpretation. (figs 5.9 (a) & (b)).

4. - the thickness of sediments under the basalt then, ranges from 10 m. (or less) in extreme N - W and Western parts to about 30 m. - (belt A). The middle part of the study area has the highest thickness of sediments with a range of 30 - 80 m. with an average of about 70 $\pm$ 1 m. In belt (C) a range of 3 - 30m. with about 20 m. average is observed.

6.2 Related error sources and precautions:

Errors in the gravity calculations could be contributed mainly in the following ways:-

i. variations in density both laterally and with depth is very important in gravity stripping. Density measurements needed a larger number of samples from boreholes taken to best represent each formation sub-stratum in order to facilitate accuracy in gravity stripping calculation.

ii. the technical aspect of well control is never perfect and errors are introduced in the depths as compared with the computed.

iii. the deeper gravity picture is subject to all uncertainties involved in the stripping corrections - errors inherent in the postulation of the overlying structures and formation thickness on the unknown profiles. This will introduce errors to the estimated bedrock depths and isopach maps constructed; contour interpolation may add to the errors.

The bedrock depths estimated from gravity and resulting maps may not absolutely correlate with the existing bedrock contour due not only to the above uncertainties but also to the fact that gravity depths possibly may take into account the

weathering depth of the granitic bedrock and weak-zones.

To take a fair care of these uncertainties in bedrock depths, intersection points of both depth contours from gravity and drillholes (extrapolated) may be used to construct a fresh average depth ccntours of smaller intervals.

6.3 Conclusion:

1. The area of investigation includes a possible downstream extension of the ancient N'gell river basin.

Gravity and magnetic results point to a possible flow of the ancient river to the south-western direction into a basement surface low resulting into a thick pile of sediments later covered by a thick basaltic flow and compacted. The thickest pile of sediments under the basalt can be observed in this area (figs 6.1 (a) - (b) and 5.9 (b)) with a maximum dipping bedrock south-westwards at a depth range of 61 - 100 m. indicating a possible stream channel.

The possibility of the river channel originally following a contact of weak/fracture zone oriented in a NE - SW in a basement low surface is evident from the results of the original Bouguer, residual and stripped, derivative and continuation maps of gravity and vertical field magnetic maps, of the study area.

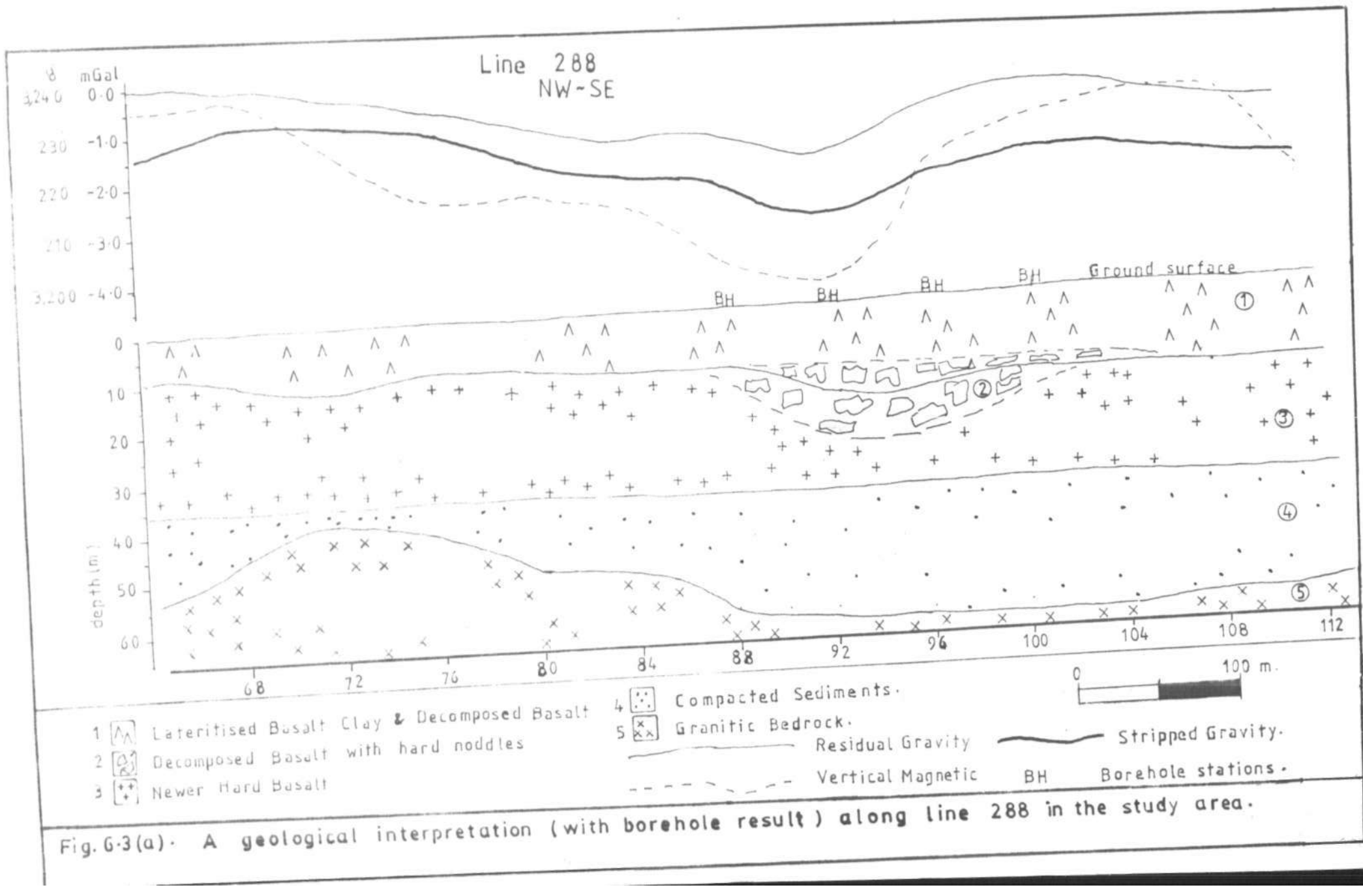
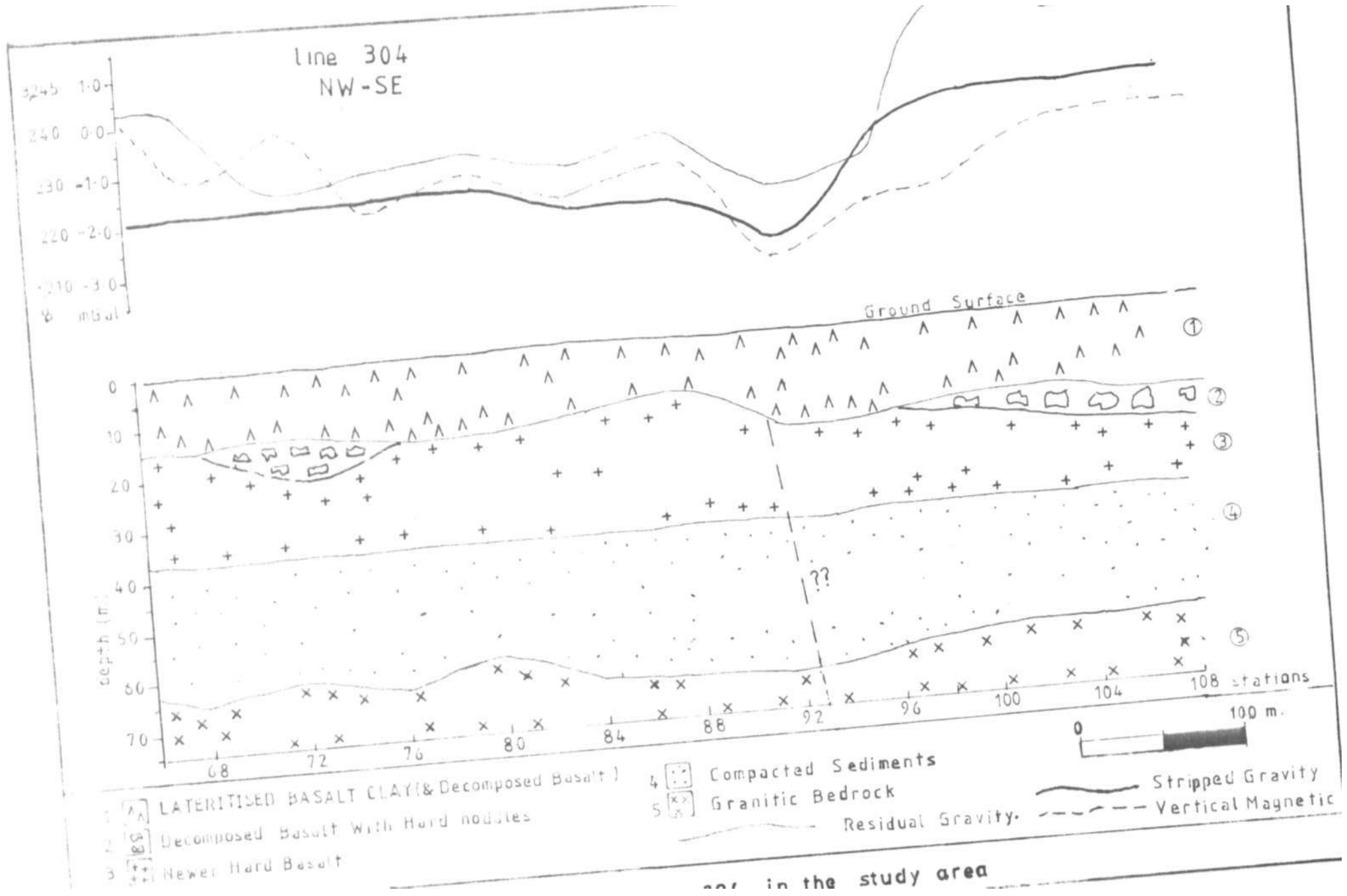


Fig. 6·3(a). A geological interpretation (with borehole result) along line 288 in the study area.



in the study area

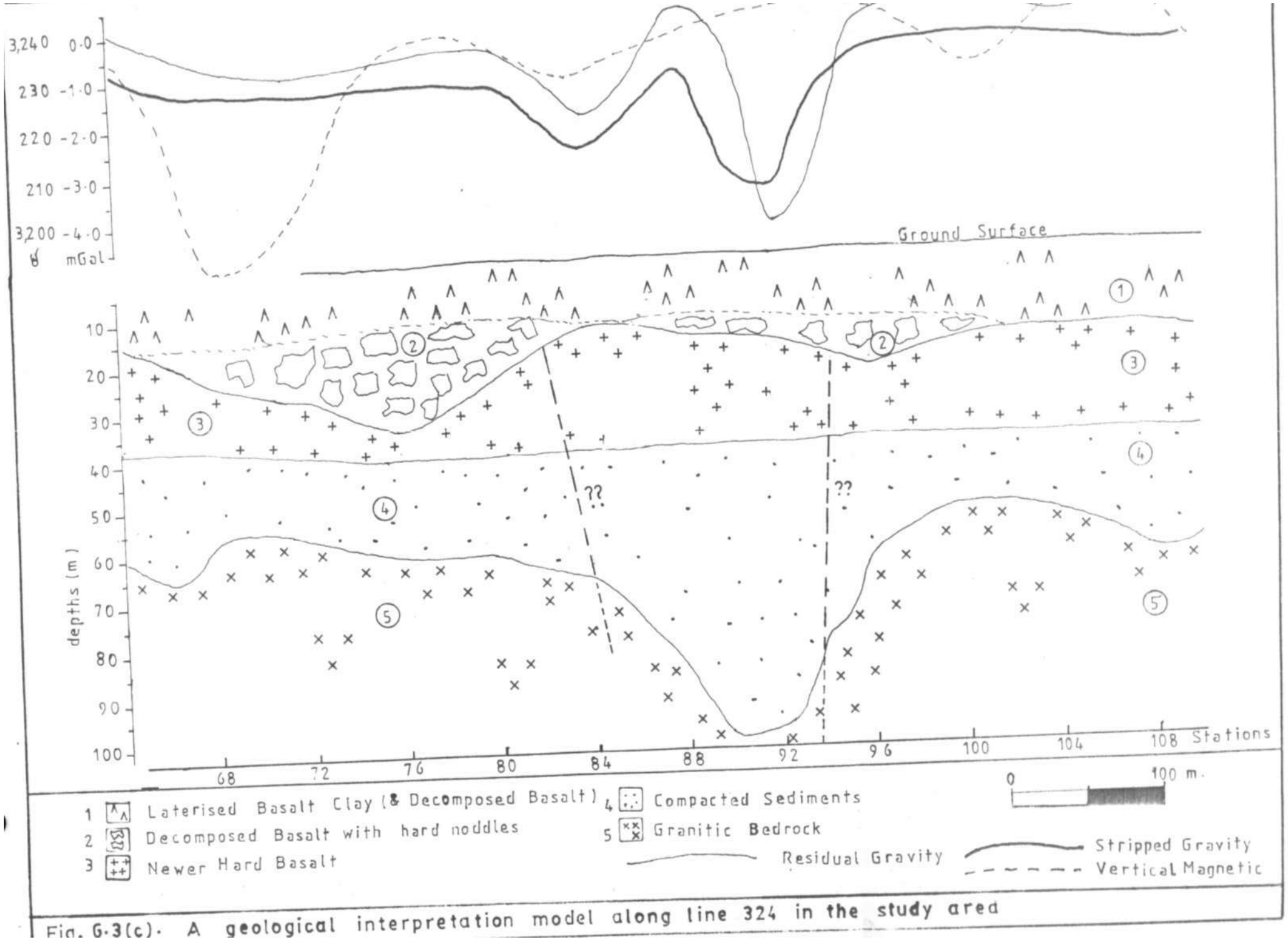


Fig. 6·3(c). A geological interpretation model along line 324 in the study area

A NW - SE linear features affecting the basalts and the sub-basalt rocks are also evident from the continuation maps.

2. It is possible practically to remove the basaltic masking effect from gravity data observed on the basalt by a stripping technique as evident from the results of the study. This can enable the interpretation of the sub-basalt cassiterite deposit by a fair estimate of the outline of the basin (figs 6.3 (a) - (c)) and probable bedrock depths and hence the ancient stream channel. A fair estimate of the depths to bedrock from stripped gravity data (taken over the basalt) is done from these results as shown in figs 5.9 (a) and 6.1 (a) - (b) and is in agreement with the results from the boreholes (fig 5.3 (a)).

3. Estimate of the depths to basalt is also fairly achieved from the results of total field magnetic data.

4. Analytical method of continuation and derivative computation techniques applied to both the gravity and magnetic data served as a practical check on the results of stripping technique applied in this study. Results yield a depth range of 36 - 45 m. for the base of the basalt and a range of 45 - 61 m and above for the base-ment surface depth.

A simple cover by hard thick basalt layer overlain by weathered lateritised basalt clay overburden gives a simple surface geological picture that hides a rather interesting sub-surface conditions of the N'Gell basin. The slight changes in surface relative elevation is possibly due to thick poorly weathered basaltic cover.

Composite geological sections are compiled from the above results and shown in fig. 6.3 (a) - (c) for the area of study.

6.4 Recommendations:

The results of this study has added a foresight as to the need for further investigation and scope of future geophysical work:

1. extension of profiles is required beyond line 336 (NE - SW) so as to fully define the extent of the anomaly in belt (B) of this study and beyond cross-lines 288 - 340 in the SE direction in belt (C) of this study. In belt (A) of this study, extension should be made on all the profile lines to NW from cross-line 116, 120... ... and beyond.

These extension areas show the nature of a pre-basalt flood plain and could be fully defined.

2. future gravity and magnetic data along profile grid systems of about 10 - 20 m. is adequate for detailed work.

In the analysis, or otherwise, stripping correction used be done with adequate density data taken with few drill-holes limited to the basalt.

3. test-drilling may be done in Belt (A) near locations 296/120, 308/116 - 112 and 280/116. These areas are likely flat bedrock flood-plains near valley-foot, and may preserve early bottom wash.

A test-drilling may also be done along cross-line 92 and 96 where the sedimentary pile is thickest, to confirm the nature of anomaly in belt (B). Mineral desposit along the flat valley bottom is possible.

4. extensive gravity and magnetic data should be taken along all existing borehole profiles on the N'gell sub-basalt basin as a follow-up of this studies. In view of future underground mining prospect under the basalt, stripped gravity data may be used to study the weathering depths and weakzones under the basalt. Isopach maps of the sub-basalt sediments and maps of weathered or weakzone of the bedrock might be helpful.

APPENDIX 1

Gravity Belt	Anomaly	**Polarity and Pairs	Interpretations Infeered
A	G2/M1	GH, MH, ML	- basic intrusive at depth (also a gravity hig indicated on 3rd and 4th spacing down-continued data; and magnetic (3rd spacing) fig. 5.3.2(c) and 5.3.1 (b).
	G3	GL/ML	- a basic intrusive in a basement depression (shows a gravity low on 3rd and 4th spacing continuation and high on Derivative Magnetic. (figs 5.3.2. (c) and 5.3.1.(b)).
	G4/M2	GH/ML GH/MH	-a thick basaltic rock layer and basic intrusive in a background of sedimentary rock (shows gravity lows and highs on the 3rd/4th spacing

	M4	GL/MH GH/ML	continuation maps (fig. 5.3.2(c) and 5.3.1.(b) and splits into alternative lows and highs on the 3rd spacing magnetic (fig. 5.3.2.(b)). - gravitation steps (probable break in hard basalt or edge/or deep basaltic weathering).
B	M3	GL/ML	-depression in the basement (see continuation maps).
	M3(b)	GL/ML GL/MH	- a basic plug within the basement masked by a basement surface depression.
	M3(c)	GH/MH	- thick basic layer over an ultrabasic or basic intrusive or plug in a sedimentary background.

C	G5/M7	MH/GL ML/GH	- weathering steps, a probable deep basaltic weathering to linear depression with basalt (shallow source).
	G6/M5	MH/GL	- an ultrabasic cr basic plug at depth within the basement (prominent on gravity and magnetic 3rd and 4th spacing continuation maps and on the derivative magnetic map (fig. 5.3.2(c) and 5.3.1(b)).
	G8	ML/GH	- linear step within basement (fig. 5.3.2(c) and 5.3.1(b)) fracture.
	G7	GL/MH	- shallow depression on the basement surface (fig. 5.3.2(c) 5.3.1.(b)).
	G9	GH/ML	- weathering step within the basalt (shallow source), (not indicated from continuation map of fig. 5.3.2(c)).
	M6	GH/ML	- intrusive plug at depth (basic or ultrabasic body).
	M5(b)	MH/GH	- basic plug in the basement (figs 5.3.2(c) and 5.3.1(b)).

Table 5.0 - Qualitative interpretation of the gravity and Magnetic anomalies polarities in the area.

** GH = Gravity high; MH = Magnetic high;
GL = Gravity low; ML = Magnetic low.

APPENDIX 2

Station No	Bore-hole results (m)		Approx. Over-burden depths (m)		Appox. Basalt thickness (m)	
	Basalt Thick-ness	Over-Burden Depth	*From Gravity	+From Mag-netic	*From Gravity	+From Mag-netic
288/100	19.2	17.3	-	-	-	-
288/96	14.6	20.4	17.6	21.4	19.0	22.9
288/92	16.2	19.2	18.9	19.8	17.7	24.3
288/88	22.0	16.2	17.1	13.7	25.0	25.5
288/84	25.9	13.1	17.1	18.3	25.0	21.8
288/80	-	-	17.1	15.2	25.0	26.9
288/76	-	-	17.2	15.2	25.0	26.9
288/72	-	-	17.1	16.2	25.1	25.9
288/68	-	-	16.1	-	26.0	-
288/64	-	-	15.1	13.7	27.0	25.5
Average	19.58 ± 1.0	17.24 ± 1.0	16.94 ± 1.0	16.70 ± 0.64	24.08 ± 0.60	24.96 ± 1.0

Table 5.5(a) - Basalt and Overburden thicknesses on the Control bore-hole section.

\+ based on Peter's, 1949.

* based on assumption of a Bouguer slab of infinite horizontal extent

Appendix 3

PROFILE LINE / COMPUTED VARIABLES	288	300	304	316	320
No. of Samples	15	13	14	14	14
Gravity * Depth Range To basalt (m)	15.50 - 18.87	8.6 - 27.07	16.85-24.34	14.53-30.55	14.52-36.36
Mean Depth To Basalt (m)	17.97	19.43	21.30	20.23	21.52
Standard Deviation	0.68	5.84	2.57	2.41	6.57
No of s samples	8	6	11	12	9
Magnetic + Depth Range to Basalt (m)	16.56-20.81	14.63-22.86	15.30-27.12	12.30-25.47	14.06-29.87
Mean Depth To Basalt (m)	17.87	19.56	20.62	18.09	19.51
Standard Deviation	1.54	2.88	3.93	3.86	3.18

Table: 5.5(b) Compiled depths to Basal ic layer from Gravity and Magnetics. A generally higher average overburden thickness is observed from the gravity data.

* based on infinite horiz. slab approx.
\+ based on Peter's, 1949

APPENDIX 4

Anomaly Closures	Average Radius (m) of Closure	Maximum Depth To Source (m)
G1	90.17	58.6
G2/M1	114.30	74.3
G3	57.15	37.2
GS1	77.47	50.4
GS2	85.09	55.3
GS3	120.65	78.4
G5/M7	107.95	70.2
G6	105.41	68.5
G7	88.90	57.8
G9	66.04	42.9
GS4	73.66	47.9
GS5	67.31	43.8
GS6	68.58	44.6
GS7	208.28	135.4

Table 5.5(c) - Depths to Source from stripped gravity closures, (based on Botts and Smiths, 1958) (GS1, GS2... are anomaly closures appearing on stripped, gravity map only).

APPENDIX 5

SURFACE ANOMALY CLOSURES	Maximum depth (h) to Bedrock or Source (m)	Maximum depth (D) of Overburden (m)
G1/M1	62.7 *	16.6 +
G2/M1	162.6 *	15.0 +
G3	71.8 *	17.5 +
M3	-	16.0 +
M3(b)	69.3 +	13.8 +
G4/M2	61.1 +	16.8 +
G5/M7	65.4 *	17.2 +
G6/M5	61.9 +	18.1 +
G7	70.2 *	22.9 +
G8	76.8 *	17.5 +
G9/M6	47.1 *	13.7 +
Mean	65.1 ± 1.0 (Bedrock Depth)	16.80 ± 1.0

TABLE 5.5(d) Depths estimated from gravity and magnetic closures.

* based on Bott and Smith (1958)

\+ based on Peter (1949)

PROFILE	RANGE OF BEDROCK DEPTH (m)	RANGE OF BEDROCK Dip. (o)	Average dip (o)
L 96	50.6 - 78.0	0.53 - 1.04	0.72 ± 0.28
L 92	52.0 - 100.0	0.80 - 3.15	1.65 ± 0.31
L 88	52.1 - 85.0	1.02 - 2.10	1.33 ± 0.65

Table 6.1: Bedr ck paramters of the Deepest zones (see figs. 6.1 (a) & 6.1(b)).

PROFILE SECTION	PROFILE Length (m)	DEPTH (h) To Source (m)
336/96-88	127.0	40.4
332/96-88	101.6	32.4
328/ "	114.3	36.4
324/ "	111.8	35.6
320/ "	109.2	34.8
316/ "	121.9	38.8
312/ "	119.4	38.0
308/ "	121.9	38.8
296/96-88	139.7	44.5
336/88-80	114.3	36.4
332/ "	111.8	35.6
328/ "	114.3	36.4
324/ "	119.4	38.0
320/ "	121.9	38.8
316/ "	119.4	38.0

Table 5.6 (e): Parameters of geological flexure on the sharp gravity zone (B); Depth (h) to centre of semi-infinite horizontal sheet approximates to base of basalt. (Telford, et al, 1980, pp 68 - 69)

APPENDIX 7.

Profile Line / Computed Variables	288	299	296	390	304	316	320	324	328	336
Number of Samples	8	4	7	6	11	10	9	10	10	8
Range of Thickness from Gravity (m)	18.4-26.5	18.7-23.8	16.6-25.8	15.0-29.1	12.5-23.2	11.5-23.2	11.3-23.3	1.5-25.0	14.5-28.0	9.8-17.8
Average Thickness (m)	24.0	21.3	21.4	21.7	18.5	19.3	18.7	19.8	20.8	15.1
Standard Deviation (m)	2.71	2.6	4.2	5.1	4.0	4.2	3.8	5.9	4.6	2.5
Range of Thickness from Magnetic (m)	21.8-25.9	18.7-39.6	22.8-39.7	19.2-27.4	14.9-26.7	16.6-23.8	12.2-23.8	12.2-30.5	15.2-24.4	10.7-29.9
Average Thickness (m)	24.3	25.0	28.0	22.5	21.4	20.9	19.5	20.9	19.4	18.3
Standard Deviation (m)	1.40	-9.95	6.25	3.88	3.93	2.61	3.72	5.89	3.46	5.37
Correlation Coefficient (Gravity/ Magnetic Thickness)	0.44	0.65	-0.50	0.71	0.87	0.80	0.99	0.62	0.65	-0.61

Table 5.6: Statistical Correlation of the basalt thickness from Gravity and Magnetics. A generally higher average thickness is here observed from Magnetics data.

REFERENCES

Ajakaiye, D.E. (1970), Gravity measurements over Nigerian Younger Granite Province - Nature Vol. 225, pp. 50 - 52.

Ajakaiye, D.E. (1976) - A Gravity Survey over the Nigerian Younger Granite Province. In: Kogbe, C.A. (1976) (ed) Geology of Nigeria pp. 207-224. Elizabethan Publ. Co. Lagos.

Ajakaiye, D.E., Ellis, R.M., Verheijen, P.J.T. (1975) Gravity and Seismic Investigation of ML6114 and EPL 9736. Final Report (Unpubl.) submitted to the ATMN.

Ajakaiye, D.E. and Burke, K.C. (1972), A Bouguer gravity map of Nigeria, Tectonophysics, Vol. 16, pp. 103 - 115.

Buchanan, M.S. (1971) - The Geology of the Jos Plateau. Bull. Geol. Surv. Nigeria No. 32, Vol. 2, Younger Granite Complexes.

Bott, M.H.P. and Smith, R.A. (1958) - The Estimation of the limiting depth of gra itating bodies Geophys. Prosp., Vol. 6 pp. 1 - 10.

Burke, K.C. and Durotoye, A.B. (1970) - The Quarternary in Nigeria. In: Dessauvagie, T.F.J. and Whiteman, A.J. (eds), African Geology pp. 325-347, Ibadan (1972).

Bond, G (1956), "A preliminary account of the Pleistocene Geology of the Plateau tin field region of Northern Nigeria", Proc. 3rd. Intern. West African Conf. Ibadan 1949. pp. 187 - 202.

Bullard, E.C. (1956) and Cooper, R.I.B. (1948), - Determination of the masses required to produce a given gravity field, Roy. Soc. London, Proc. A., Vol. 194 pp. 332-347.

Cox, C.I.B. (1979), "Sub-Basalt Tin: Its Prospecting and Minning; Proc. 15th Ann. Conf. Nig. Min. Geosc. Soc. (1976).

Constantinescu, L. and Botezatu, R., (1961) - Contributula interpretarea fizica a anomalaor cimpurilor potentiale: Petroleum de Geofizica, R.P.R.I.I.

Dobrin, M.B. (1976) - Introduction to Geophysical Prospecting pp. 426-430 McGraw Hill (1976).

De Swardt, A.M.J. (1956) - "Recent erosion surfaces on the Jos Plateau". Proc. 3rd International W. Afr. Conf. (1956), pp. 180-186.

Elkins, T.A. (1951) - The second derivative method of gravity Interpretation, Geophs. Vol. 16 pp. 29-50.

Evjen, H.M. (1936) - The place of the vertical gradient gravity interpretation. Geophys. Vol. 1., pp. 127-136.

Forsyth, W.A.L., (1960) - Inverell airborne magnetic and radiometric survey. Aust. Bur. Min. Res. Record No. 1960/101 (Unpubl.). In: Parkinson, W.D. (ed.) Introduction to Geomagnetism, PP. 191. Elsevier Sch. Publ.Co., Inc. (1982).

Falconer,J.D. and Raeburn, C., (1923) - The Northern Tinfields of Bauchi Province. Bull. geol. Surv. Nigeria, No, 4'

Falconer, J.D.,Raeburn, C and Bain, A.D. (1926) - The Southern Plateau Tinfields. Bull. geol. Surv. Nigeria, No. 9.

Grant, F.S., (1954), - A theory of regional correction of potential field data. Geophys. Vol. 19 pp. 23-45.

Grant, F.S. and West, F.G. (1965) - Interpretation Theory in Applied Geophysics New York, McGraw Hill.

Griffin, W.R., (1949), Residual gravity in theory and practice. Geophys. Vol. 14, pp. 39-56.

Henderson, R.G. and Zietz, I. (1949a). - The Computation of 2nd vertical derivative of geomagnetic fields, Geophys. Vol. 14, pp 517 - 534.

Hughs, D.S.,(1942)- The analytical bases of gravity interpretation. Geophys. Vol. 7, pp. 169 - 178.

Hammer, S. (1947) - A New calculation technique for Quantitative Interpretation in Gravity Prospecting. Geophys. Vol. 12, pp. 498.

Hammer, S.,(1963) Deep Gravity Interpretation by Stripping. Geophys. Vol. 28, pp. 369 - 378.

Jacobson, R.R.E., MacLeod, NN. and Black R. (1958), Ring Complexes in the Younger Granite Province of Northern Nigeria. Mem. geol. Soc. Lond. No. 1.

Jacobson, R.R.E., and McLeod, W.N. (1977), Geology of the Liurei, Banke and adjacent Younger Granite Ringe Pompleces. Bull. geol. surv. Nigeria, No. 33.

Kotanski, Z.J. (1976) - Probable Fold and Fault Tectonics of the fluvio-volcanic formation in the vicinity of Jos. In; Kogbe, C.A. (ed.) Geology of Nigeria pp. 429, Elizabethan Publ. (1976).

Mackay, R.A., Greenwood, R. and Rockingham, J.E. (1949) - The Geology of the Plateau Tinfields - Resourvey 1945 - 48. Bull. geol. Surv. Nigeria No. 19.

McLeod, W.N., Turner, D.C., and Wright, E.P. (1971) - The Geology of the Jos Plateau, Vol. 1: General Geol. Bull. geol. Surv. Nigeria, No. 32.

MacLeod, W.N. and Berridge, N.G. (1971) - The Geology of the Jos Plateau. Geol. Surv. Nigeria. Bull. No. 32 Vol. 2. Younger Granite Complexes.

McLeaod, W.N. and Turner, D.C. (1971) - The Geology of the Jos Plateau. Bull. geol. surv. Nigeria. No. 32 Vol. a: General Geology.

Masson-Smith, D. 1965 - Geophysical prospecting for basalt covered alluvial cassiterite on the J_os Plateau, Northern Nigeria. Overseas geol. Surv., London, Geophys. Rep. No. 27.

Mesko, A., 1966 - Two dimensional filtering and the second derivative method, Geophysics, Vol. 31, pp.606-617.

Mesko, A., 1967 - Gravity Interpretation and information theory, Annals, Universities Scientiarum. Budapest, 1967.

Naggy, D. (1964) - The gravitational effect of two dimensional masses of Arbitrary Cross Section, Unpubl. Manuscript of the Gravity Div. of the Mines and Tech. Surv. Observ. Branch, Canada.

Nettleton, L.L. (1976) - Geophysical Prospecting for Oil. New York, McGraw-Hill Book Company.

(1942) - Gravity and magnetic calculations. Geophys., Vol. 7, pp 293-310.

Netfleton, L.L. (1971) - Elementary Gravity and magnetics for Geologists and Seismologists. S.E.G. Monograph series, No. 1.

Nettleton, L. . (1954) - Regionals, residuals and structures. Geophys; Vol. 19, pp. 1-22.

Nettleton, L.L. (1939) - Determination of density for reduction of gravimeter observations, Geophys. Vol. 4 pp. 176-183.

Oyawoye, M.O. (1963) - The geology of the Nigerian Basement Complex. Journ. Nig. Min. Geol, and Metallurgical Soc. Vol. 1, 2; pp. 87 - 102.

Peters, L.J., 1949 - The direct approach to the magnetic interpretation and its practical application. Geophys., Vol. 14 pp. 290 - 319.

Petrova , G.N., Bebrov, V.N. and Pudovkin, M.I. (1980) - Geomagnetism. I.U.G.G. Publ. UNESCO (1980)

Parkinson, W.D. (1982) - Introduction to Geomagnetism Elsevier Publ. Co. Inc.

Raeburn, C. (1927) - The Tinfields of Zaria and Kano Provinces. Bull, geol. Surv. Nigeria, No. 11.

Rosenbach, O., (1953) - A contribution to the computation of "second derivative" from gravity data Geophys. Vol. 18. pp. 894-912.

Rosenbach, O. (1955) - Quantitative studies concerning the vertical gradient and 2nd derivative method of gravity interpretation. Geophys. Prosp. Vol. 2.

Roy, A,, (1961) - On some properties of residuals and derivatives. J. Geophys. Pros., V. 66 pp. 540-548.

Shaw, S.H. (1951) - Report on Magnetic and resistivity work in the Plateau tinfield. Unpubl. Rep. Overseas geol. Surv. London.

Shaw, S.H. (1951) and Cole, J.A. (1961) - The use of the electrical Resistivity method for prospecting deep-leads in the Jos Plateau Tinfield Rec. Geol. Survey, Nigeria.

Smith, R.A. (1959) - Some depth formulae for local magnetic and gravity anomalies - Geophys. Prosp. Vol. 7, pp. 55 - 63.

Smith, R.A. (1960) - Some formulae for interpreting local gravity anomalies, Geophys, Prosp . Vol. 8 pp. 607-612.

Swartz, C.A. (1954) - Some geometrical properties of residual maps. Geophys. Vol. 19, pp. 46-70.

Sharma, P.V. (1976) - Geophysical methods in Geology Amsterdam. pp. 217.

Sazhina, N and Grushinsky (1971), - Gravity Prospecting PP. 414-438. Mir. Publ. Moscow.

Trejo, G.A. (1954) - A note on the downward continuation Gravity. Geophys. Vol. 19, pp. 71 - 75.

Telford, W.M., Gilbert, L.P., Sheriff, R.E. and Keys, D.A. (1980) - Applied Geophysics pp. Cambridge University Press London.

Verheijen, P.J.T. and Ajakaiye, D.E. (1978) - A gravimeter of calibration line, Nigeria. Surv. Review. Vol. 24. 190, 373 - 380.

Vacquier, V., Steenland, N.C., Henderson, R.G. and Zeitz, I. (1951). Interpretation of aeromagnetic maps. Geol. Soc. Am., Memoir, 47.

Wright, E.P. (1971) - The Geology of the Jos Plateau. Bull. geol. Surv. Nigeria, No. 32 Vol. 1, General Geology pp. 40 - 41.